

Universidade Federal do Rio Grande do Sul
Faculdade de Medicina
Programa de Pós-Graduação em Ciências Pneumológicas

Fernando Ferreira Gazzoni

**Achados na tomografia computadorizada de alta resolução da aspergilose
pulmonar em pacientes transplantados de pulmão**

Porto Alegre, 2014

Fernando Ferreira Gazzoni

**Achados na tomografia computadorizada de alta resolução da aspergilose
pulmonar em pacientes transplantados de pulmão**

Tese apresentada ao Programa de Pós-graduação em Ciências Pneumológicas da Universidade Federal do Rio Grande do Sul, como requisito parcial à obtenção do título de Doutor em Ciências (área do conhecimento: Ciências pneumológicas).

Orientador: Prof^o. Dr. Luiz Carlos Severo

Co-orientador: Prof^o. Dr. Bruno Hochhegger

Porto Alegre, 2014

CIP - Catalogação na Publicação

Ferreira Gazzoni, Fernando

Achados na tomografia computadorizada de alta resolução da aspergilose pulmonar em pacientes transplantados de pulmão / Fernando Ferreira Gazzoni. -- 2014.
144 f.

Orientador: Luiz Carlos Severo.

Coorientador: Bruno Hochhegger.

Tese (Doutorado) -- Universidade Federal do Rio Grande do Sul, Faculdade de Medicina, Programa de Pós-Graduação em Ciências Pneumológicas, Porto Alegre, BR-RS, 2014.

1. Transplante de pulmão. 2. Aspergilose pulmonar. 3. Tomografia computadorizada. I. Severo, Luiz Carlos, orient. II. Hochhegger, Bruno, coorient. III. Título.

Elaborada pelo Sistema de Geração Automática de Ficha Catalográfica da UFRGS com os dados fornecidos pelo(a) autor(a).

Fernando Ferreira Gazzoni

Achados na tomografia computadorizada de alta resolução da aspergilose pulmonar em pacientes transplantados de pulmão

Tese apresentada ao Programa de Pós-graduação em Ciências Pneumológicas da Universidade Federal do Rio Grande do Sul, como requisito parcial à obtenção do título de Doutor em Ciências (área do conhecimento: Ciências pneumológicas).

Porto Alegre, agosto de 2014.

A Comissão Examinadora, abaixo assinada, aprova a Tese “Achados na tomografia computadorizada de alta resolução da aspergilose pulmonar em pacientes transplantados de pulmão”, elaborada por Fernando Ferreira Gazzoni, como requisito parcial para a obtenção do título de Doutor em Ciências Pneumológicas.

Comissão Examinadora:

Prof. Dr. José da Silva Moreira

Prof. Dr. Luciano Zubaran Goldani

Prof. Dr. Sydnei Hartz Alves

Prof. Dr. Luiz Carlos Severo - Orientador

Agradecimentos

Gostaria de agradecer ao Prof. Dr. Luiz Carlos Severo, pela oportunidade de fazer parte de seu grupo de pesquisa, por todos os ensinamentos na área de micologia, entusiasmo pela pesquisa científica, disponibilidade e incentivo para a realização deste trabalho desde a primeira reunião.

Ao co-orientador Prof. Dr. Bruno Hochheger pela sua dedicação, conhecimento, auxílio, incentivo e pelos trabalhos realizados juntos nesta caminhada acadêmica.

Ao Grupo de Transplante Pulmonar e ao Laboratório de Micologia da Irmandade Santa Casa de Misericórdia de Porto Alegre.

Ao Flávio de Mattos Oliveira pela sua disponibilidade e colaboração na realização deste trabalho.

Agradeço aos meus pais e irmãos, que sempre estimularam minhas iniciativas, pelo esforço dedicado, apoio e confiança.

À minha esposa Simone, que esteve ao meu lado durante o desenvolvimento dessa tese, e por tudo que significa para mim, me incentivando e dando apoio nas mais diferentes situações com bons conselhos e paciência.

Enfim, a todos que de alguma maneira colaboraram para que este trabalho fosse concretizado.

MUITO OBRIGADO

**“A ciência será sempre uma busca, jamais uma descoberta. É uma viagem, nunca
uma chegada.”**

Karl Popper

Resumo

GAZZONI, Fernando Ferreira. Achados na tomografia computadorizada de alta resolução da aspergilose pulmonar em pacientes transplantados de pulmão. 2014. 144f. Tese (Doutorado) – Programa de Pós-Graduação em Ciências Pneumológicas. Universidade Federal do Rio Grande do Sul. Porto Alegre.

O objetivo deste estudo foi avaliar os achados na tomografia computadorizada de alta resolução (TCAR) de pacientes transplantados de pulmão diagnosticados com infecção pulmonar por *Aspergillus*. Foram revisados retrospectivamente os exames de TCAR de 23 pacientes diagnosticados com aspergilose. Os exames de imagem foram realizados entre 2-5 dias após o início dos sintomas. A amostra de pacientes incluiu 12 homens e 11 mulheres com idades entre 22-59 anos (idade média: 43,6 anos). Todos os pacientes apresentaram taquipnéia, dispnéia e tosse. O diagnóstico foi estabelecido com o ensaio imunoenzimático (Platelia *Aspergillus*) para a detecção do antígeno galactomanana no lavado broncoalveolar e recuperação dos sintomas e dos achados de TCAR após tratamento com voriconazol. As TCAR foram analisadas independentemente por dois observadores que chegaram a uma decisão em consenso. O principal padrão na TCAR encontrado foi o de nódulos centrolobulares com padrão de árvore-em-brotamento associados com espessamento de paredes brônquicas que foi visualizado em 65% (n=15) dos pacientes. Este padrão foi descrito em associação com áreas de consolidação e opacidades em vidro-fosco em 13% (n=3) dos pacientes. Consolidação e opacidades em vidro-fosco foi o padrão principal em 22% (n=5) dos pacientes. O padrão de nódulos grandes com e sem o sinal do halo foi observado em 13% (n=3) dos pacientes e, em um caso, esteve associado com consolidação e opacidades em vidro-fosco. Conclui-se que os achados predominantes na TCAR em pacientes transplantados de pulmão com aspergilose foram espessamento de paredes

brônquicas e opacidades centrolobulares com padrão de árvore-em-brotamento bilateralmente. Além disso, opacidades em vidro-fosco e / ou áreas de consolidação bilaterais foram achados comuns. Os nódulos com o sinal do halo foram encontrados em apenas 13% dos pacientes.

Palavras-chave: Transplante de pulmão. Aspergilose pulmonar. Tomografia computadorizada.

Abstract:

GAZZONI, Fernando Ferreira. Achados na tomografia computadorizada de alta resolução da aspergilose pulmonar em pacientes transplantados de pulmão. 2014. 144f. Tese (Doutorado) – Programa de Pós-Graduação em Ciências Pneumológicas. Universidade Federal do Rio Grande do Sul. Porto Alegre.

The aim of this study was to assess high-resolution computed tomographic (HRCT) findings at presentation in lung transplant patients diagnosed with pulmonary *Aspergillus* infection. We retrospectively reviewed HRCT findings from 23 patients diagnosed with pulmonary aspergillosis. Imaging studies were performed 2–5 days after the onset of symptoms. The patient sample comprised 12 men and 11 women aged 22–59 years (mean age, 43.6 years). All patients had dyspnea, tachypnea, and cough. Diagnoses were established with Platelia *Aspergillus* enzyme immunoassays for galactomannan antigen detection in bronchoalveolar lavage and recovery of symptoms, and HRCT findings after voriconazole treatment. The HRCT scans were reviewed independently by two observers who reached a consensus decision. The main HRCT pattern, found in 65% (n = 15) of patients, was centrilobular tree-in-bud nodules associated with bronchial thickening. This pattern was described in association with areas of consolidation and ground-glass opacities in 13% (n = 3) of patients. Consolidation and ground-glass opacities were the main pattern in 22% (n = 5) of patients. The pattern of large nodules with and without the halo sign was observed in 13% (n = 3) of patients, and were associated with consolidation and ground-glass opacities in one case. In conclusion, the predominant HRCT findings in lung transplant patients with pulmonary aspergillosis were bilateral bronchial wall thickening and centrilobular opacities with the tree-in-bud pattern. Ground-glass opacities and/or

bilateral areas of consolidation were also common findings. Pulmonary nodules with the halo sign were found in only 13% of patients.

Keywords: Lung transplantation. Pulmonary aspergillosis. Computed tomography.

Lista de Figuras

Figura 1	Bolas fúngicas bilaterais em paciente masculino de 78 anos, com sequela de tuberculose, história de tosse há nove meses e episódio de hemoptise há um dia. A TC com janela de pulmão (a) e de mediastino (b) demonstrou cavidades de paredes espessas contendo massas com densidade de partes moles compatíveis com bolas fúngicas nos lobos superiores. A TC obtida com o paciente em decúbito ventral (c) evidenciou a mobilidade dos aspergilomas.....	2
Figura 2	Paciente feminina, 39 anos, asmática, com quadro de pneumonias de repetição, apresentando tosse, febre e expectoração com melhora clínica transitória após antibioticoterapia. TC com janela de pulmão (a) e de mediastino (b) demonstrou opacidades tubulares com distribuição brônquica e atenuação aumentada no lobo inferior direito, relacionadas à bronquiectasias com impactação mucóide decorrentes de aspergilose broncopulmonar alérgica.....	4
Figura 3	Aspergilose semi-invasiva em paciente masculino, 35 anos, com AIDS, apresentando febre, dispnéia, tosse e episódios recorrentes de hemoptise. A TC demonstrou espessamento de paredes brônquicas e consolidações com escavação nos lobos superior e inferior à direita.....	6
Figura 4	Aspergilose invasiva de vias aéreas em paciente de 45 anos, transplantado bilateral de pulmão, com febre, dispnéia e tosse. A TC demonstrou espessamento de paredes brônquicas e opacidades centrolobulares ramificadas com padrão de árvore-em-brotamento.....	8
Figura 5	Aspergilose angioinvasiva em paciente de 44 anos, submetido a transplante de medula óssea. A TC demonstrou múltiplas lesões nodulares, algumas com halo de atenuação em vidro fosco (sinal do halo), e consolidações de base pleural.....	10
Artigo 4.1	High-resolution computed tomographic findings of <i>Aspergillus</i> infection in lung transplant patients	
Figura 1	High-resolution computed tomography patterns.....	33
Figura 2	A 45 year-old unilateral right-lung transplantation recipient with dyspnea. A and B, Axial CT scans shows centrilobular nodules with the tree-in-bud pattern in the right lower lobe.....	34

Figura 3	A 56 year-old unilateral left-lung transplantation recipient with dyspnea and fever. Axial CT scans shows area of consolidation (A) and ground-glass opacities (B) in the left lower lobe.....	35
Figura 4	A 49 year-old bilateral lung transplantation recipient with dyspnea. A and B, Axial CT scans shows pulmonary nodules with the halo sign in the right lower lobe.....	36
Artigo 9.1	Letter to the editor: <i>Aspergillus fumigatus</i> fungus ball in the native lung after single lung transplantation	
Figura 1	Axial HRCT scans. In A, cavitory lung lesion in the left upper lobe filled with an opacity resembling a fungus ball (arrow). In B, a scan after moving the patient from the supine position to the prone position, demonstrating the motility of the mass (arrow).....	57
Artigo 9.2	Pulmonary diseases with imaging findings mimicking aspergilloma	
Figura 1	A 78-year-old man presented with a 9-month history of cough and one episode of hemoptysis in the last day. He denied any history of fever or night sweats. His medical history included a reported 70-pack-year smoking habit and treatment for pulmonary tuberculosis 45 years previous. Axial computed tomographic (CT) images obtained in the pulmonary (a) and mediastinal (b) windows show thick-walled cavities containing fungus balls in the upper lobes of the lungs. An axial CT image obtained with the patient in the prone position (c) shows changes in the positions of the aspergillomas.....	77
Figura 2	A 75-year-old man presented with a 3-month history of cough and one episode of hemoptysis in the last week. He denied any history of fever or night sweats. His medical history included a reported 60-pack-year smoking habit and treatment for pulmonary tuberculosis 30 years previously. (a) Magnetic resonance image (axial T1-weighted sequence) shows a thick-walled cavity containing a mildly hyperintense mass with the air crescent sign. (b) Magnetic resonance image (axial T1-weighted sequence) obtained with the patient in the prone position shows mobility of the fungus ball. (c) Photomicrograph of the surgical specimen shows a tangle of septate, dichotomously branching hyphae compatible with <i>Aspergillus</i> (Grocott-Gomori, x20).....	78

Figura 3	A 65-year-old man presented with productive cough. He denied any history of fever or night sweats. His medical history included a reported 45-pack-year smoking habit. (a) Axial computed tomographic image obtained in the pulmonary window shows a large cavity margined by pleural thickening containing a mass in the left upper lobe of the lung. (b) Microscopic examination showed yeast cells of <i>Coccidioides</i> in smear (Grocott, x250).....	79
Figura 4	A 54-year-old man presented with a 3-month history of cough. He denied any history of fever or night sweats. His medical history included a reported 40-pack-year smoking habit, diabetes, and treatment for pulmonary tuberculosis 35 years previously. (a) Axial computed tomographic image obtained in the pulmonary window shows a thick-walled cavity containing a mass with the air crescent sign in the left upper lobe of the lung. (b) Microscopic examination of biopsy specimens showed yeast cells of <i>Actinomyces</i> in smear (Gram, x250).....	80
Figura 5	A 33-year-old man presented with a 3-month history of right chest pain. He denied any history of fever or night sweats. His medical history included bronchiectasis. Axial computed tomographic images obtained in the pulmonary (a) and mediastinal (b) windows show a thin-walled cavity containing a mass with the air crescent sign in the lingula. Microscopic examination (c) of the surgical specimen confirmed the diagnosis of nocardiosis; showed weak acid-fast and Gram-positive organisms (right Ziehl-Neelsen; left Gram, x100).....	81
Figura 6	A 49-year-old woman presented with chronic cough. She denied any history of fever or night sweats. Her medical history included a reported 25-pack-year smoking habit. (a) Axial computed tomographic (CT) image shows a thin-walled cavity containing a mass with the air crescent sign in the right lower lobe of the lung. (b) A reconstructed sagittal CT image shows that the cavity is characterized by cystic bronchiectasis with a fungus ball. Microscopic examination of the surgical specimen led to the diagnosis of <i>Candida norvegensis</i> infection.....	82
Figura 7	A 79-year-old man presented with active hemoptysis. He had a history of low-grade fever and night sweats. His medical history included a reported 60-pack-year smoking habit and previous treatment for pulmonary tuberculosis. Axial (a) and coronal (b) computed tomographic images show a cavitated pulmonary mass with	

	irregular thick walls and the air crescent sign, associated with centrilobular tree-in-bud nodules in the right upper lobe of the lung. The patient underwent surgery to treat hemoptysis, which allowed confirmation of the diagnosis of <i>Mycobacterium tuberculosis</i> infection and intracavitary hematoma.....	83
Figura 8	A 63-year-old male kidney transplant recipient presented with a 1-month history of cough. His medical history included a reported 30-pack-year smoking habit and previous treatment for pulmonary tuberculosis. Axial computed tomographic (CT) images obtained in the pulmonary (a) and mediastinal (b) windows and a reconstructed coronal CT image (c) show a cavitated pulmonary mass with irregular thick walls and the air crescent sign in the left upper lobe of the lung. The patient underwent surgery and the diagnosis of scarring associated with lepidic growth adenocarcinoma was confirmed.....	84
Figura 9	A 48-year-old woman presented with chronic cough. She denied any history of fever or night sweats. Her medical history included a reported 25-pack-year smoking habit. Axial computed tomographic (CT) images obtained in the pulmonary (a) and mediastinal (b) windows and a reconstructed coronal CT image (c) show scarring in the right upper lobe and a thick-walled cavity containing a mass surrounded by gas (air crescent sign). The patient underwent surgery and the diagnosis of a fungus ball due to <i>Pseudallescheria boydii</i> was confirmed.....	85
Figura 10	A 28-year-old man presented with acute and productive cough, followed by the expectoration of clear fluid. He denied any history of fever or night sweats. Axial computed tomographic images obtained in the pulmonary (a) and mediastinal (b) windows show a cavitated pulmonary mass with irregular thick walls and the air crescent sign. The solid component represents the detached, crumpled endocyst. The patient underwent surgery and the diagnosis of hydatid cyst was confirmed.....	86
Artigo 9.3	Fungal diseases mimicking primary lung cancer: radiologic-pathologic correlation	
Figura 1	A 75-year-old man from Latin America who presented with a 3-month history of anorexia and weight loss. He also complained of haemoptysis associated with a non-productive cough. He denied any history of fever or night sweats. His medical history included a 60-pack-year smoking habit. (a) Axial computed tomography (CT) image shows a spiculated pulmonary mass associated with pleural effusion in	

	the right lower lobe, suggesting lung cancer. (b) CT image with sagittal reconstruction demonstrates the same findings. (c) Axial T2-weighted magnetic resonance image shows the pulmonary mass and septated pleural effusion. (d) Biopsy specimens contained predominantly non-caseating granulomas; intracellular and extracellular fungal elements compatible with budding forms of <i>Paracoccidioides brasiliensis</i> (Grocott, x400). (e) Axial T1-weighted magnetic resonance image shows regression of the pulmonary mass and pleural effusion 6 months after treatment (amphotericin B and itraconazole).....	111
Figura 2	An asymptomatic 65-year-old man who underwent evaluation of a pulmonary nodule newly detected on a chest X-ray. He denied any history of fever or night sweats. His medical history included a 45-pack-year smoking habit. (a) Axial computed tomography (CT) image shows a spiculated pulmonary nodule associated with adjacent bullous emphysema in the left upper lobe, suggesting lung cancer. (b) CT image with coronal reconstruction demonstrates the same findings. (c) Microscopic examination of transthoracic needle biopsy specimens showed yeast cells of <i>Histoplasma capsulatum</i> in smear. The fungal walls are black and organisms are small, uninucleate and spherical to ovoid; they have single buds and are often clustered. (Grocott, x 250).....	112
Figura 3	An asymptomatic 44-year-old man who underwent evaluation of a pulmonary nodule. He denied any history of fever or night sweats. His medical history included a 75-pack-year smoking habit. (a) A positron emission tomography (PET)/computed tomography (CT) image with coronal reconstruction demonstrates a spiculated pulmonary nodule with high uptake [standardised uptake value (SUV) = 5.5]. (b) PET/CT image with coronal reconstruction demonstrates hilar and subcarinal lymph nodes with high uptake (SUV = 8.5). (c) Microscopic examination of mediastinoscopic biopsy specimens showed yeast cells of <i>Histoplasma capsulatum</i> in smear. (Grocott, x250).....	113
Figura 4	A 53-year-old man who presented with a 3-month history of right chest pain. He denied any history of fever or night sweats. His medical history included a 33-pack-year smoking habit. (a) Axial computed tomography (CT) image shows a spiculated pulmonary mass in the right upper lobe with pleural contact, suggesting lung cancer. (b) CT image with sagittal reconstruction demonstrates the same findings. (c) Microscopic examination of transthoracic needle biopsy specimens showed yeast	

	cells of <i>Cryptococcus neoformans</i> in smear; fungal cell wall is stained in black (Grocott, x250). (d) A CT image shows regression of the pulmonary mass 7 months after treatment (fluconazole).....	114
Figura 5	An asymptomatic 49-year-old woman underwent evaluation of a pulmonary nodule discovered on a chest X-ray. She denied any history of fever or night sweats. Her medical history included a 25-pack-year smoking habit. (a) Axial computed tomography (CT) image shows a lobulated pulmonary nodule in the right upper lobe, suggesting lung cancer. (b) Microscopic examination of transthoracic needle biopsy specimens showed yeast cells of <i>Coccidioides immitis</i> (spherules in black) in smear (Grocott, x250). (c) CT image shows regression of the pulmonary nodule 3 months after treatment (itraconazole).....	115
Figura 6	A 77-year-old man who presented with a 3-month history of bloody sputum. He denied any history of fever or night sweats. His medical history included a 60-pack-year smoking habit and previous treatment of pulmonary tuberculosis. (a) Axial computed tomography (CT) image shows a cavitated pulmonary mass with irregular thick walls, suggesting lung cancer. The patient underwent surgery, which confirmed the diagnosis of cavitary colonisation by <i>Aspergillus fumigatus</i> . (b) Tissue sections contained narrow, tubular and regularly septate hyphae compatible with <i>Aspergillus fumigatus</i> (Grocott, x100). Branching is regular, progressive and dichotomous; hyphal branches tend to arise at acute angles from parent hyphae.....	116
Figura 7	A 45-year-old male kidney transplant recipient presented with a 15-day history of bloody sputum and night sweats. His medical history included a 30-pack-year smoking habit. (a) Axial computed tomography (CT) image shows a cavitated pulmonary mass with irregular thick walls. No centrilobular lesion suggesting the bronchogenic spread of a possible granulomatous infection is present. (b) CT image with coronal reconstruction demonstrates similar findings. Microscopic examination of a bronchoalveolar lavage specimen yielded findings compatible with mucormycosis. The lesion progressed despite appropriate treatment with antimycotic drugs, and the patient died 15 days after initiation of treatment. Within this context of immunosuppression, the possibility of invasive fungal infection should be favoured over lung cancer. Early diagnosis is of utmost importance in such cases.....	117

<p>Figura 8</p>	<p>An asymptomatic 59-year-old man who had undergone surgery for oesophageal cancer. He denied any history of fever or night sweats. His medical history included a 35-pack-year smoking habit. (a) Axial computed tomography (CT) image shows a new spiculated pulmonary nodule in the left upper lobe, suspicious for lung cancer or metastasis. (b) Axial positron emission tomography (PET)/CT image demonstrates high fluorodeoxyglucose uptake (standardized uptake value = 6.5) by the speculated pulmonary nodule. (c) Microscopic examination of transthoracic needle biopsy specimens showed that the pulmonary parenchyma had been replaced by necrotizing granulomatous inflammation (haematoxylin and eosin, x20). (d) Gomori methenamine silver histochemical staining showed yeast with broad-based budding typical of North American blastomycosis (x60).....</p>	<p>118</p>
-----------------	---	------------

Lista de Tabelas

Artigo 4.1	High-resolution computed tomographic findings of <i>Aspergillus</i> infection in lung transplant patients	
Tabela 1	Features of lung transplantation recipients with pulmonary aspergillosis.....	37
Artigo 9.2	Pulmonary diseases with imaging findings mimicking aspergilloma	
Tabela 1	Pulmonary diseases with imaging findings mimicking aspergilloma.....	87
Artigo 9.3	Fungal diseases mimicking primary lung cancer: radiologic-pathologic correlation	
Tabela 1	Classical features in fungal diseases that assist in differential diagnosis with lung cancer.....	119

Lista de abreviaturas e siglas

A. flavus – *Aspergillus flavus*

A. fumigatus – *Aspergillus fumigatus*

A. niger - *Aspergillus niger*

AIDS - Acquired immunodeficiency syndrome

Cm - Centímetro

DPOC- Doença pulmonar obstrutiva crônica

GM- Galactomanana

HIV - Vírus da imunodeficiência humana

ISCMPA - Irmandade Santa Casa de Misericórdia de Porto Alegre

LBA - Lavado bronco-alveolar

MIP - Maximum intensively projection

PCR- Reação em cadeia da Polimerase

RX- Raio-X

TC – Tomografia computadorizada

TCAR - Tomografia computadorizada de alta resolução

µm - Micrômetro

Sumário

Agradecimentos.....	IV
Resumo.....	VI
Abstract.....	VIII
Lista de Figuras.....	X
Lista de Tabelas.....	XVII
Lista de abreviaturas e siglas.....	XVIII
1. Introdução.....	1
2. Objetivos.....	15
2.1. Objetivo geral.....	15
2.2. Objetivo específico.....	15
3. Metodologia.....	16
4. Resultados.....	20
Artigo 4.1: High-resolution computed tomographic findings of <i>Aspergillus</i> infection in lung transplant patients.....	20
5. Discussão.....	38
6. Conclusões.....	42
7. Perspectivas.....	43
8. Referências.....	44
9. Anexos (artigos publicados em periódicos durante o doutorado).....	51
Artigo 9.1: Letter to the editor: <i>Aspergillus fumigatus</i> fungus ball in the native lung after single lung transplantation.....	52
Artigo 9.2: Pulmonary diseases with imaging findings mimicking aspergilloma.....	58
Artigo 9.3: Fungal diseases mimicking primary lung cancer: radiologic-pathologic correlation.....	88

1. Introdução:

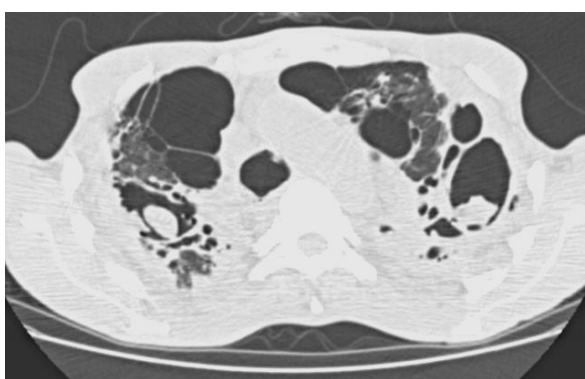
Aspergillus é um gênero de fungos filamentosos e ubíquos no ambiente, particularmente no solo, poeira e vegetação em decomposição. As espécies que mais comumente causam infecção em humanos são *A. fumigatus*, *A. flavus* e *A. niger*, especialmente a primeira citada (1,2). Ao exame dos espécimes de tecido, as suas hifas aparecem caracteristicamente como elementos septados, uniformes e tubulares, com ramificação regular, progressiva e dicotômica, em ângulo agudo, geralmente de 45 graus (1,2).

A aspergilose pulmonar compreende um espectro clínico variável de comprometimento. As manifestações desta doença são determinadas pelo número e virulência dos organismos, resposta imune do paciente e presença de doença pulmonar estrutural (1,2,3). O seu espectro pode ser dividido em cinco categorias: saprobiota (bola fúngica ou aspergiloma), reação de hipersensibilidade (aspergilose broncopulmonar alérgica), semi-invasiva, invasiva das vias aéreas e angioinvasiva (2,3).

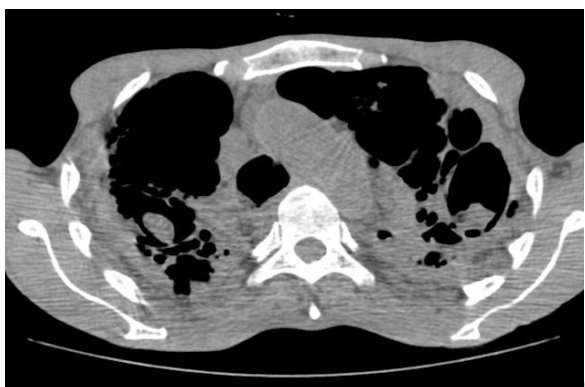
Na forma saprobiota, bola fúngica ou aspergiloma não há invasão tecidual. A bola fúngica consiste de um conglomerado entrelaçado de hifas, muco, fibrina e debris celulares, que coloniza uma cavidade pulmonar pré-existente ou brônquio ectásico. Pacientes com doença pulmonar cavitária, bolhosa ou cística, geralmente resultante de tuberculose, sarcoidose ou enfisema apresentam um maior risco de desenvolver aspergiloma (2,4). Embora os pacientes possam permanecer assintomáticos, eles comumente apresentam tosse produtiva crônica ou hemoptise, que pode ser fatal. Espessamento pleural pode ser o sinal mais precoce nas radiografias de tórax, precedendo as alterações visíveis na cavidade envolvida (3,5). Na tomografia computadorizada (TC), classicamente a cavidade contém uma massa sólida arredondada

com densidade de partes moles, que se movimenta com a mudança de decúbito (Figura 1).

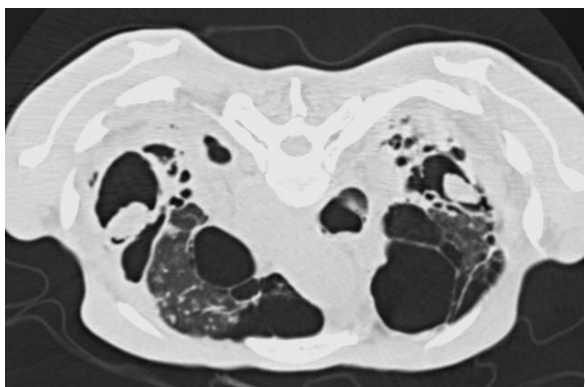
Figura 1 - Bolas fúngicas bilaterais em paciente masculino de 78 anos, com sequela de tuberculose, história de tosse há nove meses e episódio de hemoptise há um dia. A TC com janela de pulmão (a) e de mediastino (b) demonstrou cavidades de paredes espessas contendo massas com densidade de partes moles compatíveis com bolas fúngicas nos lobos superiores. A TC obtida com o paciente em decúbito ventral (c) evidenciou a mobilidade dos aspergilomas.



(a)



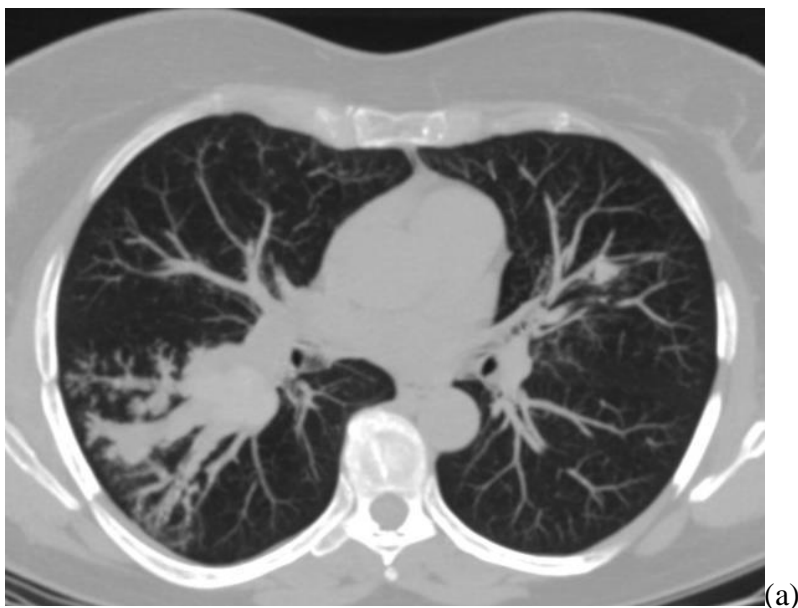
(b)



(c)

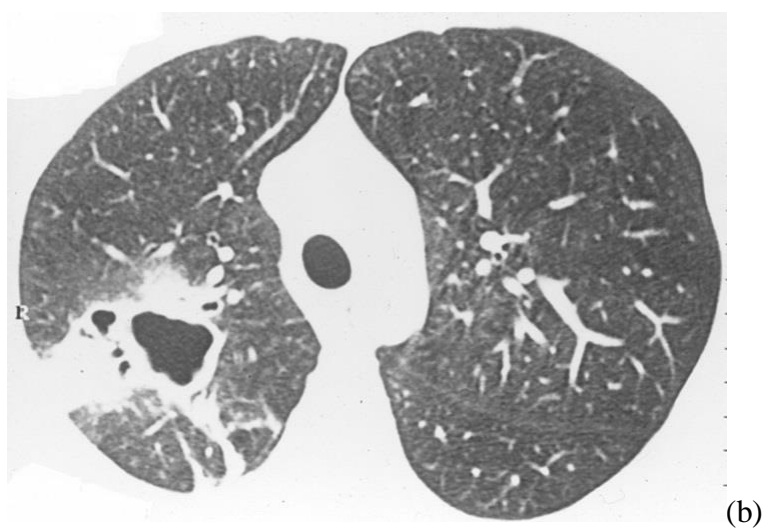
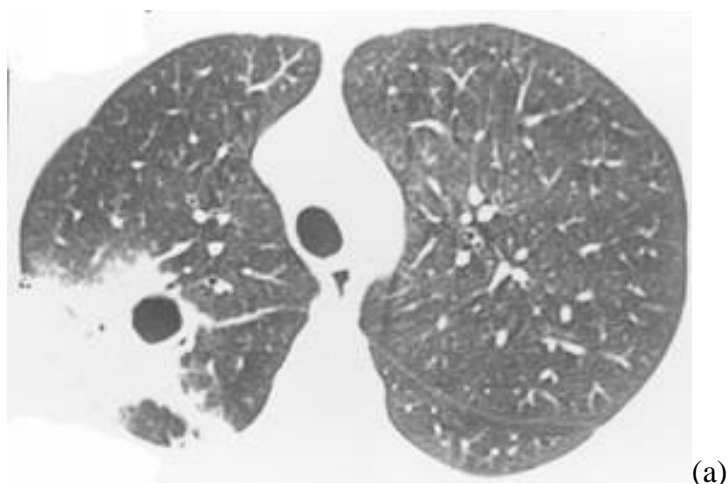
A reação de hipersensibilidade ou aspergilose broncopulmonar alérgica acomete geralmente pacientes asmáticos de longa data (3,6). Ela é causada por uma reação complexa de hipersensibilidade aos organismos, incluindo as do tipo I e III, sendo que os pacientes geralmente apresentam eosinofilia. Na análise patológica esta forma é caracterizada por plugs de muco com *Aspergillus* e eosinófilos. Isto resulta em dilatação brônquica, tipicamente envolvendo brônquios segmentares e subsegmentares. As manifestações clínicas incluem mal estar, febre baixa, tosse produtiva, dor torácica e pneumonias recorrentes. As alterações radiológicas incluem opacidades tubulares, tipo “dedo-de-luva”, com distribuição brônquica, usualmente predominando nos lobos superiores, que representam impactação mucóide e bronquiectasias. Na TC estas opacidades podem apresentar alta densidade (3,5,6) (Figura 2).

Figura 2 - Paciente feminina, 39 anos, asmática, com quadro de pneumonias de repetição, apresentando tosse, febre e expectoração com melhora clínica transitória após antibioticoterapia. TC com janela de pulmão (a) e de mediastino (b) demonstrou opacidades tubulares com distribuição brônquica e atenuação aumentada no lobo inferior direito, relacionadas à bronquiectasias com impactação mucóide decorrentes de aspergilose broncopulmonar alérgica.



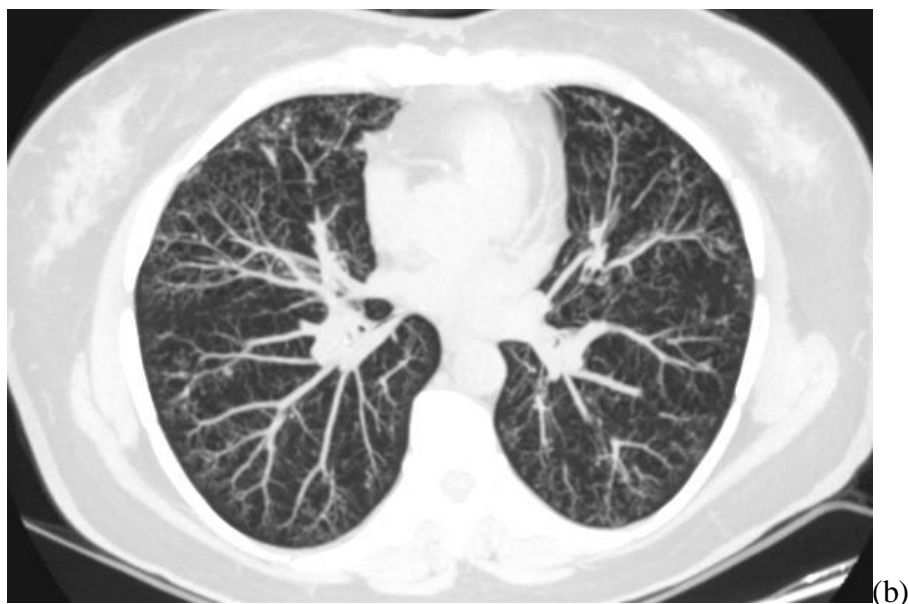
A apresentação semi-invasiva ou necrosante crônica não é usual, sendo caracterizada por necrose tecidual e inflamação granulomatosa, geralmente em pacientes moderadamente imunossuprimidos e com comorbidades (3). Histologicamente existe invasão da mucosa traqueobrônquica sem extensão ao parênquima. Esta forma assemelha-se a outras doenças pulmonares crônicas como reativação de tuberculose, actinomicose e histoplasmose. Os fatores predisponentes incluem AIDS, diabetes mellitus, leucemia, transplante de pulmão, desnutrição, alcoolismo, idade avançada, terapia prolongada com corticóide e doença pulmonar obstrutiva crônica (DPOC). As manifestações clínicas são insidiosas, caracterizadas por tosse crônica, escarro, febre e sintomas constitucionais. Assim como nas formas mais invasivas das infecções fúngicas, o grau de imunossupressão provavelmente é o fator mais importante levando a invasão da parede brônquica. As alterações radiológicas são variadas e incluem espessamento de paredes brônquicas, múltiplas opacidades nodulares, consolidações segmentares uni ou bilaterais, com ou sem cavitação ou espessamento pleural (Figura3). Estas áreas são persistentes e podem progredir vagarosamente durante meses (7,8).

Figura 3 - Aspergilose semi-invasiva em paciente masculino, 35 anos, com AIDS, apresentando febre, dispnéia, tosse e episódios recorrentes de hemoptise. A TC demonstrou espessamento de paredes brônquicas e consolidações com escavação nos lobos superior e inferior à direita.



A infecção invasiva das vias aéreas ocorre mais comumente em pacientes imunocomprometidos, especialmente nos casos de malignidades hematológicas, transplante de órgãos sólidos ou de células tronco hematopoiéticas, e corticoterapia prolongada. Caracteriza-se, na histologia, pela presença de *Aspergillus* abaixo da membrana basal da via aérea e imediatamente adjacente ao parênquima pulmonar, tipicamente associado com reação inflamatória neutrofílica. As manifestações clínicas incluem traqueobronquite, bronquiolite e broncopneumonia. Pacientes com traqueobronquite geralmente tem achados radiológicos normais ou eventualmente espessamento de paredes brônquicas. A broncopneumonia resulta em áreas de consolidação peribrônquicas (3,9). A bronquiolite manifesta-se na tomografia computadorizada de alta resolução (TCAR) pela presença de nódulos centrolobulares, ramificados com padrão de árvore-em-brotamento (Figura 4). Este achado pode ser encontrado em outras condições, incluindo disseminação endobrônquica de tuberculose, pneumonias virais e por micoplasma, dentre outras possibilidades (5,10).

Figura 4 - Aspergilose invasiva de vias aéreas em paciente de 45 anos, transplantado bilateral de pulmão, com febre, dispnéia e tosse. A TC demonstrou espessamento de paredes brônquicas e opacidades centrolobulares ramificadas com padrão de árvore-em-brotamento.

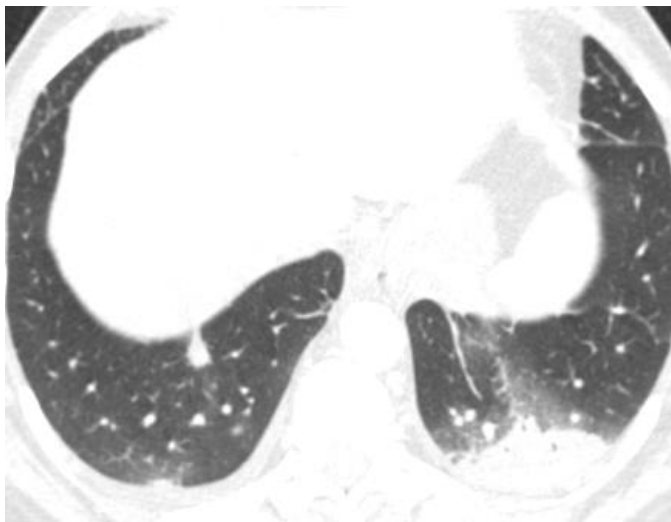


A doença angioinvasiva acontece geralmente em pacientes imunodeprimidos com importante neutropenia. Exemplos: quimioterapia intensiva para neoplasias hematológicas como linfoma e leucemia, regimes imunossupressores para doenças auto-imunes, e em casos de transplante de órgãos, especialmente medula óssea (3). Na histologia é caracterizada por invasão e oclusão de artérias pulmonares de pequeno e médio porte por hifas, o que leva a formação de nódulos necrótico-hemorrágicos e infartos hemorrágicos com base pleural (11). O diagnóstico clínico muitas vezes é retardado e a mortalidade é alta. Os achados tomográficos característicos incluem nódulos envoltos por um halo com atenuação em vidro-fosco (sinal do halo), nódulos mal definidos, cavidades, áreas de consolidação em cunha com base pleural, e opacidades com atenuação em vidro-fosco (12,13,14) (Figura 5). Em pacientes imunodeprimidos o sinal do halo é sugestivo de aspergilose angioinvasiva. No entanto, já foi descrito em uma variedade de outras situações como infecções por *Candida*, *Mucorales*, herpes simplex e citomegalovírus, granulomatose de Wegener, dentre outras (15). Na fase de convalescença, duas a três semanas após o início do tratamento, pode ocorrer o sinal do crescente, traduzindo a separação dos fragmentos necróticos do parênquima adjacente, o que resulta em crescentes de ar (12,13,14).

Figura 5 - Aspergilose angioinvasiva em paciente de 44 anos, submetido a transplante de medula óssea. A TC demonstrou múltiplas lesões nodulares, algumas com halo de atenuação em vidro fosco, o sinal do halo (a), e consolidações de base pleural (b).



(a)



(b)

O transplante de pulmão é uma importante estratégia terapêutica para muitas doenças pulmonares em fase terminal. No entanto, a sobrevida a longo prazo ainda é relativamente limitada em comparação com outros transplantes de órgãos sólidos. A complicação mais comum após o transplante é infecção, que se constitui na maior causa de mortalidade perioperatória e na segunda causa mais comum de mortalidade tardia (16,17). As infecções bacterianas predominam nas primeiras quatro semanas após o transplante, refletindo colonização do pulmão nativo ou evento perioperatório; enquanto que as infecções oportunistas virais aumentam em incidência após o primeiro mês, em decorrência dos regimes imunossupressores. As infecções fúngicas podem ocorrer em qualquer período após o transplante (17,18).

Dentre as doenças fúngicas que acometem os receptores de transplante pulmonar, a aspergilose permanece entre as infecções oportunistas mais prevalentes. É documentada em 6% a 8% de todos os receptores, a maioria dentro de 2-6 meses após o transplante (18-22). Sabe-se que os receptores de transplante pulmonar são suscetíveis à colonização das vias aéreas por *Aspergillus*, devido à comunicação direta do transplante pulmonar com o ambiente externo (17,23). Em transplantados de pulmão, a aspergilose invasiva pode ser precedida por colonização da via aérea. Exposição ambiental excessiva pode ocorrer tanto antes quanto após o transplante. Pacientes com exposição ambiental excessiva incluem fazendeiros, jardineiros, trabalhadores da construção civil e residentes em áreas rurais. Os portadores de fibrose cística tem taxas de colonização pré-transplante de até 63%. Pacientes com exposição nosocomial devido a construções em hospitais ou em outros locais também apresentam risco elevado (24). Pacientes com colonização da via aérea por *A. fumigatus* nos primeiros seis meses tem onze vezes mais chance de desenvolver doença invasiva do que aqueles não colonizados neste período (23). Outros fatores de risco incluem imunossupressão, depuração mucociliar

prejudicada, tosse diminuída devido à desnervação do pulmão, interrupção da drenagem linfática e lesões isquêmicas das vias aéreas. Doença por citomegalovírus é outro fator de risco conhecido, pois esta infecção pode contribuir para um estado mais profundo de imunossupressão (24,25,26).

As manifestações da aspergilose nos receptores de transplante pulmonar são variáveis dentro do seu espectro, desde colonização, infecção semi-invasiva, invasiva de vias aéreas até infecção angioinvasiva fulminante (17,23,24). As infecções por *Aspergillus* são responsáveis por 2 a 33% das infecções após transplante pulmonar e por 4 a 7% das mortes dos referidos transplantados (16).

Aspergilose acometendo as vias aéreas é vista em cerca de 5% dos pacientes após o transplante de pulmão, principalmente nos primeiros seis meses. Elas geralmente são assintomáticas nas fases iniciais e detectadas em broncoscopias de rotina. Pode haver sintomas como febre, tosse e hemoptise. As manifestações clínicas incluem traqueobronquite, bronquiolite e broncopneumonia. Dentre elas destaca-se, entre os receptores de pulmão, a traqueobronquite ulcerativa, que é predominantemente intraluminal com mínima invasão tecidual, e geralmente é oculta na radiografia de tórax. Na TCAR ocasionalmente pode-se identificar espessamento de paredes brônquicas ou da traquéia (3,19,27). Na broncoscopia visualizam-se lesões inflamatórias ulcerativas focais ou difusas, pseudomembranas e estenose de via aérea, comprometendo geralmente a região da anastomose (28).

Na aspergilose angioinvasiva clássica afetando indivíduos gravemente imunocomprometidos (por exemplo, neutropenia, transplante de medula óssea, etc) a tomografia computadorizada comumente revela os achados de doença angioinvasiva como nódulos mal definidos, opacidades cavitárias, consolidações em forma de cunha, nódulos com o sinal do halo e o sinal do crescente aéreo em fases finais (3,23).

Como acima relatado, sabe-se que infecções das vias aéreas por *Aspergillus* são entidades distintas da pneumonia angioinvasiva e que poderiam ocorrer desproporcionalmente em receptores de transplante de pulmão (28, 29). Dessa forma, os achados tomográficos clássicos da aspergilose pulmonar afetando indivíduos gravemente imunocomprometidos podem não se aplicar a pacientes transplantados de pulmão. Os fatores que diferenciam estes pacientes são os mecanismos de defesa local alterados pela interrupção cirúrgica do suprimento nervoso e da drenagem linfática, danos causados pela preservação e transporte do pulmão, isquemia no local da anastomose brônquica ou traqueal, administração de corticosteroides inalatórios e uso prolongado de ventilação mecânica. Outro fator relevante que está envolvido é o tipo de imunossupressão, pois são pacientes que geralmente não estão neutropênicos (30,31). No entanto, os escassos relatos dos achados da aspergilose pulmonar após transplante de pulmão incluem poucos pacientes que realizaram TC de tórax (23,30). Numa série de 30 pacientes, apenas sete realizaram TC, e todos (100%) mostraram nódulos mal definidos (30). Em outro estudo, com apenas oito casos, o padrão tomográfico mais comum entre pacientes com pneumonia por *Aspergillus* foi uma combinação de nódulos, consolidação e de opacidades em vidro-fosco, ocorrendo em cinco de oito pacientes (62,5%); o padrão de árvore-em-brotamento foi visto em apenas um paciente (12,5%), e dois (25%) pacientes tiveram nódulos com cavitação (23).

Foi relatado, ainda, que a avaliação associada dos achados da TC com os níveis séricos do antígeno galactomanana, liberado a partir da parede da célula durante o crescimento das hifas, auxilia a prever o resultado da terapia antifúngica empírica em pacientes submetidos a transplante alogênico de células tronco hematopoéticas (32). Por todos os motivos acima descritos, torna-se importante o estudo dos achados

tomográficos da aspergilose pulmonar no grupo específico de pacientes transplantados de pulmão.

2. Objetivos:

2.1. Objetivo geral:

O objetivo deste estudo é analisar os achados tomográficos de pacientes transplantados de pulmão diagnosticados com aspergilose pulmonar.

2.2. Objetivo específico:

Descrever os padrões predominantes na TCAR da aspergilose pulmonar em pacientes transplantados de pulmão.

3. Metodologia

Estudo retrospectivo, em que foi realizada revisão dos dados de todos os pacientes transplantados de pulmão na Irmandade Santa Casa de Misericórdia de Porto Alegre (ISCOMPA), que tiveram o diagnóstico de aspergilose pulmonar no período compreendido entre janeiro de 2007 e dezembro 2012.

O estudo foi aprovado pelo Comitê de Ética desta instituição e foi exclusivamente descritivo, não envolvendo a realização de qualquer intervenção terapêutica. Todas as informações clínico-epidemiológicas necessárias para o estudo foram obtidas através de revisão de prontuários, não havendo qualquer contato direto entre investigadores com os pacientes. A pesquisa teve interesse puramente científico com o compromisso de manutenção do anonimato dos sujeitos da pesquisa.

Critérios de inclusão:

- Doença respiratória aguda.
- Dispnéia, taquipnéia e tosse.
- Melhora dos sintomas e dos achados da TC após tratamento com terapia antifúngica;
- Valor >1.5 para o índice de densidade óptica no ensaio imunoenzimático Platelia *Aspergillus* para detecção do antígeno galactomanana no lavado bronco-alveolar (LBA). Este critério demonstrou especificidade de 90,4% na detecção de infecção por *Aspergillus*. (33). A galactomanana é um heteropolissacarídeo estável ao calor e liberado a partir da parede da célula. A molécula tem um núcleo manana não imunogênico com cadeias laterais apresentando unidades imunorreativas contendo unidades de galactofuranosil. Considerando que a

galactomanana é liberada predominantemente por hifas de *Aspergillus* durante o crescimento e, em menor grau pelos conídios, a sua detecção no LBA parece representar uma melhor evidência de aspergilose do que a cultura ou a reação em cadeia da polimerase (PCR). O teste disponível comercialmente (Platelia *Aspergillus*) detecta a galactomanana por utilização de anticorpos monoclonais de rato. Os resultados podem ser obtidos em 3 horas, o que é uma grande vantagem em comparação com os métodos de cultura. A galactomanana pode ser detectada em vários fluídos corporais, pois é um hidrato de carbono solúvel em água (34).

Critérios de exclusão:

Os pacientes diagnosticados com infecções virais concomitantes que potencialmente afetam o pulmão, incluindo citomegalovírus, com base em uma revisão de dados clínicos e laboratoriais, foram excluídos deste estudo.

Todos os pacientes incluídos no estudo foram considerados como tendo aspergilose invasiva comprovada ou provável, de acordo com os critérios propostos pela Organização Européia para Pesquisa e Tratamento do Câncer / Grupo de Estudo em Micoses, e conforme relatado previamente em receptores de transplante de pulmão (35).

Os exames de TCAR foram realizados em um tomógrafo de 64 detectores (LightSpeed VCT, GE Healthcare), com os seguintes parâmetros: 120 kVp, 250 mA, tempo, 0,8 segundos; pitch, 1,375. Os parâmetros técnicos incluíram aquisição volumétrica inspiratória com 1mm de colimação e 1mm de incremento usando um algoritmo de reconstrução espacial de alta-frequência. As imagens foram obtidas com

janelas para mediastino (largura 350-450HU, nível 20-40HU) e parênquima (largura 1200-1600HU; nível de -500 a-700HU). As reconstruções foram realizadas nos planos axial e coronal.

Os achados na TCAR foram classificados segundo os critérios definidos no Glossário da Sociedade Fleischner de Termos (36). As TCAR foram avaliadas quanto à presença e distribuição de nódulos, opacidades centrolobulares com padrão de árvore-em-brotamento, opacidades em vidro-fosco e consolidações. O nódulo foi definido como uma opacidade arredondada ou irregular, bem ou mal definido, medindo até 3,0 cm de diâmetro. Os nódulos foram divididos em pequenos nódulos (<10 mm de diâmetro), e nódulos grandes (> 10 mm de diâmetro). O sinal do halo é definido como um halo com atenuação em vidro-fosco que circunda um nódulo ou massa. O padrão de árvore-em-brotamento representa nódulos centrolobulares ramificados. Opacidades em vidro-fosco foram definidas como áreas nebulosas de opacidade aumentada ou atenuação sem obscurecimento dos vasos subjacentes. Consolidação foi definida como a opacificação homogênea do parênquima com obscurecimento dos vasos subjacentes. A distribuição das anormalidades foi classificada como focal (unilobar) e difusa (mais de um lobo pulmonar). A distribuição das anormalidades foi também estratificada quanto a sua localização nos lobos superiores, médio ou inferiores.

As tomografias foram avaliadas de forma independente em ordem aleatória por dois radiologistas com mais de 10 anos de experiência, sem o conhecimento de informações clínicas dos pacientes, exceto que todos os pacientes tiveram infecção por *Aspergillus*. Após análise dos dois radiologistas, as imagens foram analisadas em conjunto com um terceiro radiologista torácico, e os três radiologistas chegaram a uma decisão final em consenso. Em cada paciente, um ou dois padrões tomográficos predominantes foram definidos: 1.nódulos com padrão de árvore-em-

brotamento/espessamento de paredes brônquicas; 2.consolidação do espaço aéreo/opacidade em vidro-fosco; 3.nódulos grandes, com e sem o sinal do halo.

Os dados foram digitados no programa Excel e posteriormente exportados para SPSS (Statistical Package for the Social Sciences) v.15.0 para análise estatística. As variáveis quantitativas foram descritas em média, desvio padrão, mediana e variância. As variáveis qualitativas foram descritas como frequências absoluta e relativa.

4. Resultados:

4.1. Artigo completo publicado em periódico

HIGH-RESOLUTION COMPUTED TOMOGRAPHIC FINDINGS OF
ASPERGILLUS INFECTION IN LUNG TRANSPLANT PATIENTS

GAZZONI, F.F.; HOCHHEGGER, B.; SEVERO, L.C.; MARCHIORI, E.;
PASQUALOTTO, A.; SARTORI, A.P.G.; SCHIO, S.; CAMARGO, J.

European Journal of Radiology 2014; 83(1):79-83

História do artigo:

Submetido: 04 de Fevereiro de 2013

Aceito após revisão: 22 de Março de 2013

Abstract:

Objective: The aim of this study was to assess high-resolution computed tomographic (HRCT) findings at presentation in lung transplant patients diagnosed with pulmonary *Aspergillus* infection. **Materials and methods:** We retrospectively reviewed HRCT findings from 23 patients diagnosed with pulmonary aspergillosis. Imaging studies were performed 2–5 days after the onset of symptoms. The patient sample comprised 12 men and 11 women aged 22–59 years (mean age, 43.6 years). All patients had dyspnea, tachypnea, and cough. Diagnoses were established with Platelia *Aspergillus* enzyme immunoassays for galactomannan antigen detection in bronchoalveolar lavage and recovery of symptoms, and HRCT findings after voriconazole treatment. The HRCT scans were reviewed independently by two observers who reached a consensus decision. **Results:** The main HRCT pattern, found in 65% (n = 15) of patients, was centrilobular tree-in-bud nodules associated with bronchial thickening. This pattern was described in association with areas of consolidation and ground-glass opacities in 13% (n = 3) of patients. Consolidation and ground-glass opacities were the main pattern in 22% (n = 5) of patients. The pattern of large nodules with and without the halo sign was observed in 13% (n = 3) of patients, and were associated with consolidation and ground-glass opacities in one case. **Conclusion:** The predominant HRCT findings in lung transplant patients with pulmonary aspergillosis were bilateral bronchial wall thickening and centrilobular opacities with the tree-in-bud pattern. Ground-glass opacities and/or bilateral areas of consolidation were also common findings. Pulmonary nodules with the halo sign were found in only 13% of patients.

Keywords: Lung transplantation; Pulmonary aspergillosis; Computed tomography.

1. Introduction:

Lung transplantation is an important treatment modality for many end-stage lung diseases [1–3]. However, the long-term survival of patients undergoing lung transplantation remains relatively limited compared with survival rates in those receiving other solid organ transplants (SOTs) [1–3]. Infection is a significant problem and major cause of mortality after lung transplantation. *Aspergillus* infection, documented in 6–8% of all lung transplant recipients, is among the most significant opportunistic infections after lung transplantation [1–5].

In severely immunocompromised individuals with pulmonary aspergillosis, computed tomography (CT) commonly reveals a combination of poorly defined nodules, cavitary opacities, wedged-shaped pleural-based consolidation, ground-glass opacities, and nodules surrounded by a halo of ground-glass attenuation (“halo sign”) [6]. In the later stages of infection, an air crescent is frequently observed. The evaluation of CT findings in association with the results of serum galactomannan (GM) assays has been reported to help predict the outcome of empirical antifungal therapy in patients undergoing allogeneic hematopoietic stem-cell transplantation [6,7].

However, few reports have described the CT findings of aspergillosis in patients after lung transplantation [8,9]. The aim of this study was to assess high-resolution computed tomography (HRCT) findings at presentation in lung transplant patients diagnosed with pulmonary *Aspergillus* infection.

2. Materials and methods:

The study was approved by our institutional review board. This retrospective study reviewed data from all lung transplant recipients with pulmonary aspergillosis treated in two hospitals. The inclusion criteria for patients were: dyspnea, tachypnea, and cough; acute respiratory disease; recovery of symptoms and HRCT findings after exclusive treatment with antifungal therapy (oral voriconazole, 400 mg/day); and an index exceeding the cutoff value of 1.5 on a Platelia *Aspergillus* enzyme immunoassay (EIA) for GM antigen detection in bronchoalveolar lavage (BAL). The latter criterion has shown 90.4% specificity for the detection of *Aspergillus* infection [10]. Patients diagnosed with concomitant viral infections potentially affecting the lung, including cytomegalovirus, based on a review of clinical and laboratory data were excluded from this study.

The study sample comprised 23 patients (12 men, 11 women) with a mean age of 43.6 (range, 22–59) years who were diagnosed with *Aspergillus* infection and met the inclusion criteria. All patients were considered to have proven or probable invasive aspergillosis according to the criteria proposed by the European Organization for Research and Treatment of Cancer/Mycoses Study Group, and as previously reported in lung transplant recipients [11]. Isolated *Aspergillus* cultures from BAL and/or sputum were obtained from 12/23 patients. No patient showed eosinophilia in blood or BAL.

HRCT examinations were performed using a 64-multidetector scanner (LightSpeed VCT; GE Healthcare, Waukesha, WI, USA) with the following parameters: 120 kVp; 250 mA; time, 0.8 s; and pitch, 1.375. The technical parameters included inspiratory volumetric acquisition with 1 mm collimation at 1 mm increments using a high-spatial-frequency reconstruction algorithm. Images were obtained with mediastinal (width, 350–450 HU; level, 20–40 HU) and parenchymal (width, 1200-

1600 HU; level, -500 to -700 HU) window settings, and reconstructions were performed in the axial and coronal planes.

The HRCT scans were assessed according to criteria defined in the Fleischner Society's Glossary of Terms [12]. The presence and distribution of nodules, centrilobular opacities with the tree-in-bud pattern, ground-glass opacities, and consolidations were evaluated. A nodule was defined as a rounded or irregular opacity that was well or poorly defined and ≤ 3 cm in diameter. Nodules were classified as small (diameter < 10 mm) or large (diameter > 10 mm). The halo sign was defined as a CT finding of ground-glass opacity surrounding a nodule or mass. The tree-in-bud pattern refers to centrilobular branching structures that resemble a budding tree. Ground-glass opacities were defined as hazy areas of increased opacity or attenuation, with no obscuration of the underlying vessels. Consolidation was defined as homogeneous opacification of the parenchyma with obscuration of the underlying vessels. The distribution of abnormalities was categorized as focal (unilobar) or diffuse (more than one pulmonary lobe) and stratified using the categories of upper, middle, and lower lung lobes.

Two chest radiologists with more than 10 years of experience who were blinded to the patients' clinical information, except Aspergillus infection, independently assessed CT scans in random order. After the two radiologists had conducted independent analyses, the images were reviewed together with a third chest radiologist (with > 40 years of experience) to reach a final consensus decision. For each patient, reviewers identified one or two predominant CT patterns: tree-in-bud nodules/bronchial wall thickening; airspace consolidation/ground-glass opacity; and/or large nodules with and without the halo sign. We also evaluated white blood cell counts and correlated them with imaging findings.

3. Results:

3.1. Patients

Among the sample of 23 patients, 13 patients had undergone bilateral and 10 had undergone unilateral lung transplantation. The mean interval between lung transplantation and infection diagnosis was 7.4 (standard deviation, 1.7) months. The underlying lung diseases were emphysema (n = 5, 21%), idiopathic pulmonary fibrosis (n = 7, 30%), cystic fibrosis (n = 1, 4%), pneumoconiosis (n = 2, 8%), non-cystic fibrosis bronchiectasis (n = 4, 17%), retransplantation (n = 1, 4%), and lymphangioleiomyomatosis (n = 3, 12%).

3.2. HRCT patterns

The main HRCT pattern (Fig. 1), found in 65% (n = 15) of patients, was centrilobular tree-in-bud nodules associated with bronchial wall thickening (Fig. 2).

Consolidation and ground-glass opacities were observed in 22% (n = 5) of patients (Fig. 3). Centrilobular tree-in-bud nodules/ bronchial wall thickening was associated with areas of consolidation/ground-glass opacities in 13% (n = 3) of patients.

The pattern of large nodules with and without the halo sign was observed in 13% (n = 3) of patients (Fig. 4) and was associated with consolidation and ground-glass opacities in one case.

The mean white blood cell count was 6547 ± 1546 (cells/ μ L), and no correlation was observed between imaging findings and white blood cell counts. However, only one patient had neutropenia (498 cells/ μ L) and HRCT showed large nodules with the halo sign.

3.3. Distribution of abnormalities

Abnormalities were bilateral in 20 (87%) patients, among whom the lower lobes were affected in 17 patients and exclusively affected in 13 patients. All three patients with unilateral abnormalities had undergone unilateral transplantation, and abnormalities were described in the transplanted lung in two of these patients.

The results are summarized in Table 1.

4. Discussion:

Infection is the most common cause of perioperative mortality and the second most common cause of late (>90 days) mortality after lung transplantation [13]. Locally invasive or disseminated infection accounts for 2–33% of infections after lung transplantation and 4–7% of all deaths. Fungal infections can occur at any time after transplantation, and lung transplantation recipients are susceptible to *Aspergillus* airway colonization and invasive disease. *Aspergillus* organisms can cause indolent pneumonia or fulminant angioinvasive infection [9,13,14]. The spectrum of pulmonary aspergillosis includes aspergilloma and the allergic bronchopulmonary, semiinvasive (chronic necrotizing), airway-invasive, and angioinvasive forms of aspergillosis [15]. The increased risk for *Aspergillus* infection in lung transplantation patients is due to a complex set of factors, including immunosuppression, continuous contact with infectious organisms in the environment, impaired mucociliary clearance, diminished cough due to lung denervation, disruption of lymphatic drainage, and ischemic airway injury [14,16,17].

Aspergillus infections in the airway are seen in 5% of patients after lung transplantation, most commonly in the first 6 months. They are usually asymptomatic and are detected on surveillance bronchoscopy. Such infections may cause ulcerative

tracheobronchitis, usually with occult presentation on chest radiographs [18]. The most common pulmonary aspergillosis CT findings in severely immunocompromised individuals are a combination of poorly defined nodules, cavitary opacities, wedge-shaped consolidation, ground-glass opacities, and nodules with the halo sign, as well as the air crescent sign in later stages [9,15]. These findings, however, may not be applicable to lung transplant patients because of local defense mechanisms due to surgical disruption of the pulmonary nervous supply and lymphatic drainage, as well as damage caused by preservation and transport of the lung, and ischemia at bronchial or tracheal anastomosis sites [8,19].

Few reports have described HRCT findings in patients with pulmonary aspergillosis after lung transplantation [8,9]. In a series of 30 patients, CT was performed only in 7 patients and all (100%) showed poorly defined pulmonary nodules [18]. In another series of eight cases, the most common CT pattern among patients with *Aspergillus* pneumonia was a combination of nodules, consolidation, and ground-glass opacification, occurring in five of eight (62.5%) patients; the tree-in-bud pattern was seen in one (12.5%) patient, and two (25%) patients had nodules with cavitation [9].

In our study, the main HRCT pattern was centrilobular tree-in-bud nodules associated with bronchial wall thickening (65% of patients). The halo sign and cavitation were less frequently detected. These findings could be related to the use of new methods for the rapid diagnosis of aspergillosis, such as Platelia *Aspergillus* EIA for GM antigen detection in BAL. In a series of 30 patients [8], chest radiographs remained normal in 12 cases and only 7 patients underwent CT; if CT had been performed in all cases, findings might have been similar to our data because bronchial wall thickening and tree-in-bud nodules are best seen in CT and could be occult on chest radiographs.

Cellular bronchiolitis is characterized on CT by centrilobular nodules with the tree-in-bud pattern [17]. Thus, the findings of our study suggest that airway involvement was the predominant pattern of aspergillosis, in contrast to the predominance of the angioinvasive form in other types of severe immunosuppression. Colonization of the airway with *Aspergillus* and tracheobronchial infections represent entities distinct from invasive *Aspergillus* pneumonia, which could occur disproportionately in lung transplant recipients and may represent the earlier stages of infection [20,21]. Thus, the respiratory tracts of lung transplant patients may be colonized by *Aspergillus*, which may remain non-invasive or develop into tracheobronchitis or semi-invasive or invasive aspergillosis with deterioration of the immune response [19–26]. This finding was seen in our cases, in which the predominant pattern of airway disease represented the initial insult and the infection then became invasive in some cases, represented by the coexistence of more than one pattern on HRCT findings.

Two studies evaluated the CT findings of invasive pulmonary aspergillosis (IPA) in SOT recipients, but lung transplant recipients were not included [27,28]. Data from one of these reports suggested that consolidations or masses, the halo sign, and the angioinvasive form were less common in non-neutropenic transplant recipients than in neutropenic patients (56%, 26%, and 32% vs. 78%, 55%, and 60%, respectively) [27]. The other study compared radiologic findings from SOT recipients and neutropenic patients with IPA, finding that SOT recipients were more likely than neutropenic patients to show peribronchial consolidation (31% vs. 7%) or ground-glass opacities (38% vs. 7%), and less likely to have fever (22% vs. 80%), macronodules (35% vs. 67%), mass-like consolidation (27% vs. 67%), the halo sign (8% vs. 56%), and the air crescent sign (0% vs. 22%) [28]. Hence, the airway-invasive pattern was more

commonly observed in SOT recipients (65%) than in neutropenic patients (7%) with IPA. In our study, no correlation was observed between imaging findings and white blood cell counts. However, only one patient had neutropenia (498 cells/ μ L) and HRCT showed large nodules with the halo sign.

Both of these studies were limited by the omission of lung transplant recipients, which could have attenuated differences in radiologic findings between non-neutropenic transplant recipients and neutropenic patients. Most SOT cases were liver transplant recipients (65% and 89%, respectively). Thus, our study, which evaluated only lung transplantation and demonstrated a higher frequency of the airway pattern of this disease, supports and complements the results of the previous reports.

Our study was limited by the inability to exclude coexistent self-limited infections due to other organisms, especially viral infections, at the time of diagnosis, as in other immunocompromised individuals (e.g., patients with HIV). For this reason, we included only patients who received exclusively antifungal treatment and showed regression on the basis of CT findings. Colonization versus infection by *Aspergillus* should also be highlighted, but our patients' clinical symptoms resolved with *Aspergillus* treatment and no patient in our series showed eosinophilia in blood or BAL.

5. Conclusion:

We conclude that the predominant HRCT findings in lung transplant patients with *Aspergillus* infection were bilateral bronchial wall thickening and centrilobular opacities with the tree-in-bud pattern. Ground-glass opacities and/or bilateral areas of consolidation were also common findings. Thus, the presentation of aspergillosis in lung transplant recipients could differ from classic angioinvasive pneumonia findings, with a predominant pattern of airway impairment.

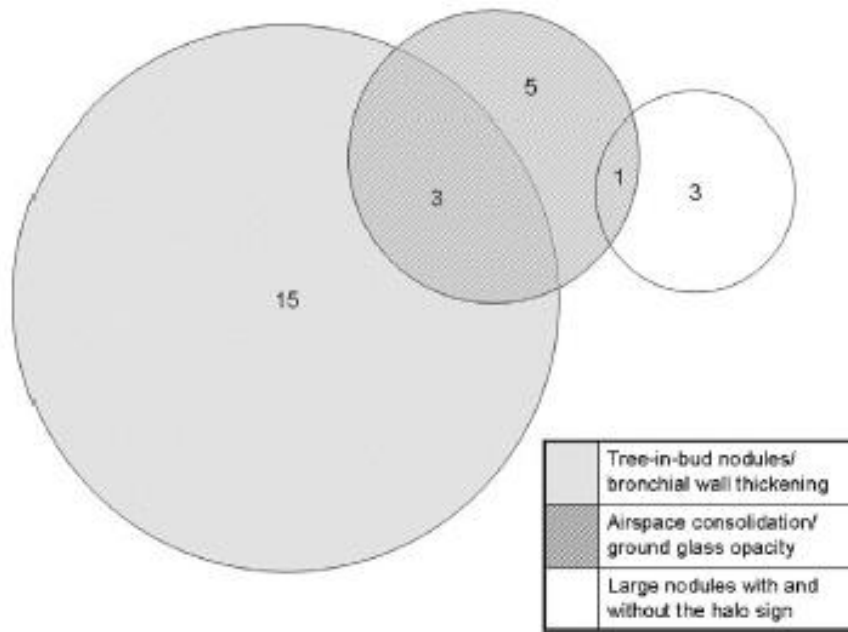
References:

- [1] Singh N, Husain S. Aspergillus infections after lung transplantation: clinical differences in type of transplant and implications for management. *Journal of Heart and Lung Transplantation* 2003;22:258–66.
- [2] Cahill BC, Hibbs JR, Savik K, et al. Aspergillus airway colonization and invasive disease after lung transplantation. *Chest* 1997;112:1160–4.
- [3] Nathan SD, Shorr AF, Schmidt ME, Burton AB. Aspergillus and endobronchial abnormalities in lung transplant recipients. *Chest* 2000;118:403–7.
- [4] Kanj SS, Welty-Wolf K, Madden J, et al. Fungal infections in lung and heart-lung transplant recipients: report of 9 cases and review of the literature. *Medicine* 1996;75:142–56.
- [5] Yeldandi V, Laghi F, McCabe MA, et al. Aspergillus and lung transplantation. *Journal of Heart and Lung Transplantation* 1995;14:883–90.
- [6] Ng YL, Paul N, Patsios D, et al. Imaging of lung transplantation: review. *AJR* 2009;192:S1–13.
- [7] Ji Y, Xu LP, Liu DH, et al. Positive results of serum galactomannan assays and pulmonary computed tomography predict the higher response rate of empirical antifungal therapy in patients undergoing allogeneic hematopoietic stem cell transplantation. *Biology of Blood and Marrow Transplantation* 2011;17(5):759–64.
- [8] Diederich S, Scadeng M, Dennis Ch, Stewart S, Flower ChDR. Aspergillus infection of the respiratory tract after lung transplantation: chest radiographic and CT findings. *European Radiology* 1998;8:306–12.
- [9] Collins J, Muller NL, Kazerooni EA, Paciocco G. CT findings of pneumonia after lung transplantation. *AJR* 2000;175:811–8.

- [10] Pasqualotto AC, Xavier MO, Sánchez LB, et al. Diagnosis of invasive aspergillosis in lung transplant recipients by detection of galactomannan in the bronchoalveolar lavage fluid. *Transplantation* 2010;90:306–11.
- [11] Ascoglu S, Rex JH, de Pauw B, et al. Defining opportunistic invasive fungal infections in immunocompromised patients with cancer and hematopoietic stem cell transplants: an international consensus. *Clinical Infectious Diseases* 2002;34:7.
- [12] Hansell DM, Bankier AA, MacMahon H, McLoud TC, Muller NL, Remy J. Fleischner society: glossary of terms for thoracic imaging. *Radiology* 2008;246:697–722.
- [13] de Perrot M, Chaparro C, McRae K, et al. Twenty-year experience of lung transplantation at a single center: influence of recipient diagnosis on long-term survival. *Journal of Thoracic and Cardiovascular Surgery* 2004;127:1493–501.
- [14] Gordon SM, Avery RK. Aspergillosis in lung transplantation: incidence, risk factors, and prophylactic strategies. *Transplant Infectious Disease* 2001;3:161–7.
- [15] Franquet T, Muller NL, Giménez A, Guembe P, de la Torre J, Bagué S. Spectrum of pulmonary aspergillosis: histologic, clinical, and radiologic findings. *Radiographics* 2001;21:825–37.
- [16] Lease ED, Zaas DW. Update on infectious complications following lung transplantation. *Current Opinion in Pulmonary Medicine* 2011;17:206–9.
- [17] Alexander BD, Tapson VF. Infectious complications of lung transplantation. *Transplant Infectious Disease* 2001;3:128–37.
- [18] Erasmuss JJ, McAdams HP, Tapson VF, Murray JG, Davis RD. Radiologic issues in lung transplantation for end-stage pulmonary disease. *AJR* 1997;169: 69–78.

- [19] Kramer MR, Denning DW, Marshall SE, et al. Ulcerative tracheobronchitis after lung transplantation: a new form of invasive aspergillosis. *The American Review of Respiratory Disease* 1991;144:552–6.
- [20] Mehrad B, Paciocco G, Martinez FJ, Ojo TC, Iannettoni MD, Lynch JP. Spectrum of *Aspergillus* infection in lung transplant recipients: case series and review of the literature. *Chest* 2001;119:169–75.
- [21] Paterson DL, Singh N. Invasive aspergillosis in transplant recipients. *Medicine* 1999;78:123–38.
- [22] Klein DL, Gamsu G. Thoracic manifestations of aspergillosis. *AJR* 1980;134:543–52.
- [23] Clarke a, Shelton J, Fraser RS. Fungal tracheobronchitis: report of nine cases and review of the literature. *Medicine* 1991;70:1–14.
- [24] Tazelaar HD, Baird AM, Mill M, Grimes MM, Schulmann LL, Smith CR. Bronchocentric mycosis occurring in transplant recipients. *Chest* 1989;96:92–5.
- [25] McAdams HP, Rosado-de-Cristenson ML, Templeton PA, Lesar M, Moran CA. Thoracic mycosis from opportunistic fungi: radiologic-pathologic correlation. *Radiographics* 1995;15:271–86.
- [26] Thompson BH, Stanford W, Galván JR, Kurihara Y. Varied radiologic appearances of pulmonary aspergillosis. *Radiographics* 1995;15:1273–84.
- [27] Park SY, Lim C, Lee SO, et al. Computed tomography findings in invasive pulmonary aspergillosis in non-neutropenic transplant recipients and neutropenic patients, and their prognostic value. *Journal of Infection* 2011;63:447–56.
- [28] Park SY, Kim SH, Choi SH, et al. Clinical and radiological features of invasive pulmonary aspergillosis in transplant recipients and neutropenic patients. *Transplant Infectious Disease* 2010;12:309–15.

Fig.1 - High-Resolution computed tomography patterns.



Footnote: Algorithms represent the number of patients in each group.

Fig. 2 - A 45 year-old unilateral right-lung transplantation recipient with dyspnea. A and B, Axial CT scans shows centrilobular nodules with the tree-in-bud pattern in the right lower lobe.

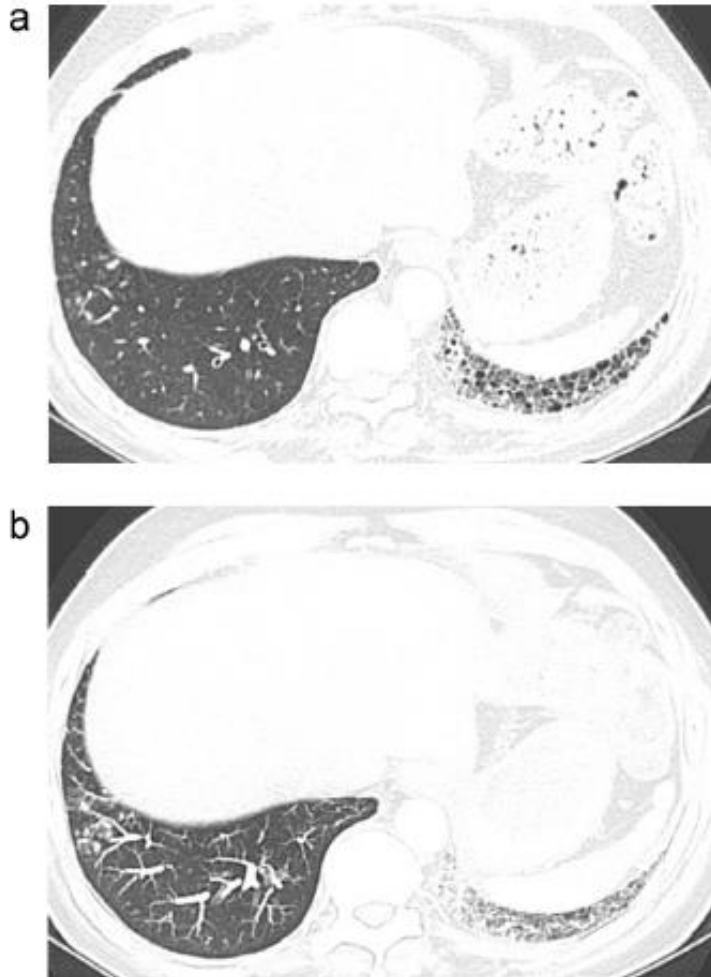


Fig. 3 - A 56 year-old unilateral left-lung transplantation recipient with dyspnea and fever. Axial CT scans shows area of consolidation (A) and ground-glass opacities (B) in the left lower lobe.

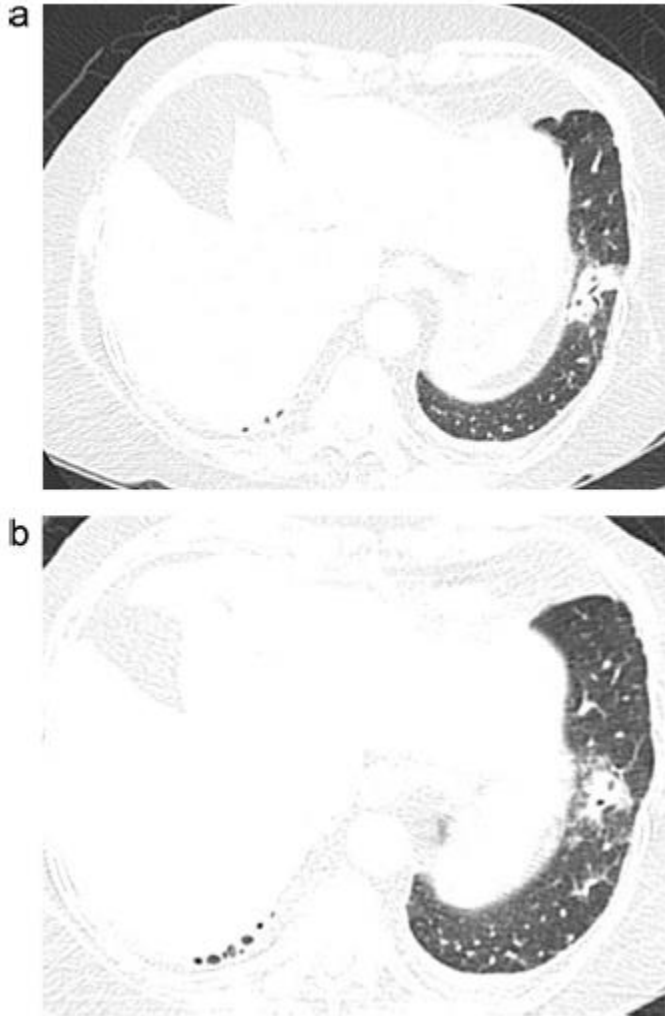


Fig. 4 - A 49 year-old bilateral lung transplantation recipient with dyspnea. A and B, Axial CT scans shows pulmonary nodules with the halo sign in the right lower lobe.

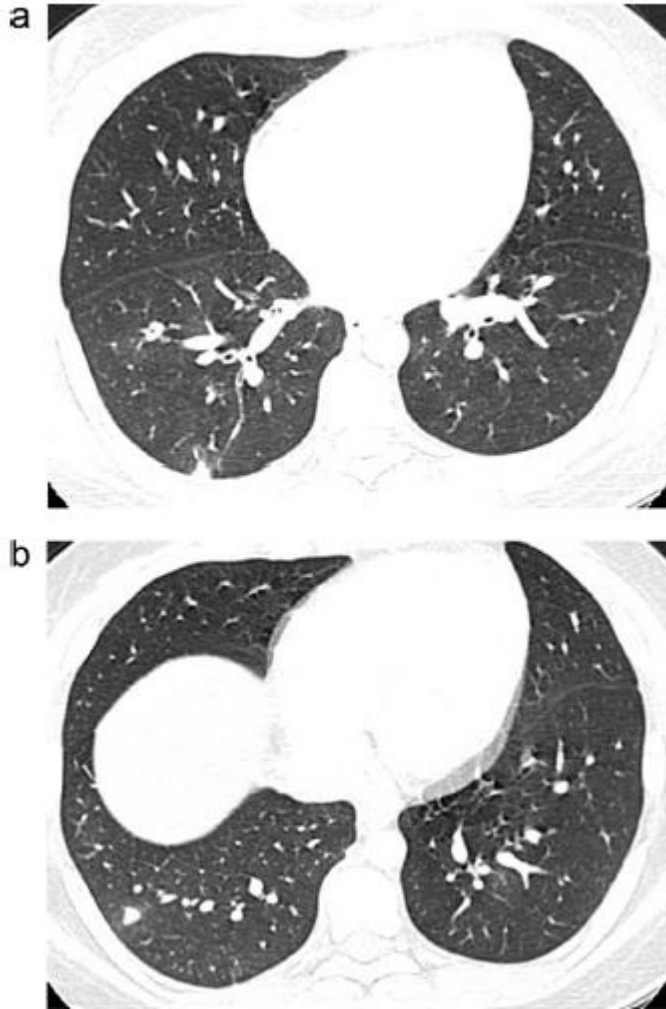


Table 1

Features of lung transplantation recipients with pulmonary aspergillosis.

Clinical characteristics:	Data ^a
Patients	23
Male gender	12 (52,17%)
Bilateral transplantation	13 (56,5%)
Age, median years (range)	43,6 (22–59)
Mean interval between lung transplantation and infection diagnosis (SD ^b)	7,4 months(1,7)
HRCT^c patterns:	
1. tree-in-bud nodules/bronchial wall thickening	15 (65%)
2. airspace consolidation/ground glass opacity	5 (22%)
3. large nodules with and without the halo sign	3 (13%)
Association of patterns 1 and 2	3 (13%)
Association of patterns 2 and 3	1 (4,3%)
Distribution of abnormalities:	
Unilateral	3 (13%)
Bilateral	20 (87%)

^a Data are presented as the number (%) of patients unless otherwise indicated.

^b SD: Standard deviation.

^c HRCT: High-resolution computed tomography.

5. Discussão:

A aspergilose pulmonar invasiva é uma infecção oportunista que afeta especialmente receptores de órgãos sólidos e pacientes com neutropenia induzida por quimioterapia (37). Embora estes pacientes estejam em risco para aspergilose invasiva, eles diferem no que diz respeito aos defeitos específicos nos mecanismos de defesa que aumentam o risco desta patologia. A neutropenia induzida pela quimioterapia é o principal defeito afetando pacientes com malignidades hematológicas, enquanto que os recipientes de transplantes tendem a apresentar disfunção de células T e fagócitos, como resultado da terapia imunossupressora. Dessa forma, os padrões da aspergilose invasiva podem diferir de acordo com o tipo de defeito imune. Na TC a aspergilose invasiva de vias aéreas pode ser considerada quando os achados predominantes revelam nódulos centrolobulares com padrão de árvore-em-brotamento, espessamento de paredes brônquicas e consolidação peribrônquica. A forma angioinvasiva é considerada quando a TC revela macronódulos, consolidações em massa, sinal do halo e sinal do crescente aéreo (37,38).

Em nosso estudo, os achados predominantes na TCAR em pacientes submetidos a transplante de pulmão com infecção por *Aspergillus* foram espessamento de paredes brônquicas e opacidades centrolobulares ramificadas com padrão de árvore-em-brotamento, visualizados em 65% dos pacientes. Opacidades em vidro-fosco e/ou áreas de consolidação bilaterais também foram achados comuns; o sinal do halo e cavitação foram menos frequentemente detectados. Apenas um paciente teve neutropenia (498 cells/ μ L) e a TCAR demonstrou nódulos grandes com sinal do halo. Desta forma, encontramos que o padrão de envolvimento da via aérea é o predominante da aspergilose nos receptores de transplante pulmonar.

Em outros dois estudos foram avaliados os achados da TC na aspergilose pulmonar invasiva em receptores de transplante de órgãos sólidos, mas transplantados de pulmão não foram incluídos (37,38). Os resultados de um destes estudos sugeriu que a apresentação angioinvasiva da aspergilose foi menos comum em receptores de transplante não-neutropênicos do que em pacientes neutropênicos (37). O outro estudo comparou achados clínicos e radiológicos de receptores de órgãos sólidos e pacientes neutropênicos com aspergilose invasiva. Os resultados demonstraram que o padrão invasivo de vias aéreas foi mais comumente observado nos receptores de órgãos sólidos (65%) do que nos pacientes com neutropenia (7%) (38). Ambos os estudos foram limitados pela omissão de receptores de transplante pulmonar. A maioria dos casos era de receptores de transplante hepático (65% e 89%, respectivamente), o que pode ter atenuado as diferenças nos achados radiológicos entre receptores de transplante não-neutropênicos e pacientes neutropênicos. Dessa forma, nosso estudo, que avaliou exclusivamente pacientes transplantados de pulmão, e demonstrou uma maior frequência do padrão de envolvimento da via aérea, suporta e complementa os resultados destes estudos prévios.

A TC é mais útil que o RX na avaliação dos pacientes transplantados de pulmão com suspeita de aspergilose, pois detecta mais facilmente pequenos nódulos e espessamento de paredes brônquicas, bem como melhor demonstra a morfologia e distribuição da doença (23,30). Dessa maneira, a estratégia diagnóstica deve incluir abordagem liberal com TC. Quando uma possível anormalidade é vista no RX, ou mesmo quando este é normal, a realização de uma TC dever ser rápida para ajudar a guiar a decisão em relação à terapêutica ou de realizar outros testes.

Pode-se salientar também que a colonização e as infecções das vias aéreas por espécies de *Aspergillus*, entidades distintas da pneumonia angioinvasiva, poderiam

ocorrer desproporcionalmente em receptores de transplante pulmonar e representar os estágios iniciais da infecção (23,28,29,30). Desta forma, o trato respiratório dos pacientes transplantados de pulmão poderia permanecer colonizado por *Aspergillus* ou desenvolver doença semi-invasiva, invasiva das vias aéreas ou angioinvasiva com a deterioração da resposta imune (28-31,39-41). Estes achados foram vistos em nossos casos, em que o padrão predominante foi o de doença da via aérea representando o insulto inicial, e a infecção tornou-se angioinvasiva em alguns casos, representado pela coexistência de mais de um padrão na TCAR.

No entanto, a diferenciação entre colonização e infecção permanece um desafio. Uma cultura ou PCR positivo para *Aspergillus* no LBA ajudam a detectar a colonização da via aérea, mas podem apenas implicar a presença de conídios no ambiente e colonização do trato respiratório. O ensaio para detecção do antígeno galactomanana também pode apresentar resultados falso-positivos quando apenas o LBA é testado. No entanto, o teste da galactomanana, por ser mais rápido, pode ser correlacionado com os achados da TCAR para permitir mais agilidade no diagnóstico (34,42), pois a terapia anti-fúngica precoce melhora a sobrevida dos pacientes transplantados de pulmão com aspergilose (38).

Como discutido anteriormente, as lesões nodulares com o sinal do halo ou o sinal do crescente historicamente foram associadas com aspergilose angioinvasiva, que ocorre em pacientes neutropênicos. As características da aspergilose acometendo as vias aéreas em pacientes não-neutropênicos são diferentes, como descrevemos em nosso estudo. No entanto, não estão incluídas na Revisão das Definições das Doenças Fúngicas Invasivas proposta pela Organização Européia para Pesquisa e Tratamento do Câncer / Grupo de Estudo em Micoses em 2008 (43). Assim, estes critérios revistos podem não refletir as características da aspergilose invasiva em receptores de

transplante de órgãos sólidos, especialmente nos casos de receptores de transplante pulmonar. A ausência dos achados tomográficos típicos da apresentação angioinvasiva não deve excluir o diagnóstico nestes casos.

6. Conclusões:

Os achados predominantes na TCAR em pacientes transplantados de pulmão com o diagnóstico de aspergilose pulmonar foram nódulos com padrão de árvore-em-brotamento e espessamento de paredes brônquicas, visualizados em 65% dos pacientes. Além disso, opacidades com atenuação em vidro-fosco e áreas de consolidação foram achados comuns. Os nódulos com o sinal do halo foram observados em apenas 13% dos pacientes. Desta forma, encontramos que o padrão de envolvimento da via aérea é o predominante da aspergilose nos receptores de transplante pulmonar.

7. Perspectivas:

Uma vez que o número de pacientes que desenvolvem infecção invasiva por *Aspergillus* em centros de transplante pulmonar é limitado, mais estudos para avaliarem a estratégia diagnóstica e abordagem preventiva ideal são necessários. Assim, continua em andamento em nossa linha de pesquisa o acompanhamento dos receptores de transplante pulmonar devido a grande importância desta infecção, que está relacionada à alta mortalidade quando não diagnosticada precocemente.

Esforços de pesquisa consideráveis também devem ser direcionados no estudo da detecção não invasiva envolvendo os antígenos do *Aspergillus* ou outros parâmetros que, associados aos achados da TCAR, devem ser amplamente utilizados nos centros de referência de transplante pulmonar.

Está em fase final a conclusão de um artigo de revisão sobre as manifestações tomográficas da aspergilose pulmonar, que será posteriormente submetido para revista indexada.

8. Referências:

1. Zmeili OS, Soubani AO. Pulmonary aspergillosis: a clinical update. *Q J Med* 2007; 100:317–34.
2. Soubani AO, Chandrasekar PH. The clinical spectrum of pulmonary aspergillosis. *Chest* 2002; 121:1988–99.
3. Franquet T, Müller NL, Giménez A, Guembe P, de la Torre J, Bagué S. Spectrum of pulmonary aspergillosis: histologic, clinical, and radiologic findings. *Radiographics* 2001; 21:825–37.
4. Aquino SL, Kee ST, Warnock ML, Gamsu G. Pulmonary aspergillosis: imaging findings with pathologic correlation. *AJR Am J Roentgenol* 1994; 163:811–5.
5. Thompson BH, Stanford W, Galván JR, Kurihara Y. Varied radiologic appearances of pulmonary aspergillosis. *Radiographics* 1995;15:1273–84.
6. McAdams HP, Rosado-de-Christenson ML, Templeton PA, Lesar M, Moran CA. Thoracic mycoses from opportunistic fungi: radiologic-pathologic correlation. *RadioGraphics* 1995; 15:271–86.
7. Binder RE, Faling LJ, Pugatch RD, Mahasen C, Snider GL. Chronic necrotizing pulmonary aspergillosis: a discrete clinical entity. *Medicine* 1982; 61:109-24.

8. Franquet T, Müller NL, Giménez A, Domingo P, Plaza V, Bordes R. Semiinvasive pulmonary aspergillosis in chronic obstructive pulmonary disease: radiologic and pathologic findings in nine patients. *AJR Am J Roentgenol* 2000; 174:51–6.
9. Logan PM, Primack SL, Miller RR, Müller NL. Invasive aspergillosis of the airways: radiographic, CT, and pathologic findings. *Radiology* 1994; 193:383–8.
10. Brown MJ, Worthy SA, Flint JD, Müller NL. Invasive aspergillosis in the immunocompromised host: utility of computed tomography and bronchoalveolar lavage. *Clin Radiol* 1998; 53:255–7.
11. Denning DW. Invasive aspergillosis. *Clin Infect Dis* 1998; 26:781–805.
12. Curtis AMB, Smith GJ, Ravin CE. Air crescent sign of invasive aspergillosis. *Radiology* 1979; 133: 17–21.
13. Geftter WB, Albelda SM, Talbot GH, Gerson SL, Cassileth PA, Miller WT. Invasive pulmonary aspergillosis and acute leukemia: limitations in the diagnostic utility of the air crescent sign. *Radiology* 1985; 157:605–10.
14. Kuhlman JE, Fishman EK, Siegelman SS. Invasive pulmonary aspergillosis in acute leukemia: characteristic findings on CT, the CT halo sign, and the role of CT in early diagnosis. *Radiology* 1985; 157:611–4.

15. Primack SL, Hartman TE, Lee KS, Müller NL. Pulmonary nodules and the CT halo sign. *Radiology* 1994; 190:513–5.
16. Ng YL, Paul N, Patsios D, Walsham A, Chung TB, Keshavjee S, et al. Imaging of lung transplantation: review. *AJR Am J Roentgenol* 2009;192:S1–13.
17. de Perrot M, Chaparro C, McRae K, Waddell TK, Hadjiliadis, Singer LG, et al. Twenty-year experience of lung transplantation at a single center: influence of recipient diagnosis on long-term survival. *Journal of Thoracic and Cardiovascular Surgery* 2004;127:1493–501.
18. Singh N, Husain S. Aspergillus infections after lung transplantation: Clinical Differences in Type of Transplant and Implications for Management. *J Heart Lung Transplant* 2003; 22: 258-66.
19. Cahill BC, Hibbs JR, Savik K, Juni BA, Dosland BM, Edin-Stibbe C, et al. Aspergillus airway colonization and invasive disease after lung transplantation. *Chest* 1997; 112:1160-4.
20. Nathan SD, Shorr AF, Schmidt ME, Burton NA. Aspergillus and endobronchial abnormalities in lung transplant recipients. *Chest* 2000; 118:403-7.
21. Kanj SS, Welty-Wolf K, Madden J, Tapson V, Baz MA, Davis RD, et al. Fungal Infections in lung and heart-lung transplant recipients: Report of 9 cases and review of the literature. *Medicine* 1996; 75:142-56.

22. Yeldandi V, Laghi F, McCabe MA, Larson R, O'Keefe P, Husain A, et al. Aspergillus and lung transplantation. *J Heart Lung Transplant* 1995; 14:883-90.
23. Collins J, Muller NL, Kazerooni EA, Paciocco G. CT findings of pneumonia after lung transplantation. *AJR Am J Roentgenol* 2000;175:811-8.
24. Gordon SM, Avery RK. Aspergillosis in lung transplantation: incidence, risk factors, and prophylactic strategies. *Transplant Infect Dis* 2001; 3:161-7.
25. Lease ED, Zaas DW. Update on infectious complications following lung transplantation. *Curr Opin Pulm Med* 2011;17:206-9.
26. Alexander BD, Tapson VF. Infectious complications of lung transplantation. *Transplant Infect Dis* 2001;3:128-37.
27. Erasmuss JJ, McAdams HP, Tapson VF, Murray JG, Davis RD. Radiologic issues in lung transplantation for end-stage pulmonary disease. *AJR Am J Roentgenol* 1997;169: 69-78.
28. Mehrad B, Paciocco G, Martinez FJ, Ojo TC, Iannettoni MD, Lynch JP. Spectrum of Aspergillus infection in lung transplant recipients: case series and review of the literature. *Chest* 2001;119:169-75.
29. Paterson DL, Singh N. Invasive aspergillosis in transplant recipients. *Medicine* 1999;78:123-38.

30. Diederich S, Scadeng M, Dennis C, Stewart S, Flower CD. Aspergillus infection of the respiratory tract after lung transplantation: chest radiographic and CT findings. *European Radiology* 1998;8:306–12.
31. Kramer MR, Denning DW, Marshall SE, Rossi DJ, Berry G, Lewiston NJ, et al. Ulcerative tracheobronchitis after lung transplantation: a new form of invasive aspergillosis. *Am Rev of Respir Dis* 1991;144:552–6.
32. Ji Y, Xu LP, Liu DH, Chen YH, Han W, Zhang XH, et al. Positive results of serum galactomannan assays and pulmonary computed tomography predict the higher response rate of empirical antifungal therapy in patients undergoing allogeneic hematopoietic stem cell transplantation. *Biol Blood Marrow Transplant* 2011;17:759–64.
33. Pasqualotto AC, Xavier MO, Sánchez LB, de Oliveira Costa CD, Schio SM, Camargo SM, et al. Diagnosis of invasive aspergillosis in lung transplant recipients by detection of galactomannan in the bronchoalveolar lavage fluid. *Transplantation* 2010;90:306–11.
34. Aquino VR, Goldani LZ, Pasqualotto AC. Update on the contribution of galactomannan for the diagnosis of invasive aspergillosis. *Mycopathologia* 2007;163:191-202.

35. Ascioglu S, Rex JH, de Pauw B, Bennett JE, Bille J, Crokaert F, et al. Defining opportunistic invasive fungal infections in immunocompromised patients with cancer and hematopoietic stem cell transplants: an international consensus. *Clin Infect Dis* 2002; 34:7-14.
36. Hansell DM, Bankier AA, MacMahon H, McLoud TC, Müller NL, Remy J. Fleischner society: glossary of terms for thoracic imaging. *Radiology* 2008; 246:697–722.
37. Park SY, Lim C, Lee SO, Choi SH, Kim YS, Woo JH, et al. Computed tomography findings in invasive pulmonary aspergillosis in non-neutropenic transplant recipients and neutropenic patients, and their prognostic value. *J Infect* 2011; 63:447–56.
38. Park SY, Kim SH, Choi SH, Sung H, Kim MN, Woo JH, et al. Clinical and radiological features of invasive pulmonary aspergillosis in transplant recipients and neutropenic patients. *Transpl Infect Dis* 2010; 12:309–15.
39. Klein DL, Gamsu G. Thoracic manifestations of aspergillosis. *AJR Am J Roentgenol* 1980; 134:543–52.
40. Clarke A, Shelton J, Fraser RS. Fungal tracheobronchitis: report of nine cases and review of the literature. *Medicine* 1991; 70:1 14.
41. Tazelaar HD, Baird AM, Mill M, Grimes MM, Schulmann LL, Smith CR. Bronchocentric mycosis occurring in transplant recipients. *Chest* 1989; 96:92–5.

42. Becker MJ, Lugtenburg EJ, Cornelissen JJ, Van Der Schee C, Hoogsteden HC, De Marie S. Galactomannan detection in computerized tomography-based bronchoalveolar lavage fluid and serum in haematological patients at risk for invasive pulmonary aspergillosis. *Br J Haematol* 2003;121:448–57.

43. De Pauw B, Walsh TJ, Donnelly JP, Stevens DA, Edwards JE, Calandra T, et al. Revised definitions of invasive fungal disease from the European Organization for Research and Treatment of Cancer/Invasive Fungal Infections Cooperative Group and the National Institute of Allergy and Infectious Diseases Mycoses Study Group (EORTC/MSG) Consensus Group. *Clin Infect Dis* 2008; 46: 1813-21.

9. Anexos:**Artigos publicados em periódicos durante o doutorado**

9.1

LETTER TO THE EDITOR: ASPERGILLUS FUMIGATUS FUNGUS BALL IN THE
NATIVE LUNG AFTER SINGLE LUNG TRANSPLANTATION

GAZZONI, F.F.; HOCHHEGGER, B.; SEVERO, L.C.; CAMARGO, J.J.

Jornal Brasileiro de Pneumologia, 2013;39(3):393-395

História do artigo:

Submetido: 11 de Novembro de 2012.

Aceito após revisão: 07 de Dezembro de 2012.

To the Editor:

A 49-year-old woman underwent right lung transplantation due to pulmonary emphysema, with favorable evolution in the early postoperative period. A year later she was readmitted to our department with productive cough. During that admission, the patient was treated for cytomegalovirus pneumonia and received broad-spectrum antibacterial therapy.

At outpatient follow-up, cavities appeared in the native lung, which gradually increased in size. Ten months later, she was admitted for the resection of a hyperinflated cavity. Chest X-rays showed an increase in the cavity in the left upper lobe with herniation of the lung and compression of the transplanted lung. Chest CT at various positions showed a round mass with soft tissue density within a lung cavity that moved when the patient changed position, thus strengthening the hypothesis of a fungus ball (Figure 1). Bullectomy was performed, and the histopathologic examination showed fungal colonization by *Aspergillus fumigatus* in emphysematous bullae and bronchiectasis. She was treated with itraconazole and had a satisfactory response.

Lung transplantation has become an acceptable treatment option for many end-stage lung diseases and could be single or double (1,2). However, *Aspergillus* sp. infections continue to be an important cause of morbidity and mortality in these patients. *Aspergillus* sp. is an ubiquitous fungus that can cause clinical entities of varying severity, such as asymptomatic colonization, aspergilloma, tracheobronchitis, active parenchymal disease, and angioinvasive aspergillosis (1-6).

Airway colonization is a common occurrence in such patients because of the exposure of the transplanted lung to the environment and impaired local host defenses, including mucociliary clearance. In addition, colonization of the native lung, which

commonly occurs in end-stage lung disease, is an important source of post-transplantation aspergillosis in single lung transplantation recipients. *Aspergillus* sp. colonization has also been related to cytomegalovirus infection and chronic rejection (1-4).

Patients who undergo unilateral transplantation are often older and have a higher prevalence of COPD as an underlying disease, a condition that might predispose to airway colonization by *Aspergillus* sp (1-3).

The most accurate way to perform the diagnosis is the demonstration of characteristic, acute branching, broad, septate hyphae showing zones of growth in biopsy/surgical/autopsy specimens and positive cultures for *Aspergillus* sp (3,5,6).

Our patient presented with *Aspergillus fumigatus* fungal ball (aspergilloma) in emphysematous bullae and bronchiectasis in the native lung 26 months after transplantation, with a satisfactory response to medical and surgical treatment. She also had a history of cytomegalovirus infection one year after transplantation as another risk factor. The diagnosis was made through imaging and evaluation of surgical specimens. In fact, aspergilloma affecting the native lung in single lung transplantation recipients has been reported only rarely in retrospective studies (3,4).

Aspergilloma is characterized by *Aspergillus* sp. infection without tissue invasion. It leads to the conglomeration of intertwined fungal hyphae mixed with mucus and cellular debris within a pre-existing pulmonary cavity, bulla, or ectatic bronchus. The most common underlying causes are tuberculosis and sarcoidosis. Although patients might remain asymptomatic, the most common clinical manifestation is hemoptysis (5,6). Risk factors for a poor prognosis of aspergilloma include the severity of the underlying lung disease, increase in size or in the number of lesions on chest X-

rays, immunosuppression (including transplantation), increasing *Aspergillus*-specific IgG titles, recurrent large volume hemoptysis, and sarcoidosis. This highlights the importance of radiological findings, cultures, reviews of the level of immunosuppression, and environmental factors for the early diagnosis and prevention of further complications, such as angioinvasive disease. Treatment should be considered only when patients become symptomatic, usually with hemoptysis. There is no consensus on the best treatment approach; however, surgical resection of the cavity and removal of the fungus ball are usually indicated in patients with recurrent hemoptysis if their pulmonary function is sufficient to allow surgery (4-6).

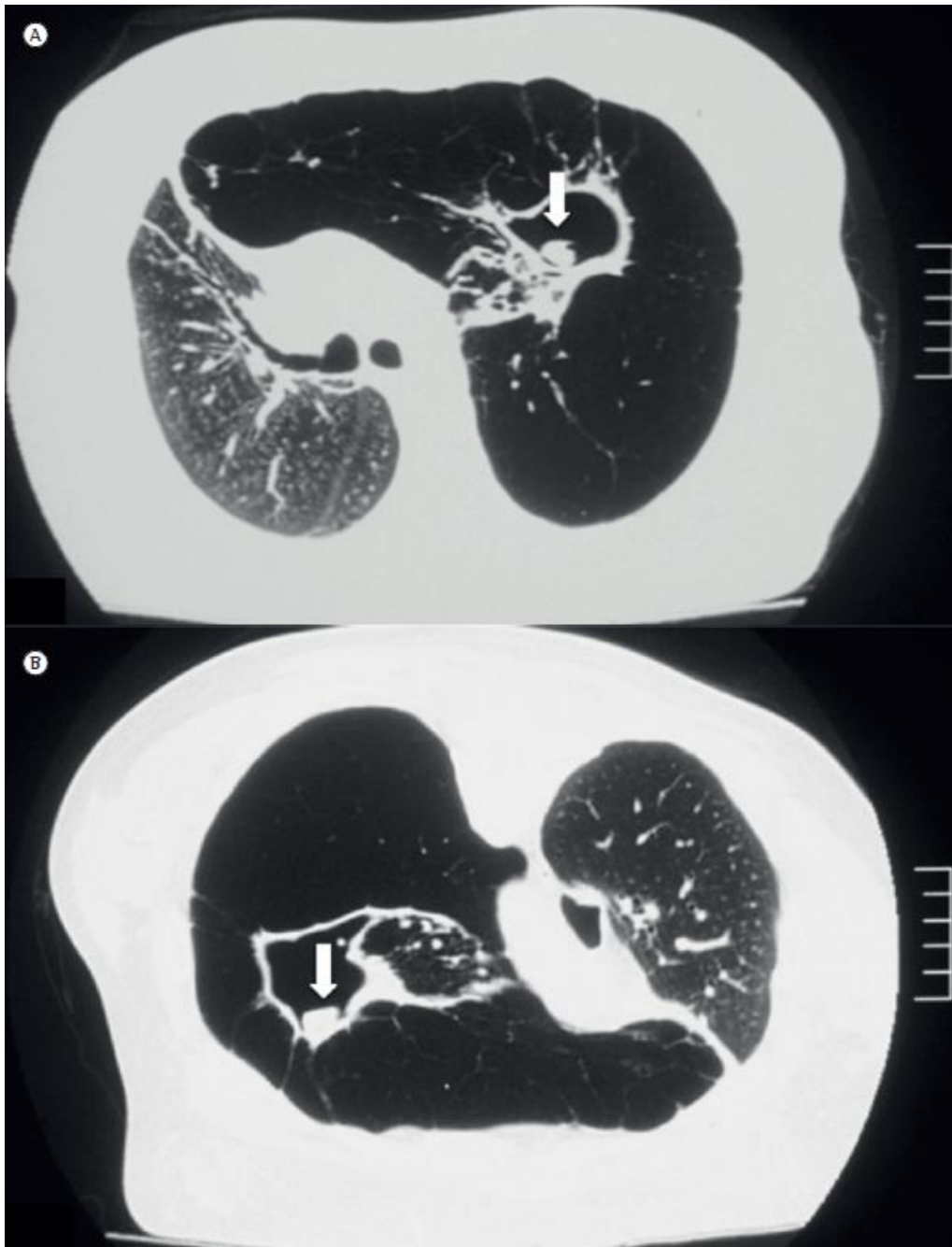
On CT scans and X-rays, aspergillomas are characterized by the presence of a round or oval mass with soft tissue density within a lung cavity. The mass can be separated from the wall of the cavity by an air space of variable size, resulting in the “air crescent” sign. The aspergilloma usually moves when the patient changes position, as was seen in our case. Another finding of aspergillomas is the thickening of the cavity wall and adjacent pleura, which might be the earliest radiological sign (5,6).

In summary, the susceptibility of the native lung to *Aspergillus* sp. infections might be an additional factor to be considered in choosing the ideal transplantation procedure. In cases of single lung transplantation, radiological and clinical attention is especially directed to the transplanted organ. However, the native lung, structurally damaged, can be a nidus for *Aspergillus* sp. and provide a source of infection.

References:

1. Singh N, Husain S. Aspergillus infections after lung transplantation: clinical differences in type of transplant and implications for management. *J Heart Lung Transplant*. 2003;22(3):258-66.
2. McAdams HP, Erasmus JJ, Palmer SM. Complications (excluding hyperinflation) involving the native lung after single-lung transplantation: incidence, radiologic features, and clinical importance. *Radiology*. 2001;218(1):233- 41.
3. Westney GE, Kesten S, De Hoyos A, Chapparro C, Winton T, Maurer JR. Aspergillus infection in single and double lung transplant recipients. *Transplantation*. 1996;61(6):915-9.
4. Fitton TP, Bethea BT, Borja MC, Yuh DD, Yang SC, Orens JB, et al. Pulmonary resection following lung transplantation. *Ann Thorac Surg*. 2003;76(5):1680-5; discussion 1685-6.
5. Franquet T, Müller NL, Giménez A, Guembe P, de La Torre J, Bagué S. Spectrum of pulmonary aspergillosis: histologic, clinical, and radiologic findings. *Radiographics*. 2001;21(4):825-37.
6. Kousha M, Tadi R, Soubani AO. Pulmonary aspergillosis: a clinical review. *Eur Respir Rev*. 2011;20(121):156- 74.

Figure 1 - Axial HRCT scans. In A, cavitory lung lesion in the left upper lobe filled with an opacity resembling a fungus ball (arrow). In B, a scan after moving the patient from the supine position to the prone position, demonstrating the motility of the mass (arrow).



9.2

PULMONARY DISEASES WITH IMAGING FINDINGS MIMICKING
ASPERGILLOMA

GAZZONI, F.F.; SEVERO, L.C.; MARCHIORI, E.; GUIMARÃES, M.D.; GARCIA,
T.S.; IRION, K.L.; CAMARGO, J.J.; FELICETTI, J.C.; OLIVEIRA, F.M.;
HOCHHEGGER, B.

Lung 2014; 192:347–357

História do artigo:

Submetido: 21 de Novembro de 2013.

Aceito: 24 de Fevereiro de 2014.

ABSTRACT:

Patients with preexisting lung cavities are at risk of developing intracavitary fungal colonization. Because *Aspergillus* spp. are the most commonly implicated fungi, these fungal masses are called aspergillomas. Their characteristic “ball-in-hole” appearance, however, may be found in a variety of other conditions that can produce radiologic findings mimicking aspergilloma. In this paper, we review the main diseases that may mimic the radiographic findings of aspergilloma, with brief descriptions of clinical, radiologic, and histopathologic findings.

Keywords: Lung disease; Fungi; *Aspergillus*; Aspergilloma; Computed tomography.

INTRODUCTION:

Pulmonary aspergillosis refers to a clinical spectrum of lung diseases caused by species of the *Aspergillus* genus (usually *A. fumigatus*). *Aspergillus* spp. are ubiquitous fungi found in organic debris, dust, compost, foods, spices, and rotted plants. In tissue sections, *Aspergillus* hyphae characteristically appear as uniform, narrow (3–6- μ m wide), tubular, and regularly septate (usually 45°) elements. Branching is regular, progressive, and dichotomous. Hyphal branches tend to arise at acute angles from parent hyphae [1, 2].

The spectrum of pulmonary aspergillosis can be divided into five categories: saprophytic (aspergilloma), hypersensitivity reaction (allergic bronchopulmonary aspergillosis), and semi-invasive (chronic necrotizing), airway-invasive, and angioinvasive aspergillosis [1, 2]. The manifestations of this disease are determined by the number and virulence of organisms, the patient's immune response, and the presence of structural lung disease. They range from invasive pulmonary disease in severely immunocompromised patients to chronic necrotizing aspergillosis in patients with chronic lung disease and/or mildly compromised immune systems. Allergic bronchopulmonary aspergillosis, a hypersensitivity reaction to *Aspergillus* antigens, mainly affects patients with asthma, whereas aspergilloma is an *Aspergillus* sp. fungus ball seen mainly in patients with cavitary lung disease [1, 2].

A fungus ball consists of masses of fungal mycelia, inflammatory cells, fibrin, mucus, and tissue debris; it colonizes pulmonary cavities, usually in the upper lobes [2]. Because the most commonly implicated fungi are *Aspergillus* sp., these fungal masses are called aspergillomas. Patients at risk of aspergilloma development have cavitary, bullous, or cystic lung disease that is commonly a result of tuberculosis (TB), sarcoidosis, or emphysema. These patients have chronic productive cough or

hemoptysis, which can be life-threatening. Pleural thickening may be the earliest sign on chest radiographs, preceding visible changes in the involved cavity or cyst [3, 4]. Classically, the cavity contains a mass or fungus ball (Figs. 1, 2). However, because this “ball-in-hole” aspect may be found in other diseases, clinicians must be aware of the differential diagnosis of this radiologic finding.

In this paper, we review the main pathologies that may mimic the radiographic findings of aspergilloma, including coccidioidomycosis, actinomycosis, nocardiosis, candidiasis, lung adenocarcinoma, intracavitary hematoma due to TB, pseudallescheriasis/scedosporiosis, and hydatid cyst, with brief descriptions of clinical, radiologic, and histopathologic findings.

Coccidioidomycosis

Coccidioidomycosis is caused by inhalation of spores of the dimorphic fungus *Coccidioides immitis* or *C. posadasii*. It is endemic in the southwestern United States and northern Mexico and also is found in parts of Argentina, Brazil, Colombia, Guatemala, Honduras, Nicaragua, Paraguay, and Venezuela [5]. Sixty percent of individuals with acute infection are asymptomatic; the remainder present with mild to moderate flu-like symptoms, which disappear within a few weeks. Approximately 5 % of patients develop residual pulmonary disease. These patients are generally asymptomatic, and the lesions regress spontaneously after a few years in half of individuals. However, extrapulmonary dissemination, including that to the skin, bones, and central nervous system, occurs in 0.5–1.0 % of these patients [6].

The majority of patients with acute (primary) coccidioidomycosis have mild reactions and normal radiographic appearance. Approximately 40 % of patients are symptomatic, with radiographically visible areas of consolidation. Associated hilar

lymph-node enlargement is seen in 20 % of cases. The consolidation usually resolves over a period of several weeks. Chronic pulmonary coccidioidomycosis is characterized radiologically by nodules or cavities (usually solitary), most of which are discovered incidentally in asymptomatic patients; approximately 25 % of lesions result from incomplete resolution of acute bronchopneumonia. Cavities <2.5 cm in diameter tend to resolve spontaneously within 1 year, but those >5.0 cm persist [5]. Cavitory pulmonary disease due to coccidioidomycosis is common, but a coccidioidal fungus ball occurs rarely in a preexisting cavity (Fig. 3a). This ball presents as a mass within a cavity that is mobile with positional change. This finding simulates an *Aspergillus* fungus ball, which also may invade cavities of coccidioidomycosis [6, 7].

The diagnosis of coccidioidomycosis is based on clinical suspicion supported by microbiologic, histopathologic, and/or serologic evidence. On histopathologic examination, the presence of spherules in tissue specimens is virtually pathognomonic of this condition (Fig. 3b). The main distinguishing feature of *Coccidioides* spherules is the presence of endospores. A few fungi or fungus-like organisms, including *Rhinosporidium seeberi*, *Prototheca wickerhamii*, *Emmonsia parva*, and *E. crescens*, may superficially resemble spherules. Histopathologic findings in immunocompromised patients and in uncontrolled disease are abscesses with spherules, endospores, and neutrophils; findings in patients with competent cell-mediated immunity are well-formed granulomas, with very few organisms visible within the lesion [5, 8].

Actinomycosis

Actinomycosis is a chronic disease characterized by abscess formation, tissue fibrosis, and draining sinuses. It is caused by non-spore-forming anaerobic or microaerophilic bacterial species of the genus *Actinomyces*. Agents of actinomycosis

are commensals and normal inhabitants of the oropharynx, gastrointestinal tract, and female genital tract in humans. Actinomycosis usually occurs in immunocompetent persons but may occur in immunosuppressed patients. Most clinical forms are cervicofacial, thoracic, abdominopelvic, and cerebral. Thoracic actinomycosis may involve the lungs, pleura, mediastinum, or chest wall. The portal of entry is usually a break in the integrity of the mucosa or pulmonary aspiration. Infection in the lungs usually leads to the development of chronic pneumonia. Cough, low-grade fever, weight loss, and chest pain are the clinical findings [9].

The radiologic findings of pulmonary actinomycosis include: airspace consolidation; multifocal mass-like lesions, usually peripheral and not limited to pulmonary segments; cavitation with a thick irregular wall; mild enlargement of mediastinal lymph nodes; small pleural effusion or empyema; smooth, localized, mild pleural thickening adjacent to the airspace consolidation; and chest wall invasion. Actinomycotic intracavitary lung colonization leading to the formation of a fungus ball mimicking aspergilloma also has been reported (Fig. 4a), most frequently in patients with diabetes [10]. Computed tomography (CT) of intracavitary lung colonization shows a masslike lesion within a cavity. The “ball-in-hole” components may be actinomycete mycelia, with or without coexistent fungal infection in the cavities [11-13].

The presence of sulfur granules in the lesions is a characteristic histopathologic finding of actinomycosis. Microscopically, these granules are distinctive conglomerate masses of organisms that appear round or oval and have basophilic or amphophilic masses with a radiating rosette or fringe of eosinophilic clubs on the surface (Fig. 4b). Gram-staining reveals masses of Gram-positive branching filaments. Another histologic

feature of actinomycosis is an inflammatory pseudotumor of the organizing pneumonia type with marked fibroblastic proliferation and diffuse chronic inflammatory cells [13].

Nocardiosis

Nocardiosis is an opportunistic infection caused by *Nocardia*, an aerobic Gram-positive bacillus with microscopically visible branching hyphae. *Nocardia* may be found in soil, decomposing vegetation, and fresh and salt water. Approximately two-thirds of infections caused by this bacterium occur in immunocompromised patients. The incidence of nocardiosis is increasing, presumably due to the growing number of patients receiving immunosuppressive therapies for solid organ or hematopoietic stemcell transplants, hematologic, and solid tissue cancers, and autoimmune inflammatory conditions. The most common clinical presentation is pulmonary nocardiosis, because inhalation is the primary route of bacterial exposure. Symptoms can include productive or nonproductive cough, chest pain, hemoptysis, fever, night sweats, weight loss, and progressive fatigue. Other regions that may be affected include the central nervous system and skin, through hematogenous dissemination [14].

The predominant CT finding of nocardiosis is multifocal lung consolidation. Other findings include solitary lung nodules or multiple nodules of various sizes. A halo of ground-glass opacity surrounding a nodule or mass also may be present. Central low attenuation can occur in nodules or areas of consolidation, likely reflecting abscess formation; this characteristic is more visible on contrast enhanced CT because of rim enhancement. Over time, nodules or consolidations may cavitate. In such cases, endobronchial spreading can occur and is characterized by the presence of small centrilobular nodules [15]. Rarely, *Nocardia* may invade these cavities, mimicking

aspergilloma (Fig. 5) [16]. A small number of patients present pleural involvement and chest wall extension [15, 16].

Histopathologic examination reveals necrosis and abscess with accumulation of neutrophils, lymphocytes, and macrophages, but no granuloma formation. The definitive diagnosis of nocardiosis is obtained by the isolation and identification of the organism from biopsy or aspirate samples from affected sites or from respiratory secretion. *Nocardia* are Gram-positive and weak acid-fast bacteria (Fig. 5c). The weak acid fastness of *Nocardia* species, demonstrated by Kinyoun staining (modified Ziehl–Neelsen technique) is highly useful for differentiation from other actinomycetes, such as *Actinomyces* and *Streptomyces* species, which also are Gram-positive branching bacteria [16, 17].

Candidiasis

Candida species are common commensals from the oral cavity and genital tracts in up to 75% of individuals [18]. *Candida albicans* is a fungal pathogen that infects mainly mucocutaneous and urinary sites, and less frequently the lung. Pulmonary candidiasis is seen mainly in patients with hematologic malignancies (acute leukemia and lymphoma) and in intravenous drug users. Lung invasion is the result of dissemination or aspiration from the upper airway; the latter is particularly common in chronic debilitating disease [19].

The chest radiologic manifestations of candidiasis include patchy unilateral or bilateral airspace consolidation and poorly defined nodules, reflecting the presence of necrotizing bronchopneumonia. Occasionally, miliary disease is seen [19]. Furthermore, a large cavitation and even pulmonary abscess may be observed. These fungi can

accumulate in the airways in association with pulmonary disease, and thus occasionally manifest as a fungus ball mimicking aspergilloma on CT (Fig. 6) [19, 20].

The presence of *Candida* in respiratory specimens may be due to contamination, and this infection has no specific clinical radiologic picture. Therefore, the definitive diagnosis requires demonstration of the fungus in lung tissue with associated inflammation. *Candida* spp. are identified in tissue as oval-budding yeast and hyphae [19, 20].

Intracavitary Hematoma Due to Tuberculosis

TB is an infectious disease caused by organisms of the *Mycobacterium tuberculosis* complex (*M. tuberculosis*, *M. bovis*, and *M. africanum*). Infection occurs when susceptible persons inhale droplets produced by the exhalations of persons with respiratory tract TB [21]. Patients with active pulmonary TB may be asymptomatic, have mild or progressive dry cough, or present with multiple symptoms including fever, fatigue, weight loss, night sweats, and cough producing bloody sputum [22]. Massive hemoptysis can occur in active TB and inactive disease, with sequelae including bronchiectasis, cavitary disease with or without aspergilloma, and recurrent secondary pulmonary infection. One cause of hemoptysis is Rasmussen aneurysm (cavity disease), usually characterized by a solitary arterial aneurysm caused by focal inflammatory changes in the pulmonary artery wall. Abundant systemic bronchial circulation surrounds the site of infection, and the pulmonary vessels in and around a TB cavity form aneurysmal sacs, which can erode and bleed into the cavity, leading to hematoma formation. Little is known about the natural history of these aneurysms, but Sanika et al. [23] reported that they appear to be a major cause of persistent bleeding.

The radiologic finding of intracavitary hematoma mimicking aspergilloma in cavitary TB is a mass within a cavity (Fig. 7). This mass can have a blood density. CT with intravenous contrast may show filling of the pulmonary artery aneurysm when this is the cause of the pathologic process [22].

Adenocarcinoma

Lung cancer is the leading cause of cancer deaths in the United States and throughout the world [24]. Four cell types account for more than 95% of all primary lung neoplasms: (I) adenocarcinoma, (II) squamous cell carcinoma, (III) large cell carcinoma, and (IV) small cell carcinoma. Mixtures of these cell types may occur within the same primary neoplasm, and some tumors are too poorly differentiated to be further classified. Rapid growth, early metastatic spread, and responsiveness to chemotherapy and radiation therapy distinguish small cell carcinoma from the other types, which has led to the dichotomous classification of small cell or non-small-cell carcinoma. Adenocarcinoma is the most common cell type seen in women and nonsmokers [24].

The typical radiographic manifestation of lung cancer is a solitary pulmonary nodule or mass with well-margined, lobulated, irregular, or spiculated margins. Peripheral adenocarcinoma is the most common pathologic type of lung cancer and is detected with increasing frequency [25]. Peripheral adenocarcinoma may grow circumferentially around the lung and invade the pleura. Air bronchograms are frequent. Adenocarcinoma can have a lepidic pattern of growth, with cuboidal or columnar cells lining the walls of distal airspaces. A well-circumscribed peripheral solitary nodule or mass, frequently with a halo of ground-glass opacity, is the most common radiologic finding. Less common patterns include cavitation, multiple nodules, or extensive alveolar lung disease involving one or more lobes [25]. Lung cancer mimicking

aspergilloma, with the air crescent sign, is very rare. Even in lung cancers deriving from previous pulmonary injury, the majority of lesions are located at or derived from a fibrotic or granulomatous lesion, instead of a TB cavity. When lung cancer does occur in a previously existing TB cavity, an irregular and progressively enlarging nodular lesion is present within the cavity, in addition to typical fibronodular lesions distributed in the lung (Fig. 8). The tumor infiltrates the lung parenchyma with a paracatricial effect, inducing emphysematous or cystic changes between the tumor infiltrating bands [26].

Microscopically, adenocarcinoma is characterized by the formation of glands and papillary structures. The presence of significant mucin is an immunohistochemical finding.

Cases of aspergilloma within a malignant pulmonary cavity also have been reported. Lung cancers, such as adenocarcinoma and squamous cell carcinoma, have been reported in association with *Aspergillus* [27–29]. The patient's clinical history and positron emission tomography can help in the differential diagnosis of these lesions [26].

Pseudallescheriasis/Scedosporiosis

Pseudallescheria boydii (or *Scedosporium apiospermum*, the asexual anamorph) is an ascomycetous fungus that causes a wide array of human infections, which can affect practically all organs of the body [30–32]. These infections have been recognized for a long time, but a marked increase in the incidence of severe invasive infections, mainly in immunocompromised hosts, has been noted in recent years. This saprophytic fungus is ubiquitous worldwide, occurring in nutrient-rich, poorly aerated environments, such as polluted water [30, 31].

Pulmonary scedosporiosis may be caused by the asexual (*S. apiospermum*) and/or sexual (*P. boydii*) phase of the fungus. The spectrum of disease in the respiratory tract is similar in terms of variety and severity to that caused by *Aspergillus* [30, 31]. Differential diagnosis is mandatory because of the frequent resistance of *Scedosporium* to a variety of commonly used antimycotic agents. Symptoms include fever, cough, chest pain, and hemoptysis, but patients may be asymptomatic. Radiologic examination may show a crescent-shaped radiolucency capping a fungus ball, as seen in aspergilloma (Fig. 9). However, radiologic findings can be less specific, characterized by diffuse infiltration and consolidation [33].

The definitive diagnosis of respiratory tract intracavitary colonization by *S. apiospermum* (or *P. boydii*, the teleomorph) requires recovery of the organism by culture from the cavity. However, serum precipitins may be of aid in diagnosis and can be used in screening. When cultural confirmation is not possible, histopathologic examination can provide proof of the etiologic agent. On hematoxylin and eosin-stained sections, an *S. apiospermum* fungus ball is composed primarily of tangled, septate, hyaline hyphae, which can be distinguished from *Aspergillus* by direct immunofluorescence [30].

The classification of *P. boydii* as a complex comprising at least six different species (*P. boydii*, *P. angusta*, *P. ellipsoidea*, *P. fusoidea*, *P. minutispora*, and *S. aurantiacum*) has recently been proposed [31, 32].

Hydatid Disease

Hydatid disease is a zoonosis produced by the larval stage of the *Echinococcus* tapeworm [34, 35]. The infection has two principal varieties: the more widespread disease is caused by the larval form of the dog tapeworm *Echinococcus granulosus* and

is characterized by the formation of one or more expanding unilocular cysts, whereas the less common alveolar form is caused by *Echinococcus multilocularis* and produces destructive invasive lesions resembling malignancy. Dogs and carnivores are definitive hosts, and sheep and other ruminants are intermediate hosts. Humans are infected secondarily by the ingestion of food or water that has been contaminated by dog feces containing the eggs of the parasite and may become intermediate hosts. After the outer capsule of the egg has been ingested, the freed embryo enters a branch of the portal vein by passing through the duodenal mucosa. Most embryos become lodged in the hepatic capillaries, where they grow into hydatid cysts. Some pass through the capillary sieve and become lodged in the lungs and other organs [34, 36].

A hydatid cyst has three layers: (a) the outer pericyst, composed of modified host cells that form a dense and fibrous protective zone; (b) the middle laminated membrane, which is acellular and allows the passage of nutrients; and (c) the inner germinal layer, where the scolices and laminated membrane are produced [34].

The lungs are the second most frequent site of hematogenous spread in adults and probably the most common site in children. Cysts are multiple in 30 % of cases and located in the lower lobes in 60 % of cases. Calcification in pulmonary cysts is very rare [34, 35].

Clinical symptoms include coughing attacks, hemoptysis, and chest pain. After cyst rupture, expectoration of cyst fluid and scolices may occur. Rupture into the pleural cavity also may occur [34, 35].

Imaging appearances vary according to the growth of the parasite and its relationship to adjacent lung tissue. Uncomplicated cysts appear as well-defined masses. Cyst growth produces erosions in the bronchioles that are included in the pericyst, and air is introduced between the pericyst and the laminated membrane. This presentation is

known as the “crescent” or “meniscus” sign, a thin radiolucent crescent in the upper part of the cyst [34, 37]. Some authors consider it to be a sign of impending rupture [34]. This radiographic finding is the same as that found in aspergilloma, and hydatid disease may mimic this condition despite having a totally different etiologic agent (Fig. 10) [36, 37].

If air continues to enter the space between the pericyst and laminated membrane, the two layers separate completely and the cyst shrinks and ruptures, allowing the passage of air into the endocyst. An air-fluid level inside the endocyst and air between the pericyst and endocyst with an “onion peel” appearance constitute the “Cumbo” sign [34, 35]. After the partial expectoration of fluid, the cyst empties and collapsed membranes can be seen inside it, forming the “serpent” sign [34, 35]. When fluid is entirely evacuated by expectoration, the remaining solid components will fall to the most dependent part of the cavity (“mass within a cavity”) [34, 35]. CT and magnetic resonance imaging can demonstrate the stages of hydatid cysts described above [34–37], and thus allow the inclusion of hydatid disease in the differential diagnosis of aspergilloma in combination with laboratory test results.

Conclusions

A variety of pulmonary conditions, including those caused by other fungi, mycobacteria, neoplasia, and zoonoses (summarized in Table 1), can present with radiologic findings that mimic aspergilloma. Physicians should be aware of these diseases and corresponding clinical, radiologic, and histopathologic findings. A detailed anamnesis, including the acquisition of information about the patient’s travelling habits, migration, recreational activities, and residence in endemic areas, as well as the history

of any type of immunosuppression, also is essential. Precise diagnosis is crucial and may have implications for disease management and prognosis.

References

1. Zmieli OS, Soubani AO (2007) Pulmonary aspergillosis: a clinical update. *Q J Med* 100:317–334.
2. Soubani AO, Chandrasekar PH (2002) The clinical spectrum of pulmonary aspergillosis. *Chest* 121:1988–1999.
3. Aquino SL, Kee ST, Warnock ML, Gamsu G (1994) Pulmonary aspergillosis: imaging findings with pathologic correlation. *Am J Roentgenol* 163:811–815.
4. Thompson BH, Stanford W, Galvin JR, Kurihara Y (1995) Varied radiologic appearances of pulmonary aspergillosis. *Radiographics* 15:1273–1284.
5. Anstead GM, Graybill JR (2006) Coccidioidomycosis. *Infect Dis Clin North Am* 20(621):643.
6. Osaki T, Morishita H, Maeda H et al (2005) Pulmonary coccidioidomycosis that formed a fungus ball with 8-years duration. *Intern Med* 44(2):141–144.
7. Winn RE, Johnson R, Galgiani JN, Butler C, Pluss J (1994) Cavitary coccidioidomycosis with fungus ball formation. Diagnosis by fiberoptic bronchoscopy with coexistence of hyphae and spherules. *Chest* 105(2):412–416.
8. Tonelli AR, Khalife WT, Cao M, Young VB (2008) Spherules, hyphae, and air-crescent sign. *Am J Med Sci* 335(6):504–506.
9. Smego RA, Foglia G (1998) Actinomycosis. *Clin Infect Dis* 26:1255–1263.
10. Severo LC, Kaemmerer A, Camargo JJ, Porto NS (1989) Actinomycotic intracavitary lung colonization. *Mycopathologia* 108:1–4.
11. Coodley EL, Yoshinaka R (1994) Pleural effusion as the major manifestation of actinomycosis. *Chest* 106(5):1615–1617.

12. Hsieh MJ, Shieh WB, Chen KS, Yu TJ, Kuo HP, Tsai YH (1996) Pulmonary actinomycosis appearing as a “ball-in-hole” on chest radiography and bronchoscopy. *Thorax* 51(2):221–222.
13. Sarodia BD, Farver C, Erzurum S, Maurer JR (1999) A young man with two large lung masses. *Chest* 116(3):814–818.
14. Wilson JW (2012) Nocardiosis: updates and clinical overview. *Mayo Clin Proc* 87(4):403–407.
15. Kanne JP, Yandow DR, Mohammed TL, Meyer CA (2011) CT findings of pulmonary nocardiosis. *AmJ Roentgenol* 197(2):266–272.
16. Tilak R, Agarwal D, Lahiri T, Tilak V (2008) Pulmonary nocardiosis presenting as fungal ball—a rare entity. *J Infect Dev Ctries* 2(2):143–145.
17. Baldi BG, Santana AN, Takagaki TY (2006) Pulmonary and cutaneous nocardiosis in a patient treated with corticosteroids. *J Bras Pneumol* 32(6):592–595.
18. Cartledge J, Freedman A (2011) Candidiasis. *HIV Med* 12:70–74.
19. Abel AT, Parwer S, Sanyal SC (1998) Pulmonary mycetoma probably due to *Candida albicans* with complete resolution. *Respir Med* 92(8):1079–1080.
20. Bachh AA, Haq I, Gupta R, Varudkar H, Ram MB (2008) Pulmonary candidiasis presenting as mycetoma. *Lung India* 25(4):165–167.
21. Burrell J, Williams CJ, Bain G, Conder G, Hine AL, Misra RR (2007) Tuberculosis: a radiologic review. *Radiographics* 27(5):1255–1273.
22. Kim HY, Song KS, Goo JM, Lee JS, Lee KS, Lim TH (2001) Thoracic sequelae and complications of tuberculosis. *Radiographics* 21:839–860.
23. Sanyika C, Corr P, Royston D, Blyth DF (1999) Pulmonary angiography and embolization for severe hemoptysis due to cavitary pulmonary tuberculosis. *Cardiovasc Intervent Radiol* 22:457–460.

24. Patel JD (2005) Lung cancer in women. *J Clin Oncol* 23(14):3212–3218.
25. Parl CM, Goo JM, Lee HJ, Lee CH, Chun EJ, Im JG (2007) Nodular ground-glass opacity at thin section CT: histologic correlation and evaluation of change at follow-up. *Radiographics* 27(2):391–408.
26. Wang L, Chu H, Chen Y, Perng R (2007) Adenocarcinoma of the lung presenting as a mycetoma with an air crescent sign. *Chest* 131(4):1239–1242.
27. Smahi M, Serraj M, Ouadnoui Y, Chbani L, Znati K, Amarti A (2011) Aspergilloma in combination with adenocarcinoma of the lung. *World J Surg Oncol* 27(9):27.
28. Torpoco I, Yousuiddin M, Pate JW (1976) Aspergilloma within a cavitation. *Chest* 3:561–562.
29. Nilsson J, Restrepo CS, Jagirdar J (2013) Two cases of endobronchial carcinoid masked by superimposed aspergillosis: a review of the literature of primary lung cancers associated with *Aspergillus*. *Ann Diagn Pathol* 17:131–136.
30. Severo LC, Oliveira FM, Irion K (2004) Respiratory tract intracavitary colonization due to *Scedosporium apiospermum*: report of four cases. *Rev Inst Med Trop Sao Paulo* 46(1):43–46.
31. Kim M, Ahn MH, Kang JS, Lee H, Joo SI, Park SS, Kim EC (2009) Pulmonary fungal ball of *Pseudallescheria boydii* identified by LSU rDNA D2 region sequencing. *Korean J Clin Microbiol* 12(2):87–91.
32. Gilgado F, Cano J, Gene´ J, Guarro J (2005) Molecular phylogeny of the *Pseudallescheria boydii* species complex: proposal of two new species. *J Clin Microbiol* 43(10):4930–4942.
33. Al Refai` M, Duhamel C, Le Rochais JP, Icard P (2002) Lung scedosporiosis: a differential diagnosis of aspergillosis. *Eur J Cardiothorac Surg* 21(5):938–939.

34. Pedrosa I, Sai'z A, Arrazola J, Ferreiro's J, Pedrosa CS (2000) Hydatid disease: radiologic and pathologic features and complications. *Radiographics* 20(3):795–817.
35. Polat P, Kantarci M, Alper F, Suma S, Koruyucu MB, Okur A (2003) Hydatid disease from head to toe. *Radiographics* 23(2):475–494.
36. Manzoor MU, Faruqui ZS, Ahmed Q, Uddin N, Khan A (2008) Aspergilloma complicating newly diagnosed pulmonary echinococcal (hydatid) cyst: a rare occurrence. *Br J Radiol* 81(972):e279–e281.
37. Algin O, Go'kalp G, Topal U (2011) Signs in chest imaging. *Diagn Interv Radiol* 17(1):18–29.

Fig. 1 - A 78-year-old man presented with a 9-month history of cough and one episode of hemoptysis in the last day. He denied any history of fever or night sweats. His medical history included a reported 70-pack-year smoking habit and treatment for pulmonary tuberculosis 45 years previous. Axial computed tomographic (CT) images obtained in the pulmonary (a) and mediastinal (b) windows show thick-walled cavities containing fungus balls in the upper lobes of the lungs. An axial CT image obtained with the patient in the prone position (c) shows changes in the positions of the aspergillomas.

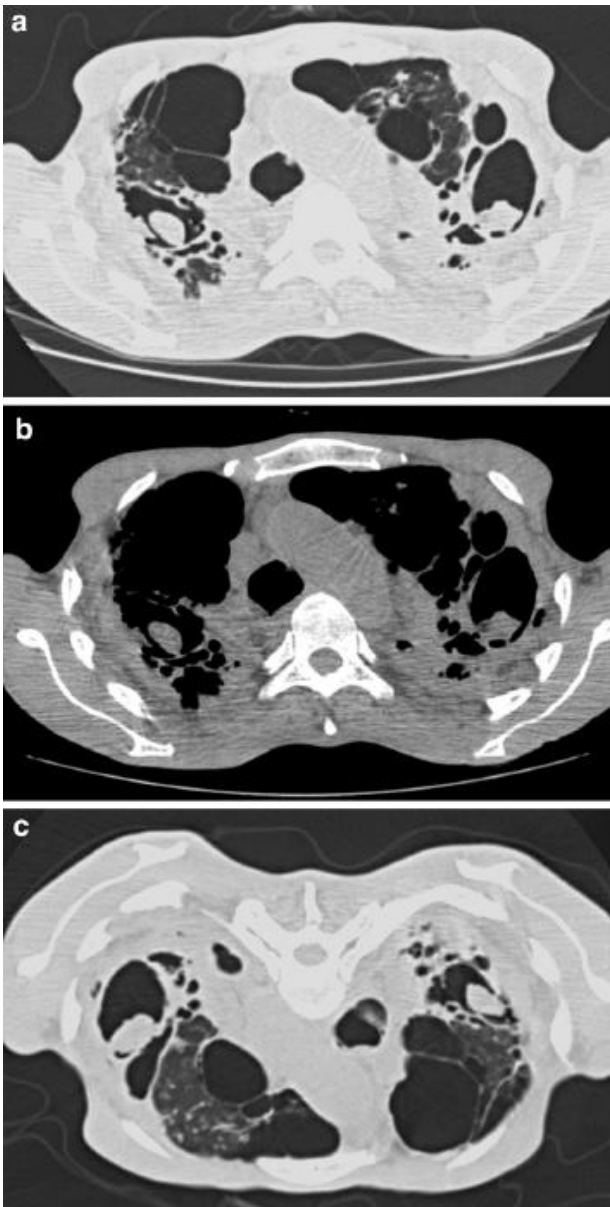


Fig. 2 - A 75-year-old man presented with a 3-month history of cough and one episode of hemoptysis in the last week. He denied any history of fever or night sweats. His medical history included a reported 60-pack-year smoking habit and treatment for pulmonary tuberculosis 30 years previously. (a) Magnetic resonance image (axial T1-weighted sequence) shows a thick-walled cavity containing a mildly hyperintense mass with the air crescent sign. (b) Magnetic resonance image (axial T1-weighted sequence) obtained with the patient in the prone position shows mobility of the fungus ball. (c) Photomicrograph of the surgical specimen shows a tangle of septate, dichotomously branching hyphae compatible with *Aspergillus* (Grocott-Gomori, x 20).

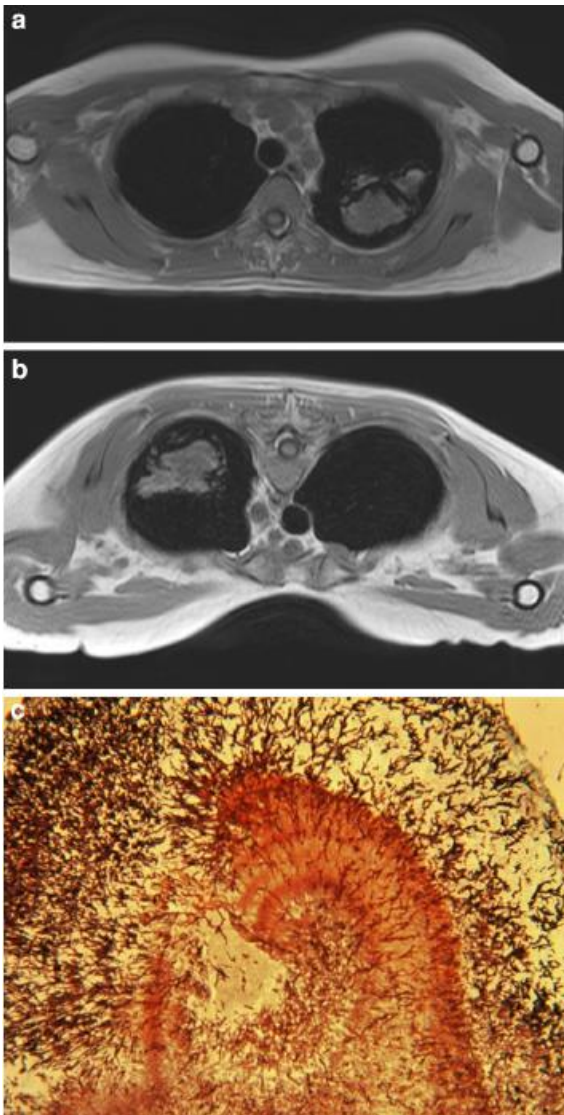


Fig. 3 - A 65-year-old man presented with productive cough. He denied any history of fever or night sweats. His medical history included a reported 45-pack-year smoking habit. (a) Axial computed tomographic image obtained in the pulmonary window shows a large cavity margined by pleural thickening containing a mass in the left upper lobe of the lung. (b) Microscopic examination showed yeast cells of *Coccidioides* in smear (Grocott, x 250).

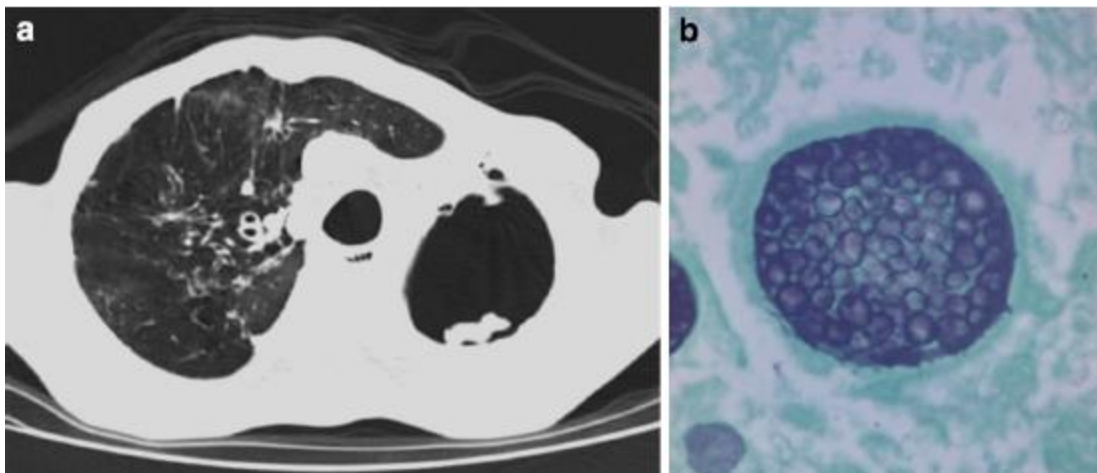


Fig. 4 - A 54-year-old man presented with a 3-month history of cough. He denied any history of fever or night sweats. His medical history included a reported 40-pack-year smoking habit, diabetes, and treatment for pulmonary tuberculosis 35 years previously. (a) Axial computed tomographic image obtained in the pulmonary window shows a thick-walled cavity containing a mass with the air crescent sign in the left upper lobe of the lung. (b) Microscopic examination of biopsy specimens showed yeast cells of *Actinomyces* in smear (Gram, x250).

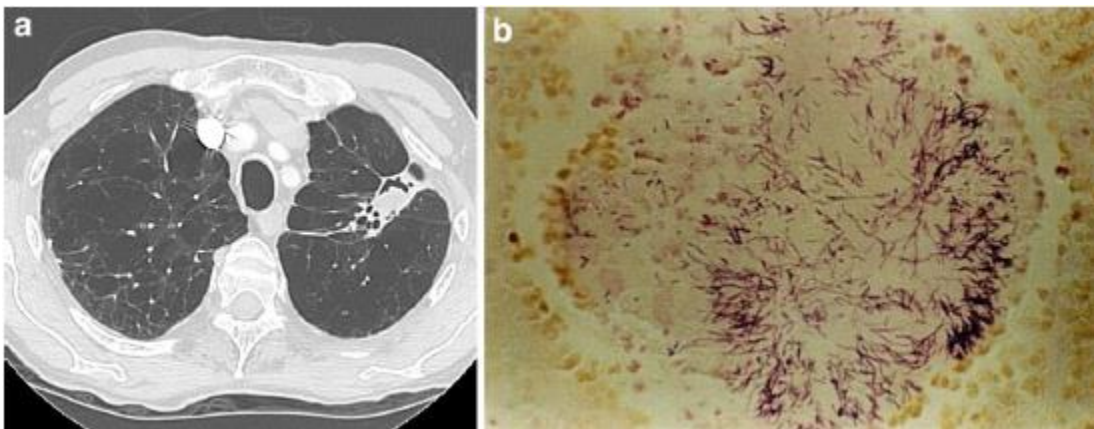


Fig. 5 - A 33-year-old man presented with a 3-month history of right chest pain. He denied any history of fever or night sweats. His medical history included bronchiectasis. Axial computed tomographic images obtained in the pulmonary (a) and mediastinal (b) windows show a thin-walled cavity containing a mass with the air crescent sign in the lingula. Microscopic examination (c) of the surgical specimen confirmed the diagnosis of nocardiosis; showed weak acid-fast and Gram-positive organisms (right Ziehl-Neelsen; left Gram, x100).

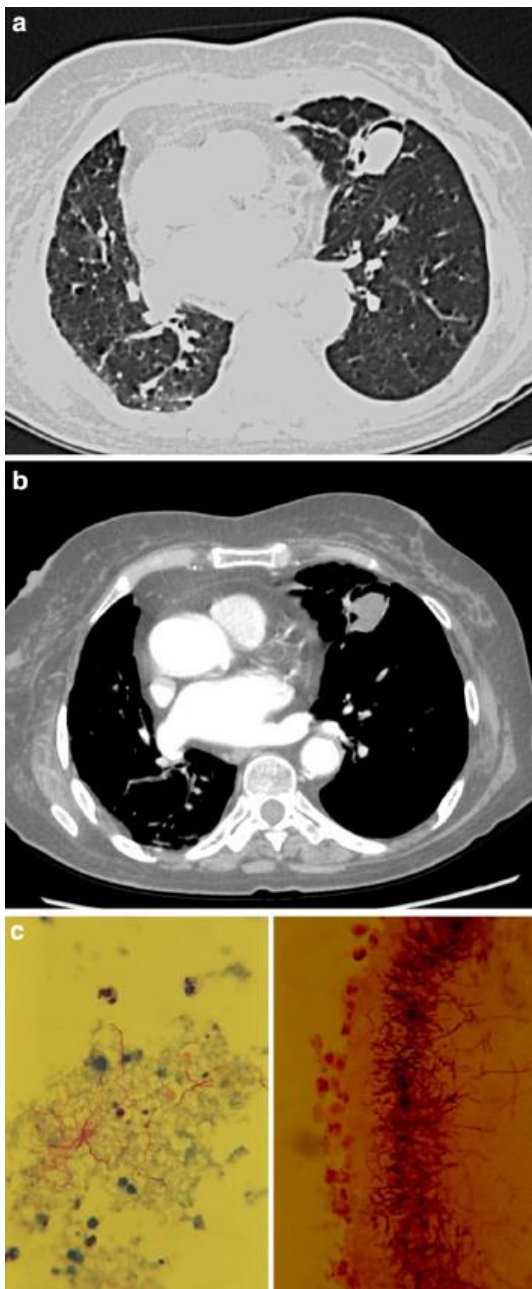


Fig. 6 - A 49-year-old woman presented with chronic cough. She denied any history of fever or night sweats. Her medical history included a reported 25-pack-year smoking habit. (a) Axial computed tomographic (CT) image shows a thin-walled cavity containing a mass with the air crescent sign in the right lower lobe of the lung. (b) A reconstructed sagittal CT image shows that the cavity is characterized by cystic bronchiectasis with a fungus ball. Microscopic examination of the surgical specimen led to the diagnosis of *Candida norvegensis* infection.

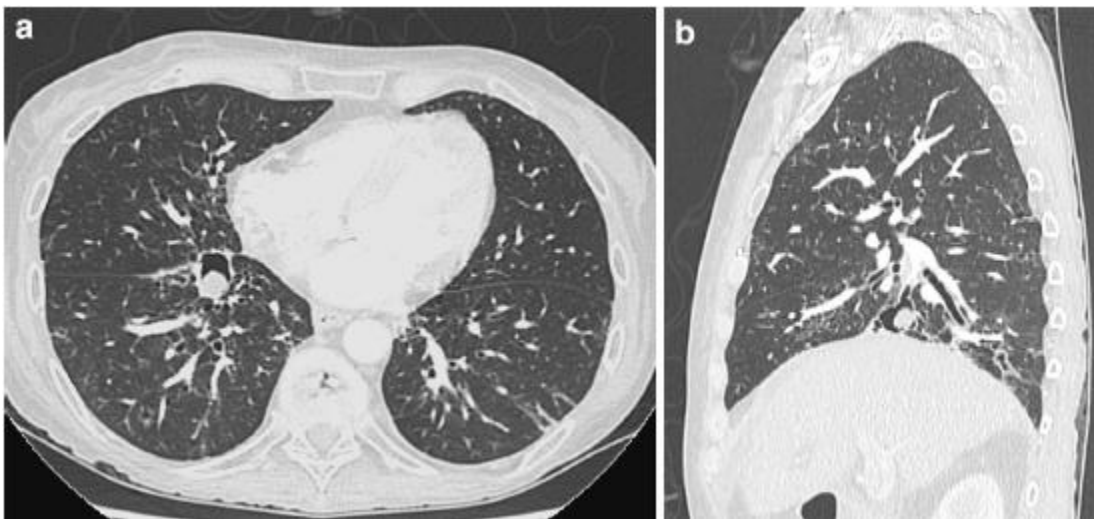


Fig. 7 - A 79-year-old man presented with active hemoptysis. He had a history of low-grade fever and night sweats. His medical history included a reported 60-pack-year smoking habit and previous treatment for pulmonary tuberculosis. Axial (a) and coronal (b) computed tomographic images show a cavitated pulmonary mass with irregular thick walls and the air crescent sign, associated with centrilobular tree-in-bud nodules in the right upper lobe of the lung. The patient underwent surgery to treat hemoptysis, which allowed confirmation of the diagnosis of *Mycobacterium tuberculosis* infection and intracavitary hematoma.

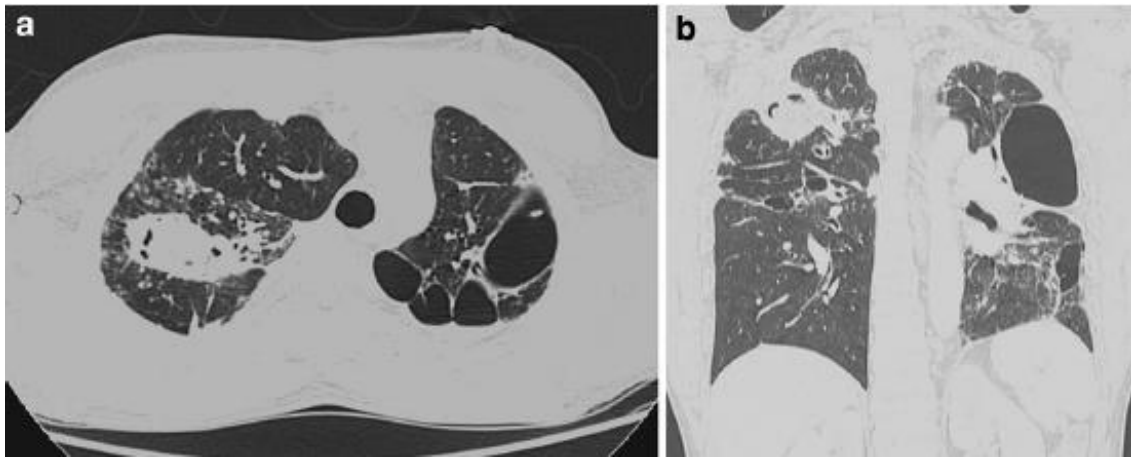


Fig.8 - A 63-year-old male kidney transplant recipient presented with a 1-month history of cough. His medical history included a reported 30-pack-year smoking habit and previous treatment for pulmonary tuberculosis. Axial computed tomographic (CT) images obtained in the pulmonary (a) and mediastinal (b) windows and a reconstructed coronal CT image (c) show a cavitated pulmonary mass with irregular thick walls and the air crescent sign in the left upper lobe of the lung. The patient underwent surgery and the diagnosis of scarring associated with lepidic growth adenocarcinoma was confirmed.

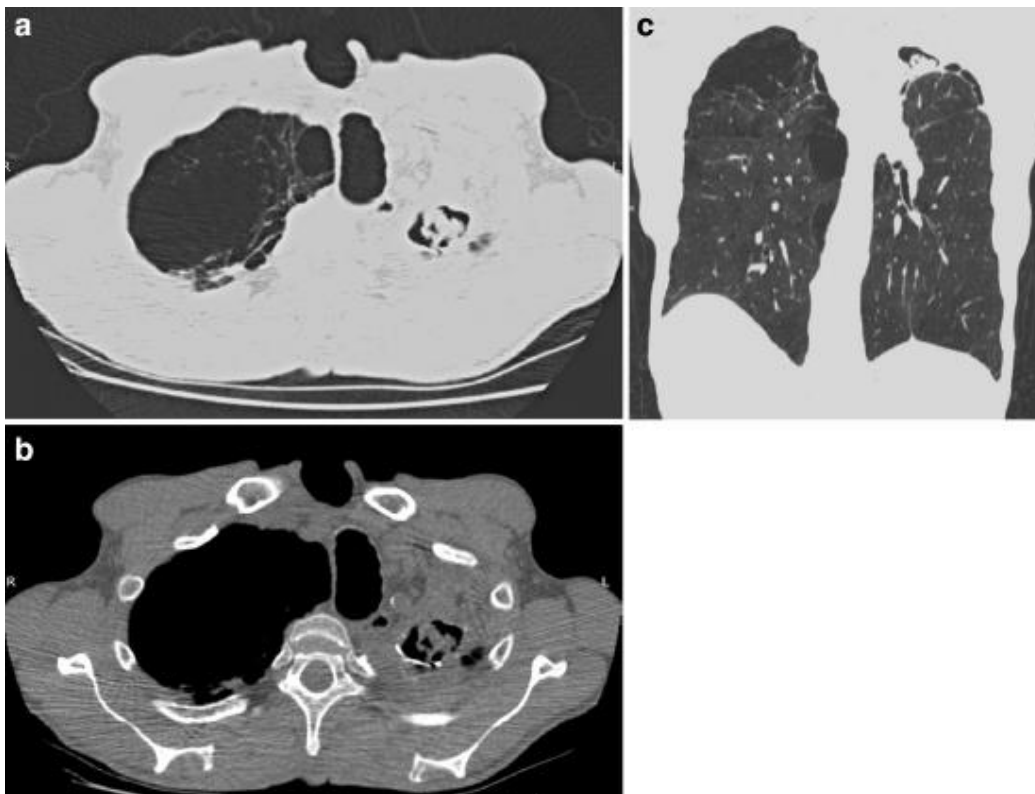


Fig. 9 - A 48-year-old woman presented with chronic cough. She denied any history of fever or night sweats. Her medical history included a reported 25-pack-year smoking habit. Axial computed tomographic (CT) images obtained in the pulmonary (a) and mediastinal (b) windows and a reconstructed coronal CT image (c) show scarring in the right upper lobe and a thick-walled cavity containing a mass surrounded by gas (air crescent sign). The patient underwent surgery and the diagnosis of a fungus ball due to *Pseudallescheria boydii* was confirmed.

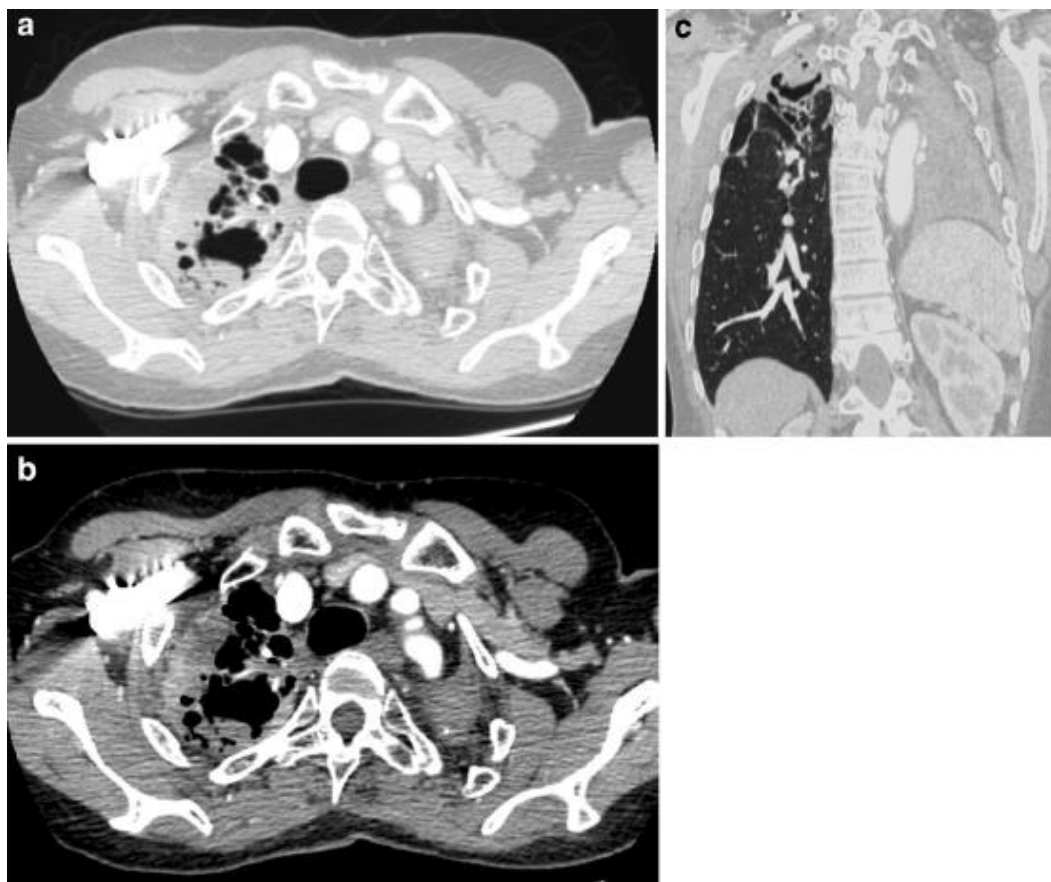


Fig.10 - A 28-year-old man presented with acute and productive cough, followed by the expectoration of clear fluid. He denied any history of fever or night sweats. Axial computed tomographic images obtained in the pulmonary (a) and mediastinal (b) windows show a cavitated pulmonary mass with irregular thick walls and the air crescent sign. The solid component represents the detached, crumpled endocyst. The patient underwent surgery and the diagnosis of hydatid cyst was confirmed.

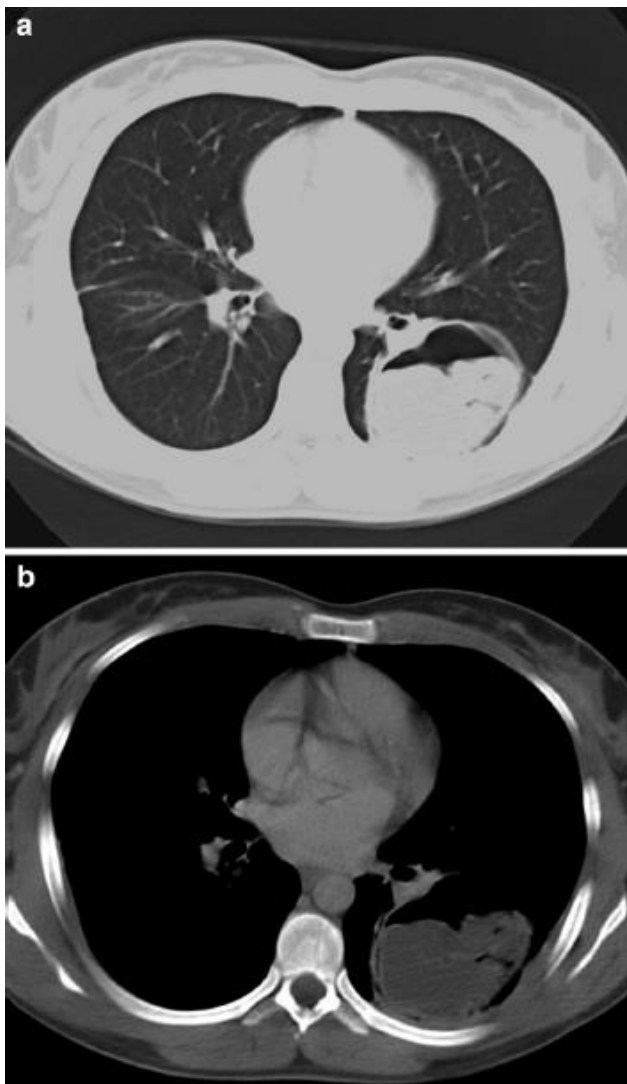


Table 1 Pulmonary diseases with imaging findings mimicking aspergilloma

Lung disease/etiology	Characteristics	Presentation as a fungus ball	Typical radiological findings	Diagnosis
Coccidioidomycosis [5–8] <i>C. immitis</i> and <i>C. posadasii</i>	Primary fungal pathogen	Coccidioidal fungus ball occurs rarely in a preexisting cavity	Peripheral lung nodules that are predominantly cavitated	Culture, biopsy, ID. Presence of spherules in tissue specimens
Actinomycosis [9, 10, 13] <i>Actinomyces</i> spp.	Usually in immunocompetent persons	Actinomycotic intracavitary lung colonization has also been reported	Airspace consolidation; mass-like lesions, not limited to pulmonary segments; cavitation; chest wall invasion	Culture, biopsy. Sulfur granules are characteristic in histopathology
Nocardiosis [14–16] <i>Nocardia</i> spp.	Opportunistic infection	Rarely may invade cavities mimicking aspergilloma	Multifocal consolidation and nodules; cavitation	Culture, biopsy, aspirate. Gram-positive, weak acid-fast bacillus
Candidiasis [19, 20] <i>Candida</i> spp.	Opportunistic infection	These fungi can accumulate in the airways, and occasionally manifest as a fungus ball	Patchy unilateral or bilateral consolidation and poorly defined nodules; cavitation; military disease	Biopsy; diagnosis requires demonstration of the fungus in lung tissue with associated inflammation
Intracavitary hematoma due to tuberculosis [21–23] <i>Mycobacterium tuberculosis</i> complex	Pulmonary artery aneurysm	Intracavitary hematoma can mimic aspergilloma	A mass within a cavity, that can have a blood density	CT with intravenous contrast may show filling of the arterial aneurysm. Bacilloscopy, culture
Lung cancer [24–26] Adenocarcinoma	The tumor infiltrates the lung parenchyma with a paracavitary effect	Lung cancer mimicking aspergilloma is rare. Progressively enlarging nodular lesion within a cavity	Well-circumscribed peripheral solitary nodule or mass	Biopsy
Pseudallescheriasis/Scedosporiosis [30–33] <i>Pseudallescheria boydii</i> or <i>Scedosporium apiospermum</i>	Saprophytic fungus	The spectrum of disease is similar to that caused by <i>Aspergillus</i> . CT may show a “ball-in-hole” aspect, as seen in aspergilloma	It can be less specific with diffuse infiltration and consolidation	Culture, biopsy. Septate hyphae, which can be distinguished from <i>Aspergillus</i> by direct IF
Hydatid disease [34–36] Larval stage of the <i>Echinococcus</i> tapeworm	Humans may become intermediate hosts	Cyst growth produces erosions in the bronchioles, and air is introduced between the pericyst and the laminated membrane (“crescent” sign, as seen in aspergilloma)	Imaging appearances vary according to growth of the parasite	Serological tests; examination of the fluid of the cyst

ID immunodiffusion; IF immunofluorescence; CT computed tomography

9.3

FUNGAL DISEASES MIMICKING PRIMARY LUNG CANCER: RADIOLOGIC-
PATHOLOGIC CORRELATION

GAZZONI, F.F.; SEVERO, L.C.; MARCHIORI, E.; GUIMARÃES, M.D.; GARCIA,
T.S.; IRION, K.L.; GODOY, M.C.; SARTORI, A.P.G.; HOCHHEGGER, B.

Mycoses, 2014, 57, 197–208

História do artigo:

Submetido: 20 de Abril de 2013.

Aceito após revisão: 24 de Setembro de 2013.

Abstract:

A variety of fungal pulmonary infections can produce radiologic findings that mimic lung cancers. Distinguishing these infectious lesions from lung cancer remains challenging for radiologists and clinicians. In such cases, radiographic findings and clinical manifestations can be highly suggestive of lung cancer, and misdiagnosis can significantly delay the initiation of appropriate treatment. Likewise, the findings of imaging studies cannot replace the detection of a species as the aetiological agent. A biopsy is usually required to diagnose the infectious nature of the lesions. In this article, we review the clinical, histologic and radiologic features of the most common fungal infections that can mimic primary lung cancers, including paracoccidioidomycosis, histoplasmosis, cryptococcosis, coccidioidomycosis, aspergillosis, mucormycosis and blastomycosis.

Keywords: Fungal; fungal infections; fungal diseases; lung cancer; computed tomography.

INTRODUCTION:

Lung cancer is the leading cause of cancer-related deaths worldwide, with a 5-year survival rate of less than 15%. In 2010, approximately 28% of all cancer deaths were related to lung cancer [1]. Radiology is the main tool used for the diagnosis and staging of lung cancer. Recent studies have demonstrated that lowdose computed tomography (CT) screening can reduce mortality related to lung cancer by at least 20% [1]. In this context, knowledge of the main radiologic mimickers of this cancer is critical.

The main radiologic features suggestive of lung cancer include a parenchymal nodule or mass with irregular margins, lobulations, a thick-walled cavity and chest wall invasion [2–4]. However, several pulmonary infectious diseases occasionally cause inflammatory lung lesions resembling pulmonary carcinoma [2–4]. Despite improvements in imaging studies, serologic/microbiologic testing and interventional bronchoscopic/ radiologic procedures, accurate diagnosis remains challenging [3]. The diversity of infectious agents involved, including bacteria [2], mycobacteria [2,3], fungi [4,5], and viruses [6], adds further difficulty. In a series of 2908 patients with a presumed diagnosis of lung cancer who underwent biopsy, fungal infection was the most common pulmonary infection that mimicked cancer, accounting for 46% of diagnosed infections [3]. The clinical manifestations and radiographic findings of such infections are indistinguishable from those produced by pulmonary neoplasms [2,3,7].

In this article, we review the clinical, histologic and radiologic features of the most common fungal infections that mimic primary lung cancers, including paracoccidioidomycosis (PCM), histoplasmosis, cryptococcosis, coccidioidomycosis, aspergillosis, mucormycosis, and blastomycosis.

DISCUSSION:

Paracoccidioidomycosis

Paracoccidioidomycosis is the most common systemic mycosis in Latin America. Although most cases occur in developing countries, recent immigration patterns have increased the numbers of cases appearing in the United States and Europe [8]. PCM is caused by dimorphic fungi *Paracoccidioides brasiliensis* and *P. lutzii*, which are transmitted by an airborne route [8–10]. Depending on the immune status of the host, the primary infection can resolve or develop into a progressive disease with an acute, subacute or chronic course [8,9]. Lung involvement usually presents non-specifically with cough, progressive dyspnoea and diffuse inspiratory crackles on physical examination.

Computed tomography is the method of choice for the evaluation of pulmonary PCM. CT findings are pleomorphic and include ground-glass attenuation, consolidation, small or large nodules, the ‘reversed halo’ sign, masses, cavitations, interlobular septal thickening, emphysema and fibrotic lesions [8,11–13]. In rare cases, the presence of a mass or spiculated nodule suggesting lung cancer is the main feature of PCM (Fig. 1) [9].

Biopsy should be performed to establish the correct diagnosis as soon as possible [9]. Typical histologic findings include granulomatous inflammation with extensive interstitial and conglomerate fibrosis, necrosis, arterial intimal fibrosis and directly identifiable fungi. In the absence of the characteristic budding forms of *Paracoccidioides* on histologic specimens, infection by this organism can be difficult to distinguish from other fungal infections. In addition to microbiologic and histologic methods, immunodiffusion (ID) is an important tool for the diagnosis of PCM, with a

sensitivity of 84.3% and specificity of 98.9% [9]. PCM can also affect and mimic cancer in almost all other sites, such as the larynx, central nervous system (CNS) and colon [14,15].

Histoplasmosis

Histoplasmosis is a fungal infection caused by the dimorphic fungus *Histoplasma capsulatum*, classically considered to be endemic mycosis. Currently, it is highly prevalent in certain areas of the United States (central and southern US, Mississippi and Ohio river valleys), Mexico, Panama and several Caribbean islands and South American countries [16,17]. The clinical features of histoplasmosis vary, including asymptomatic infection, chronic disease mimicking tuberculosis in patients with underlying emphysema and disseminated severe forms affecting patients with acquired immunodeficiency syndrome or haematologic malignancies and allograft recipients [16–18]. The majority of infections caused by *H. capsulatum* are asymptomatic or subclinical, self-limiting illnesses [19,20].

The histopathologic findings of histoplasmosis are epithelioid granulomas that caseate, then fibrose (resembling lesions caused by *Mycobacteria tuberculosis*). In silver staining, the fungal walls are black and organisms are small (2–4 µm in diameter), uninucleate and spherical to ovoid; they have single buds and are often clustered.

In a retrospective 3-year series, histoplasmosis was the most common fungal infection that mimicked lung cancer [3]. In endemic regions, this fungal infection should thus be included in the differential diagnosis of neoplasia [16]. The most common radiologic finding of acute pulmonary histoplasmosis is the presence of bilateral and mediastinal hilar lymph node enlargement associated with bilateral perihilar reticulonodular infiltrate [16–20]. The radiologic findings of chronic

pulmonary histoplasmosis are similar to those of adult or reinfection tuberculosis: progressive infiltrate in the upper lobe, cavitation and signs of fibrosis. Mediastinal enlargement can be seen principally on chest CT images of patients with mediastinal fibrosis secondary to histoplasmosis [19,20]. The presence of a solitary nodule or multiple nodules with central calcification is characteristic of the nodular form, histoplasmoma [19–21]. Typically, histoplasmomas have laminated calcific rings [16,20]. The presence of this feature on a chest radiograph can lead to a misdiagnosis of lung cancer (Fig. 2) [18]; thus, recognition of the benign pattern of calcification is important to distinguish this infection from bronchogenic carcinoma [22–25].

Currently, F-18 fluorodeoxyglucose positron emission tomography (FDG-PET) is widely used and considered to be accurate for the evaluation of lung cancer. However, the PET finding of intense F-18 FDG uptake in a lesion is a common finding in both histoplasmosis and lung cancer, significantly reducing the accuracy of PET as a diagnostic modality for lung cancer in endemic regions of histoplasmosis (Fig. 3) [24]. In an endemic region of granulomatous diseases, the specificity of FDG-PET for the diagnosis of lung cancer was 40% [24].

Serological tests available for the diagnosis of histoplasmosis include the complement fixation (CF) using histoplasmin, and the ID assay. Diagnosis is based on a fourfold rise in CF antibody titre. A single titre equal to or greater than 1:32 is suggestive, but not diagnostic. The CF test is less specific than the ID assay because cross-reactions occur with other fungal and granulomatous infections [26,27]. The ID assay is approximately 80% sensitive, but is more specific than the CF assay. Tests for antibody are most useful in patients who have chronic forms of histoplasmosis that have

allowed enough time for antibody to develop. In patients who have acute pulmonary histoplasmosis, the documentation of a fourfold rise in antibody titre to *H. capsulatum* can be diagnostic. However, it may require 2–6 weeks for the appearance of antibodies. The utility is also lower in immunosuppressed patients, who mount a poor immune response [28]. The antigen detection method is more useful for the serological diagnosis of disseminated histoplasmosis in AIDS patients. In this population, Histoplasma antigen was detected in urine in 95% and in serum in 86% of patients, respectively [29].

Cryptococcosis

Cryptococcosis is an infection caused by an encapsulated fungus of the genus *Cryptococcus* (*C. neoformans* or *C. gattii*). The infection caused by the species *C. neoformans* has become the most relevant opportunistic infection in the HIV era. *Cryptococcus gattii* is considered to be a primary fungal pathogen because it virtually always affects immunocompetent patients [30]. *Cryptococcus neoformans* is a ubiquitous fungus, found particularly in soil contaminated by pigeon droppings and in tree hollows [25,30–32]. *Cryptococcus gattii* occurs mainly in tropical and subtropical climates and is associated with certain species of the Eucalyptus tree. However, a recent outbreak of *C. gattii* in Vancouver Island shows that the distribution of *C. gattii* is changing, with its ability to associate itself with a wide variety of trees, such as firs and oaks [30].

Pulmonary cryptococcosis (PC) is caused by the inhalation of spores from *Cryptococcus* spp., with effects ranging from a self-limiting, asymptomatic pulmonary infection to severe pneumonia in cases of immunosuppression or massive inoculation of the yeast [25,33,34]. Patients with acute PC can present fever, productive cough, chest pain and weight loss. The CNS could be affected, with cerebral and meningeal

involvement, as a result of dissemination from the lungs [33,34]. In immunocompromised patients, symptoms related to the systemic dissemination of the organism, typically to the CNS, usually predominate [31–34].

Radiographically, PC may manifest as a solitary lung nodule or mass, multiple nodules, segmental or lobar consolidation, or, rarely, interstitial pneumonia (more common in immunosuppressed patients). Associated features include cavitation, lymphadenopathy and pleural effusion [25,31–34]. When presenting as a solitary nodule or mass, cryptococcosis can mimic lung cancer (Fig. 4) [3,25,32].

The manifestations of infection by *C. neoformans* and *C. gattii* can be different [30,35]. *Cryptococcus neoformans* affects immunocompromised patients, with a tendency to cause diffuse pulmonary involvement associated with meningitis. *Cryptococcus gattii*, however, are more likely to cause focal pulmonary disease in immunocompetent hosts with large inflammatory masses, called cryptococcomas [30,35]. *Cryptococcus gattii* is less likely to cause CNS disease than *C. neoformans*, but more likely to form cryptococcomas in brain [30,35].

Cryptococcus antigen detection using latex agglutination assays on cerebrospinal fluid (CSF) or serum specimens is useful in the initial diagnosis. The reported sensitivity for latex agglutination assays ranges from 54% to 100%, with higher sensitivity in patients with CNS infection or pneumonia [35]. False-negative results may occur in cases with encapsulated nodules, or when patients have an overwhelming disease such that the amount of serum antigen in the sample is in excess of the amount of antibody in the assay, the prozone effect [35,36]. False-positive results may occur with *Trichosporon beigeli* infection [35].

Therefore, the diagnosis of pulmonary disease requires direct evidence of *Cryptococcus* in sputum, bronchial washing, bronchoalveolar lavage fluid or lung

tissue. Histopathological identification of the cryptococcosis is based on the micromorphological and staining features of the cryptococcal cells, and include histochemical techniques of haematoxylin and eosin (HE) and Grocott's silver stain (GMS), as well as Mayer's mucicarmine method (MM), which stains the capsule magenta [25,37]. The Fontana–Masson procedure is a special technique, which stains fungal melanin reddish-brown, useful in the uncommon cases of capsule deficient form [37]. However, these direct and histological stains do not differentiate between the species; only culture leads to *Cryptococcus* species and variety identification [35].

Coccidioidomycosis

Coccidioidomycosis is a systemic mycosis caused by dimorphic fungi, endemic to arid and semiarid regions in the south-western United States and northern Mexico, and in certain areas of Central and South America [38–41]. Initially, it was thought that coccidioidomycosis was only caused by the fungus *Coccidioides immitis*. Based on molecular phylogeny studies, the existence of another species has been recently demonstrated. It is currently established that *C. immitis* is a fungus that is endemic in California, particularly in the San Joaquin Valley. The other species was 'hidden' with *C. immitis* and was designated as *C. posadasii*, after Alexandre Posadas, the man who discovered it. *C. posadasii* is prevalent in all the remaining endemic areas of the American continent, from the Southern United States to Argentina. The semiarid north-eastern region of Brazil has recently been identified as an area endemic for coccidioidomycosis [41].

Approximately 60% of human primary infections are asymptomatic; the majority of symptomatic cases are characterised by mild-to-severe acute pulmonary infection that generally resolves spontaneously. Progressive pulmonary

coccidioidomycosis is generally chronic and develops after the first infection, with symptoms failing to resolve after 2 months [38–40].

Progressive pulmonary coccidioidomycosis may have the following presentations: 1) nodular or cavitory lesions, sometimes as an incidental radiologic finding; 2) cavitory lung disease with fibrosis and 3) miliary pulmonary dissemination with non-specific clinical and radiologic manifestations. The most common finding on chest X-rays is multiple, peripherally distributed lung nodules associated with parenchymal consolidation. Chest CT images reveal peripheral lung nodules that are predominantly cavitated [5,41,42]. This pathology usually simulates metastatic cancer. However, due to its chronic progression, the inclusion of progressive pulmonary coccidioidomycosis in the differential diagnosis of lung cancer and other granulomatous lung diseases is important (Fig. 5) [5,43].

Coccidioides sp. inhaled into the lung develop into thin-walled spherules that rupture and release numerous endospores, causing a granulocytic response that is histologically non-specific unless spherules and endospores can be recognised. As the inflammatory response progresses, an epithelioid granuloma containing large histiocytes and giant cells is formed [38–41]. Central necrosis and a variable degree of fibrosis may be observed as healing occurs. The diagnosis of coccidioidomycosis is made by the isolation of *Coccidioides* sp. in culture or by positive results from smear microscopy (10% potassium hydroxide test), periodic acid- Schiff (PAS) staining or silver staining of any suspect material (e.g. sputum, CSF, skin exudate, lymph node aspirate); the characteristic parasitic form is the spherule [41]. Agar gel ID is the most widely used diagnostic test [5,41,42].

Aspergillosis

Pulmonary aspergillosis refers to a clinical spectrum of lung diseases caused by species of the *Aspergillus* genus (usually *A. fumigatus*), a ubiquitous genus of soil fungi. The manifestations of pulmonary aspergillosis are determined by the number and virulence of organisms and the patient's immune response. The spectrum can be subdivided into five categories: saprophytic aspergillosis (aspergilloma), hypersensitivity reaction (allergic bronchopulmonary aspergillosis), semiinvasive (chronic necrotising) aspergillosis, airway-invasive aspergillosis and angioinvasive aspergillosis [43,44]. Angioinvasive disease and aspergilloma have been reported to mimic malignancy [3,7,45]. In a 3-year review, only one case of aspergillosis was recorded among fungal infections accounting for 46% of lesions simulating neoplasms. In another series, 3/13 cases of inflammatory lesions imitating pulmonary carcinoma were subsequently identified as aspergilloma [7].

Aspergilloma is the most common pulmonary manifestation of aspergillosis that mimics neoplasia. It is characterised by *Aspergillus* colonisation without tissue invasion. The fungus colonises an existing pulmonary cavity, bulla or ectatic bronchus, forming a mass of intertwined fungal hyphae admixed with mucus and cellular debris. The most common underlying causes of the infection are tuberculosis and sarcoidosis. Although patients remain asymptomatic, the most common clinical manifestation is haemoptysis [25,43,46]. On CT, aspergilloma is characterised by the presence of a solid, round mass with soft-tissue density within a lung cavity [46]. These characteristics can simulate neoplasia (Fig. 6). However, the aspergilloma usually moves when the patient changes position [43]. Therefore, the acquisition of CT images with the patient in the dorsal and ventral decubitus positions is important for differential

diagnosis. Another finding of aspergilloma is thickening of the cavity wall and adjacent pleura, which may be the earliest radiographic sign [43].

The angioinvasive form of aspergillosis has also been described as simulating neoplasia. It is characterized by hyphal invasion and occlusion of small-to-medium sizes arteries and destruction of normal lung tissue [43–46]. Angioinvasive aspergillosis occurs almost exclusively in immunocompromised patients with severe neutropenia due to haematologic malignancies, and those who have undergone haematopoietic stem cell transplantation [44–47]. Among the recipients of solid-organ transplants the incidence of angioinvasive disease is lower because neutropenia is not the principal immunologic defect affecting these patients [48,49]. Angioinvasive aspergillosis is manifested clinically as a rapid progressive respiratory illness with cough, chest pain and haemoptysis. These clinical features are distinct from lung cancer, and suggest an infectious, rather than neoplastic disease. Characteristic CT findings consist of nodules surrounded by a halo of ground-glass attenuation (halo sign), or pleura-based, wedge-shaped areas of consolidation. The reversed halo sign (ground-glass opacity surrounded by a halo of consolidation) may also suggest this infection [44–47].

In tissue sections, *Aspergillus* hyphae characteristically appear as uniform, narrow (3–6 μm in width), tubular and regularly septate (usually 45°) elements. Branching is regular, progressive and dichotomous. Hyphal branches tend to arise at acute angles from parent hyphae. Special stains for fungi, like PAS and GMS are superior to HE for the characterisation of hyphal morphology [44,46].

Mucormycosis

Mucormycoses are a group of invasive, often fatal, opportunistic infections caused by fungi belonging to the class *Zygomycetes*, order *Mucorales*. Most clinically significant infections are caused by fungi of the genera *Lichtheimia*, *Rhizopus*, *Mucor* and *Cunninghamella* [50–55]. Risk factors for infection include haematologic malignancy, diabetes, organ transplantation, immunosuppression, graft-vs.-host disease and desferoxamine therapy. The majority of these risk factors act by impairing neutrophil function [55]. Six distinct clinical syndromes are recognised: rhinocerebral, pulmonary, abdominopelvic, cutaneous, widely disseminated and miscellaneous mucormycosis.

The clinical presentation is associated with the predisposing conditions of the host. The principal presentation is the rhinocerebral form, which typically affects diabetic patients in ketoacidosis. Pulmonary infection is the second-most common form, accounting for more than 30% of infections [51]. The clinical hallmark of pulmonary mucormycosis is rapidly progressive pneumonia with angioinvasion and tissue necrosis, which is far more common in patients with haematologic malignant neoplasms. Symptoms include fever, cough, chest pain and dyspnoea. An indolent clinical course with a better outcome is commonly seen in diabetic patients [25,50]. Due to the rapidly progressive clinical picture, mucormycosis infection is not often confused with lung cancer. However, such misdiagnoses have been reported in the literature [53]. Thus, the radiological findings must be correlated with the clinical scenario.

The radiologic manifestations of pulmonary mucormycosis are non-specific and include progressive lobar or multilobar consolidation, pulmonary masses and nodules and the reversed halo sign [25,47,51]. Cavitation is seen in up to 40% of cases, but the air crescent sign is uncommon. The upper lobes are most commonly involved [51]. This

infection may be associated with mediastinal or hilar adenopathy, vascular invasion and extrapulmonary involvement [51]. Horner's syndrome is rarely seen [54]. Rarely, radiologic aspects of mucormycosis have been described to simulate lung neoplasm (Fig. 7) [2,54].

On histopathologic examination, *Zygomycetes* hyphae are broad and irregular with right-angled branching, as opposed to *Aspergillus* hyphae, which are thinner with more acute-angled branching [50–55]. Pulmonary angioinvasion, vascular thrombosis or necrosis may be observed [55]. The mortality rate associated with mucormycosis is high; massive haemoptysis, secondary bacterial infection and acute respiratory failure are the most common causes of death [24,50–55]. Early diagnosis is of utmost importance because the early initiation of high-dose antifungal therapy is associated with improved outcomes.

It is very important to note that other invasive mycoses, like scedosporiosis and fusariosis, may affect lungs. Likewise, the clinical and radiological aspects of these infections are similar to those observed in other invasive filamentous fungi infections, such as invasive aspergillosis and mucormycosis [56–59].

Blastomycosis

Blastomycosis is an uncommon fungal pathologic condition. It is caused by *Blastomyces dermatitidis*, a thermally dimorphic fungus endemic to Canada and the upper Midwest of the United States. Outside of North America, blastomycosis has been found in Africa [60]. Human exposure occurs when fungi in soil with organic content are disturbed, especially during outdoor activities. Inhaled airborne spores cause primary lung infection, which may become disseminated [60]. Affected patients may be asymptomatic or present with chronic clinical manifestations or even acute fulminant

illness. Blastomycosis is not considered an opportunistic infection, but immunocompromised patients with AIDS or a history of transplantation more often have diffuse disease. Chronic pulmonary symptoms occur more frequently than acute symptoms [60–62]. Patients present with chest pain, low-grade fever, mild productive cough and haemoptysis. General symptoms of malaise, fatigue and weight loss are also often present.

Blastomycosis is sometimes found in patients referred for the evaluation of a nodule or mass suspicious for lung cancer [60,61]. Nodules or masses are the second-most common radiologic finding in blastomycosis, occurring in up to 31% of cases [61]. The lesions are usually well circumscribed and 3–10 cm in diameter; they tend to be paramediastinal or perihilar [62]. These manifestations can be difficult to differentiate from lung cancer (Fig. 8). In a series of 35 patients with North American blastomycosis, lung masses were resected in 55% of patients due to high suspicion for bronchogenic carcinoma [63]. Pleural effusions are uncommon [64]. The diagnosis of blastomycosis is often delayed because it can mimic many other diseases, including bacterial pneumonia, malignancy and tuberculosis.

Pathologic findings are suppurative or granulomatous lesions with numerous organisms in epithelioid and giant cells or located freely in microabscesses. The organism is spherical and single budding, with a broad base containing multiple basophilic nuclei in a double walled central body [61–64].

CONCLUSION:

A variety of fungal pulmonary infections can present with radiologic findings that mimic lung cancer. Distinguishing between these infectious lesions and lung cancer remains challenging. Physicians should be aware of the clinical and radiologic features of these fungal diseases (summarised in Table 1). The geographic distribution of endemic areas must be considered when evaluating a patient for suspected fungal disease. A detailed anamnesis is essential, including the acquisition of information about the patient's travelling habits, migration, recreational activities and residence in endemic areas, as well as the history of any type of immunosuppression. Radiologists and clinicians need to work in collaboration, as the clinical context is essential for the appropriate interpretation of images. When a lung infection is considered to be likely (or possible), serologic tests, sputum smear, bronchoscopy with bronchoalveolar lavage and image-guided biopsy can be performed to assist in the diagnosis. The tissue material should be sent not only for histopathology but also for direct exam and culture. Precise diagnosis is crucial for the administration of appropriate treatment and to avoid unnecessary high-risk surgical procedures in these patients.

References

1. Aberle DR, Adams AM, Berg CD et al. Reduced lung-cancer mortality with low-dose computed tomographic screening. *N Engl J Med* 2011; 365: 395–409.
2. Madhusudhan KS, Gamanagatti S, Seith A, Hari S. Pulmonary infections mimicking cancer: report of four cases. *Singapore Med J* 2007; 48: e327–31.
3. Rolston KV, Rodriguez S, Dholakia N, Whimbey E, Raad I. Pulmonary infections mimicking cancer: a retrospective, three-year review. *Support Care Cancer* 1997; 5: 90–93.
4. Soubani AO, Chandrasekar PH. The clinical spectrum of pulmonary aspergillosis. *Chest* 2002; 121: 1988–99.
5. Chung CR, Lee YC, Rhee YK et al. Pulmonary coccidioidomycosis with peritoneal involvement mimicking lung cancer with Peritoneal Carcinomatosis. *Am J Respir Crit Care Med* 2011; 183: 135–6.
6. Karakelides H, Aubry MC, Ryu JH. Cytomegalovirus pneumonia mimicking lung cancer in an immunocompetent host. *Mayo Clin Proc* 2003; 78: 488–90.
7. Schweigert M, Dubecz A, Beron M, Ofner D, Stein HJ. Pulmonary infections imitating lung cancer: clinical presentation and therapeutical approach. *Ir J Med Sci* 2013; 182: 73–80.
8. Barreto MM, Marchiori E, Amorim VB et al. Thoracic paracoccidioidomycosis: radiographic and CT findings. *Radiographics* 2012; 32: 71–84.
9. Rodrigues Gda S, Severo CB, Oliveira Fde M, Moreira Jda S, Prolla JC, Severo LC. Association between paracoccidioidomycosis and cancer. *J Bras Pneumol* 2010; 36: 356–62.

10. Teixeira Mde M, Theodoro RC, Derengowski Lda S, Nicola AM, Bagagli E, Felipe MS. Molecular and morphological data support the existence of a sexual cycle in species of the genus *Paracoccidioides*. *Eukaryot Cell* 2013; 12: 380–9.
11. Gasparetto EL, Escuissato DL, Davaus T et al. Reversed halo sign in pulmonary paracoccidioidomycosis. *AJR* 2005; 184: 1932–4.
12. Marchiori E, Valiante PM, Mano CM et al. Paracoccidioidomycosis: high-resolution computed tomography-pathologic correlation. *Eur J Radiol* 2011; 77: 80–84.
13. Souza AS Jr, Gasparetto EL, Davaus T, Escuissato DL, Marchiori E. High-resolution CT findings of 77 patients with untreated pulmonary paracoccidioidomycosis. *Am J Roentgenol* 2006; 187: 1248–52.
14. Maym_o Argá~naraz M, Luque AG, Tosello ME, Perez J. Paracoccidioidomycosis and larynx carcinoma. *Mycoses* 2003; 46: 229–32.
15. Chojniak R, Vieira RA, Lopes A, Silva JC, Godoy CE. Intestinal paracoccidioidomycosis simulating colon cancer. *Rev Soc Bras Med Trop* 2000; 33: 309–12.
16. Gurney JW, Conces DJ. Pulmonary histoplasmosis. *Radiology* 1996; 199: 297–306.
17. Ferreira MS, Borges AS. Histoplasmosis. *Rev Soc Bras Med Trop* 2009; 42: 192–8.
18. Severo LC, Oliveira FM, Irion K, Porto NS, Londero AT. Histoplasmosis in Rio Grande do Sul, Brazil: a 21-year experience. *Rev Inst Med Trop Sao Paulo* 2001; 43: 183–7.
19. Baum GL, Green RA, Schwarz J. Enlarging pulmonary histoplasma. *Am Rev Respir Dis* 1960; 82: 721–6.
20. Goodwin RA Jr, Snell JD Jr. The enlarging histoplasma. Concept of a tumor-like phenomenon encompassing the tuberculoma and coccidioidoma. *Am Rev Respir Dis* 1969; 100: 1–12.

21. Palayew MJ, Frank H. Benign progressive multinodular pulmonary histoplasmosis. A radiological and clinical entity. *Radiology* 1974; 111: 311–4.
22. Yousem SA, Thompson VC. Pulmonary hyalinizing granuloma. *Am J Clin Pathol* 1971; 87: 1–6.
23. Engleman P, Liebow AA, Gmelich J, Friedman PJ. Pulmonary hyalinizing granuloma. *Am Rev Respir Dis* 1977; 115: 997–1008.
24. Deppen S, Putnam JB Jr, Andrade G et al. Accuracy of FDG-PET to diagnose lung cancer in a region of endemic granulomatous disease. *Ann Thorac Surg* 2011; 92: 428–32.
25. McAdams HP, Rosado-de-Christenson ML, Templeton PA, Lesar M, Moran CA. Thoracic mycoses from opportunistic fungi: radiologicpathologic correlation. *Radiographics* 1995; 15: 271–86.
26. Picardi JL, Kauffman CA, Schwarz J, Phair JP. Detection of precipitating antibodies to *Histoplasma capsulatum* by counterimmunoelectrophoresis. *Am Rev Respir Dis* 1976; 114: 171–6.
27. Wheat J, French ML, Kamel S, Tewari RP. Evaluation of cross-reactions in *Histoplasma capsulatum* serologic tests. *J Clin Microbiol* 1986; 23: 493–9.
28. Kauffman CA, Israel KS, Smith JW, White AC, Schwarz J, Brooks GF. Histoplasmosis in immunosuppressed patients. *Am J Med* 1979; 64: 923–32.
29. Wheat LJ, Kauffman CA. Histoplasmosis. *Infect Dis Clin N Am* 2003; 17: 1–19, vii.
30. Severo CB, Gazzoni AF, Severo LC. Chapter 3 - Pulmonary cryptococcosis. *J Bras Pneumol* 2009; 35: 1136–44.
31. Fox DL, M€uller NL. Pulmonary cryptococcosis in immunocompetent patients: CT findings in 12 patients. *Am J Roentgenol* 2005; 185: 622–6.

32. Patz EF Jr, Goodman PC. Pulmonary cryptococcosis. *J Thorac Imaging* 1992; 7: 51–55.
33. Litman ML, Walter JE. Cryptococcosis: current status. *Am J Med* 1968; 45: 922–32.
34. Campbell GD. Primary pulmonary cryptococcosis. *Am Rev Respir Dis* 1966; 94: 236–43.
35. Galanis E, Hoang L, Kibsey P, Morshed M, Phillips P. Clinical presentation, diagnosis and management of *Cryptococcus gattii* cases: Lessons learned from British Columbia. *Can J Infect Dis Med Microbiol* 2009; 20: 23–28.
36. Stamm AM, Polt SS. False negative cryptococcal antigen test. *JAMA* 1980; 244: 1359.
37. Gazzoni AF, Oliveira F de M, Salles EF et al. Unusual morphologies of *Cryptococcus* spp. in tissue specimens: report of 10 cases. *Rev Inst Med Trop Sao Paulo* 2010; 52: 145–9.
38. Desai NR, McGoey R, Troxclair D, Simeone F, Palomino J. Coccidioidomycosis in nonendemic area: case series and review of literature. *J La State Med Soc* 2010; 162: 97–103.
39. Thompson GR 3rd. Pulmonary coccidioidomycosis. *Semin Respir Crit Care Med* 2011; 32: 754–63.
40. Capone D, Marchiori E, Wanke B et al. Acute pulmonary coccidioidomycosis: CT findings in 15 patients. *Br J Radiol* 2008; 81: 721–4.
41. Deus Filho A. Chapter 2: Coccidioidomycosis. *J Bras Pneumol* 2009; 35: 920–30.
42. Petrini B, Sk€old CM, Bronner U, Elmberger G. Coccidioidomycosis mimicking lung cancer. *Respiration* 2003; 70: 651–4.

43. Franquet T, M€uller NL, Gim_enez A, Guembe P, de la Torre J, Bague S. Spectrum of pulmonary aspergillosis: histologic, clinical, and radiologic findings. *RadioGraphics* 2001; 21: 825–37.
44. Kenney HH, Agrons GA, Shin JS; Armed Forces Institute of Pathology. Best cases from the AFIP. Invasive pulmonary aspergillosis: radiologic and pathologic findings. *Radiographics* 2002; 22: 1507–10.
45. Wilkinson MD, Fulham MJ, McCaughan BC, Constable CJ. Invasive aspergillosis mimicking stage IIIA non-small-cell lung cancer on FDG positron emission tomography. *Clin Nucl Med* 2003; 28: 234–5.
46. Gefter WB. The spectrum of pulmonary aspergillosis. *J Thorac Imaging* 1992; 7: 56–74.
47. Godoy MC, Viswanathan C, Marchiori E et al. The reversed halo sign: update and differential diagnosis. *Br J Radiol* 2012; 85: 1226–35.
48. Park SY, Lim C, Lee SO et al. Computed tomography findings in invasive pulmonary aspergillosis in non-neutropenic transplant recipients and neutropenic patients, and their prognostic value. *J Infect* 2011; 63: 447–56.
49. Park SY, Kim SH, Choi SH et al. Clinical and radiological features of invasive pulmonary aspergillosis in transplant recipients and neutropenic patients. *Transpl Infect Dis* 2010; 12: 309–15.
50. Severo CB, Guazzelli LS, Severo LC. Chapter 7: zygomycosis. *J Bras Pneumol* 2010; 36: 134–41.
51. McAdams HP, Rosado de Christenson M, Strollo DC, Patz EF Jr. Pulmonary mucormycosis: radiologic findings in 32 cases. *Am J Roentgenol* 1997; 168: 1541–8.

52. Marchiori E, Marom EM, Zanetti G, Hochegger B, Irion KL, Godoy MC. Reversed halo sign in invasive fungal infections: criteria for differentiation from organizing pneumonia. *Chest* 2012; 142: 1469–73.
53. Marchiori E, Zanetti G, Escuissato DL et al. Reversed halo sign: high-resolution CT scan findings in 79 patients. *Chest* 2012; 141: 1260–6.
54. Kotoulas C, Psathakis K, Tsintiris K, Sampaziotis D, Karnesis L, Laoutidis G. Pulmonary mucormycosis presenting as Horner's syndrome. *Asian Cardiovasc Thorac Ann* 2006; 14: 86–87.
55. Chung JH, Godwin JD, Chien JW, Pipavath SJ. Case 160: Pulmonary mucormycosis. *Radiology* 2010; 256: 667–70.
56. Tamm M, Malouf M, Glanville A. Pulmonary scedosporium infection following lung transplantation. *Transpl Infect Dis* 2001; 3: 189–94.
57. Boutati EI, Anaissie EJ. *Fusarium*, a significant emerging pathogen in patients with hematologic malignancy: ten years' experience at a cancer center and implications for management. *Blood* 1997; 90: 999–1008.
58. Freidank H. Hyalohyphomycoses due to *Fusarium* spp.—two case reports and review of the literature. *Mycoses* 1995; 38: 69–74.
59. Horre R, Jovanic B, Marklein G et al. Fatal pulmonary scedosporiosis. *Mycoses* 2003; 46: 418–21.
60. Fang W, Washington L, Kumar N. Imaging manifestations of blastomycosis: a pulmonary infection with potential dissemination. *Radiographics* 2007; 27: 641–55.
61. Bradsher RW, Chapman SW, Pappas PG. Blastomycosis. *Infect Dis Clin North Am* 2003; 17: 21–40.
62. Kuzo RS, Goodman LR. Blastomycosis. *Semin Roentgenol* 1996; 31: 45–51.

63. Brown LR, Swensen SJ, Van Scoy RE, Prakash UB, Coles DT, Colby TV. Roentgenologic features of pulmonary blastomycosis. *Mayo Clin Proc* 1991; 66: 29–38.
64. Failla PJ, Cerise FP, Karam GH, Summer WR. Blastomycosis: pulmonary and pleural manifestations. *South Med J* 1995; 88: 405–10.

Figure 1 - A 75-year-old man from Latin America who presented with a 3-month history of anorexia and weight loss. He also complained of haemoptysis associated with a non-productive cough. He denied any history of fever or night sweats. His medical history included a 60-pack-year smoking habit. (a) Axial computed tomography (CT) image shows a spiculated pulmonary mass associated with pleural effusion in the right lower lobe, suggesting lung cancer. (b) CT image with sagittal reconstruction demonstrates the same findings. (c) Axial T2-weighted magnetic resonance image shows the pulmonary mass and septated pleural effusion. (d) Biopsy specimens contained predominantly non-caseating granulomas; intracellular and extracellular fungal elements compatible with budding forms of *Paracoccidioides brasiliensis* (Grocott, x400). (e) Axial T1-weighted magnetic resonance image shows regression of the pulmonary mass and pleural effusion 6 months after treatment (amphotericin B and itraconazole).

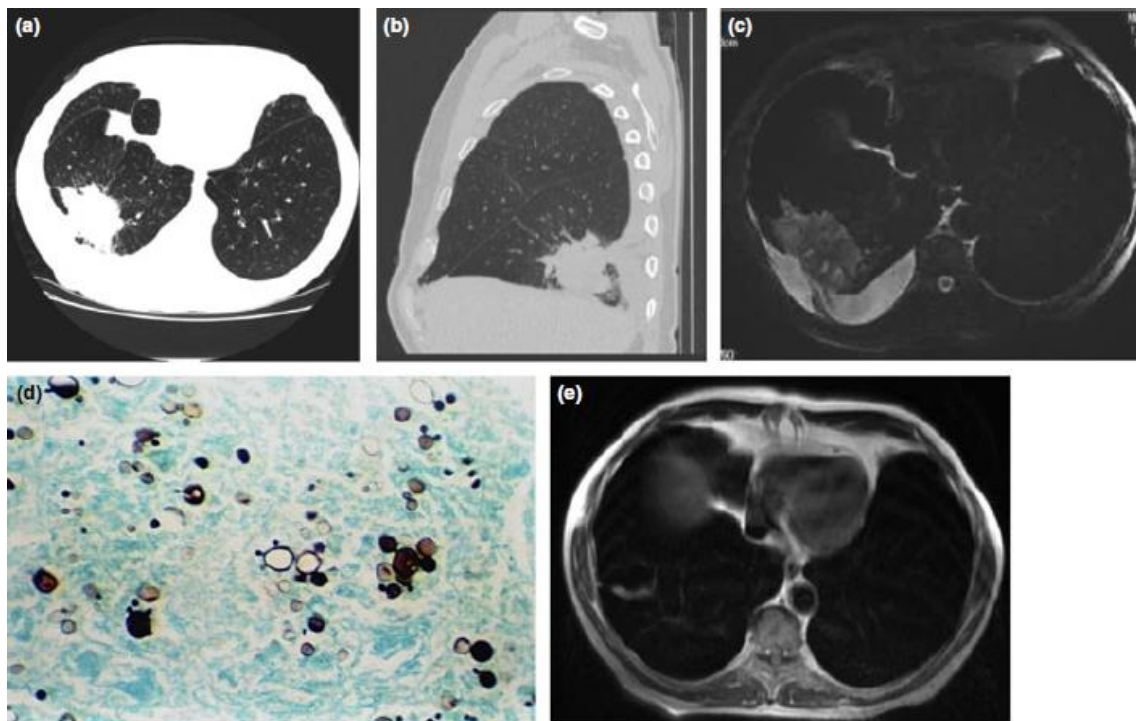


Figure 2 - An asymptomatic 65-year-old man who underwent evaluation of a pulmonary nodule newly detected on a chest X-ray. He denied any history of fever or night sweats. His medical history included a 45-pack-year smoking habit. (a) Axial computed tomography (CT) image shows a spiculated pulmonary nodule associated with adjacent bullous emphysema in the left upper lobe, suggesting lung cancer. (b) CT image with coronal reconstruction demonstrates the same findings. (c) Microscopic examination of transthoracic needle biopsy specimens showed yeast cells of *Histoplasma capsulatum* in smear. The fungal walls are black and organisms are small, uninucleate and spherical to ovoid; they have single buds and are often clustered (Grocott, x 250).

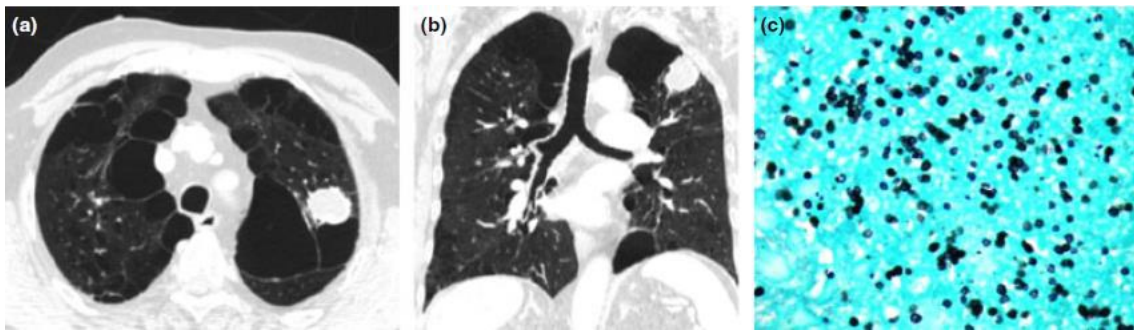


Figure 3 - An asymptomatic 44-year-old man who underwent evaluation of a pulmonary nodule. He denied any history of fever or night sweats. His medical history included a 75-pack-year smoking habit. (a) A positron emission tomography (PET)/computed tomography (CT) image with coronal reconstruction demonstrates a spiculated pulmonary nodule with high uptake [standardised uptake value (SUV) = 5.5]. (b) PET/CT image with coronal reconstruction demonstrates hilar and subcarinal lymph nodes with high uptake (SUV = 8.5). (c) Microscopic examination of mediastinoscopic biopsy specimens showed yeast cells of *Histoplasma capsulatum* in smear (Grocott, x250).

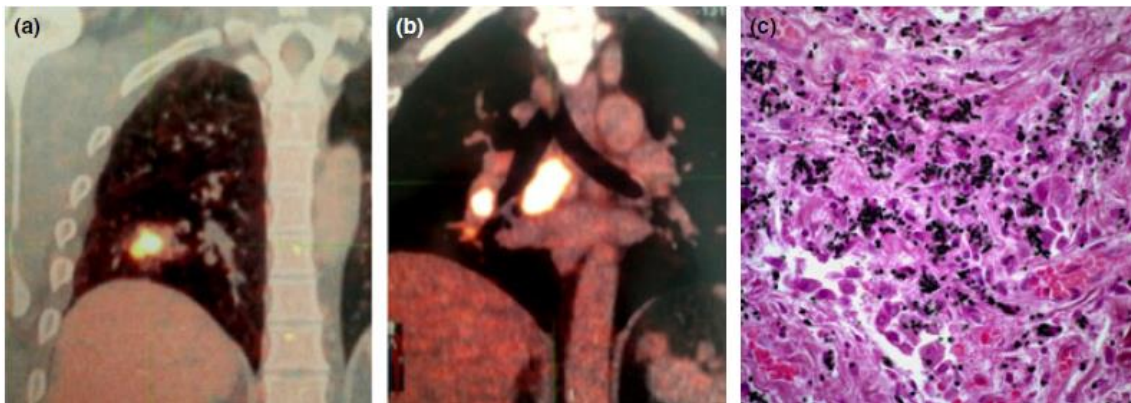


Figure 4 - A 53-year-old man who presented with a 3-month history of right chest pain. He denied any history of fever or night sweats. His medical history included a 33-pack-year smoking habit. (a) Axial computed tomography (CT) image shows a spiculated pulmonary mass in the right upper lobe with pleural contact, suggesting lung cancer. (b) CT image with sagittal reconstruction demonstrates the same findings. (c) Microscopic examination of transthoracic needle biopsy specimens showed yeast cells of *Cryptococcus neoformans* in smear; fungal cell wall is stained in black (Grocott, x250). (d) A CT image shows regression of the pulmonary mass 7 months after treatment (fluconazole).

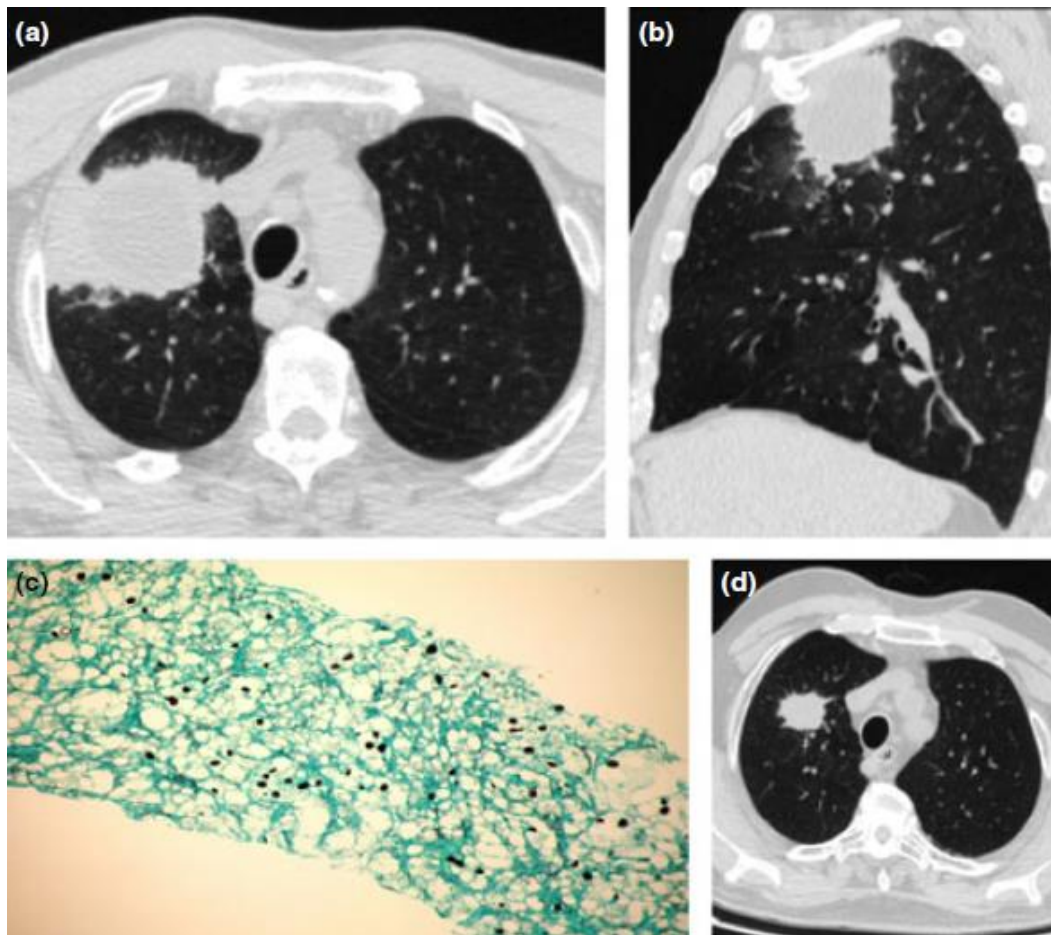


Figure 5 - An asymptomatic 49-year-old woman underwent evaluation of a pulmonary nodule discovered on a chest X-ray. She denied any history of fever or night sweats. Her medical history included a 25-pack-year smoking habit. (a) Axial computed tomography (CT) image shows a lobulated pulmonary nodule in the right upper lobe, suggesting lung cancer. (b) Microscopic examination of transthoracic needle biopsy specimens showed yeast cells of *Coccidioides immitis* (spherules in black) in smear (Grocott, x250). (c) CT image shows regression of the pulmonary nodule 3 months after treatment (itraconazole).

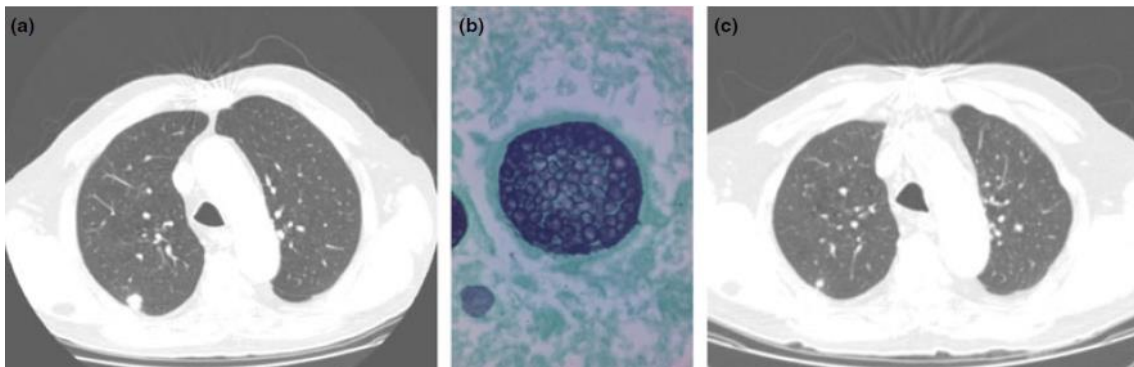


Figure 6 - A 77-year-old man who presented with a 3-month history of bloody sputum. He denied any history of fever or night sweats. His medical history included a 60-pack-year smoking habit and previous treatment of pulmonary tuberculosis. (a) Axial computed tomography (CT) image shows a cavitated pulmonary mass with irregular thick walls, suggesting lung cancer. The patient underwent surgery, which confirmed the diagnosis of cavitary colonization by *Aspergillus fumigatus*. (b) Tissue sections contained narrow, tubular and regularly septate hyphae compatible with *Aspergillus fumigatus* (Grocott, x100). Branching is regular, progressive and dichotomous; hyphal branches tend to arise at acute angles from parent hyphae.

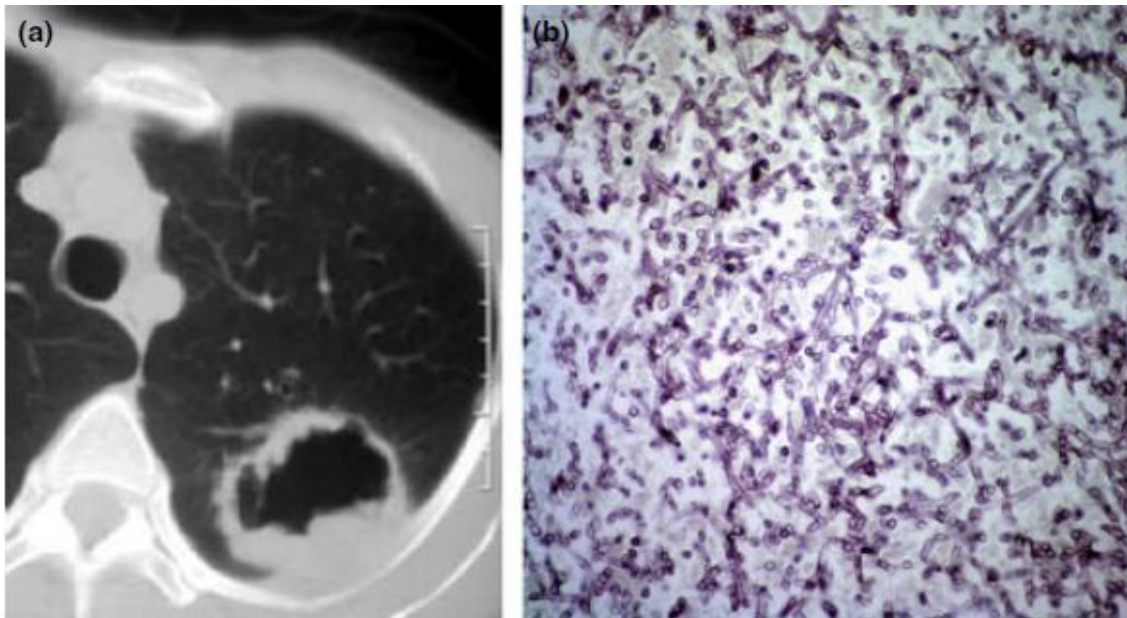


Figure 7 - A 45-year-old male kidney transplant recipient presented with a 15-day history of bloody sputum and night sweats. His medical history included a 30-pack-year smoking habit. (a) Axial computed tomography (CT) image shows a cavitated pulmonary mass with irregular thick walls. No centrilobular lesion suggesting the bronchogenic spread of a possible granulomatous infection is present. (b) CT image with coronal reconstruction demonstrates similar findings. Microscopic examination of a bronchoalveolar lavage specimen yielded findings compatible with mucormycosis. The lesion progressed despite appropriate treatment with antimycotic drugs, and the patient died 15 days after initiation of treatment. Within this context of immunosuppression, the possibility of invasive fungal infection should be favoured over lung cancer. Early diagnosis is of utmost importance in such cases.

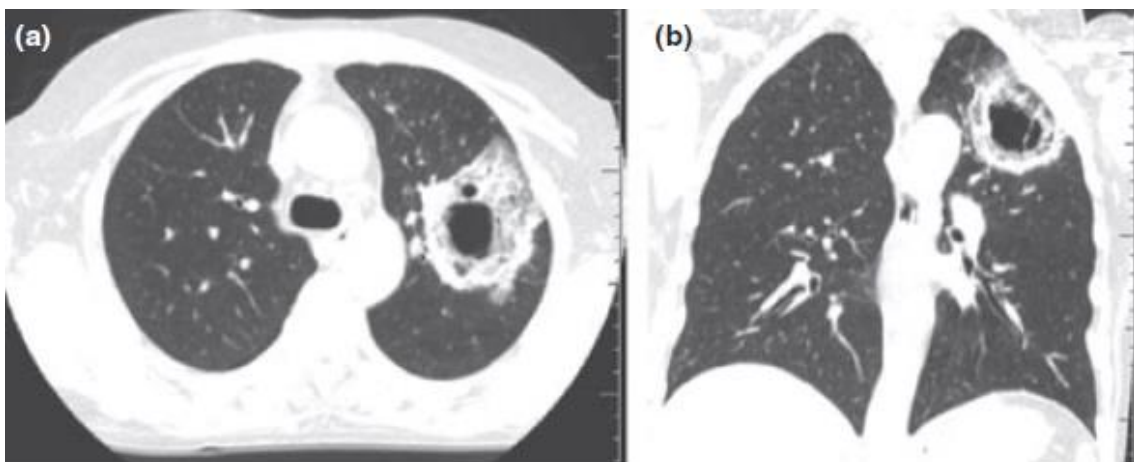


Figure 8 - An asymptomatic 59-year-old man who had undergone surgery for oesophageal cancer. He denied any history of fever or night sweats. His medical history included a 35-pack-year smoking habit. (a) Axial computed tomography (CT) image shows a new spiculated pulmonary nodule in the left upper lobe, suspicious for lung cancer or metastasis. (b) Axial positron emission tomography (PET)/CT image demonstrates high fluorodeoxyglucose uptake (standardized uptake value = 6.5) by the speculated pulmonary nodule. (c) Microscopic examination of transthoracic needle biopsy specimens showed that the pulmonary parenchyma had been replaced by necrotizing granulomatous inflammation (haematoxylin and eosin, x20). (d) Gomori methenamine silver histochemical staining showed yeast with broad-based budding typical of North American blastomycosis (x60).

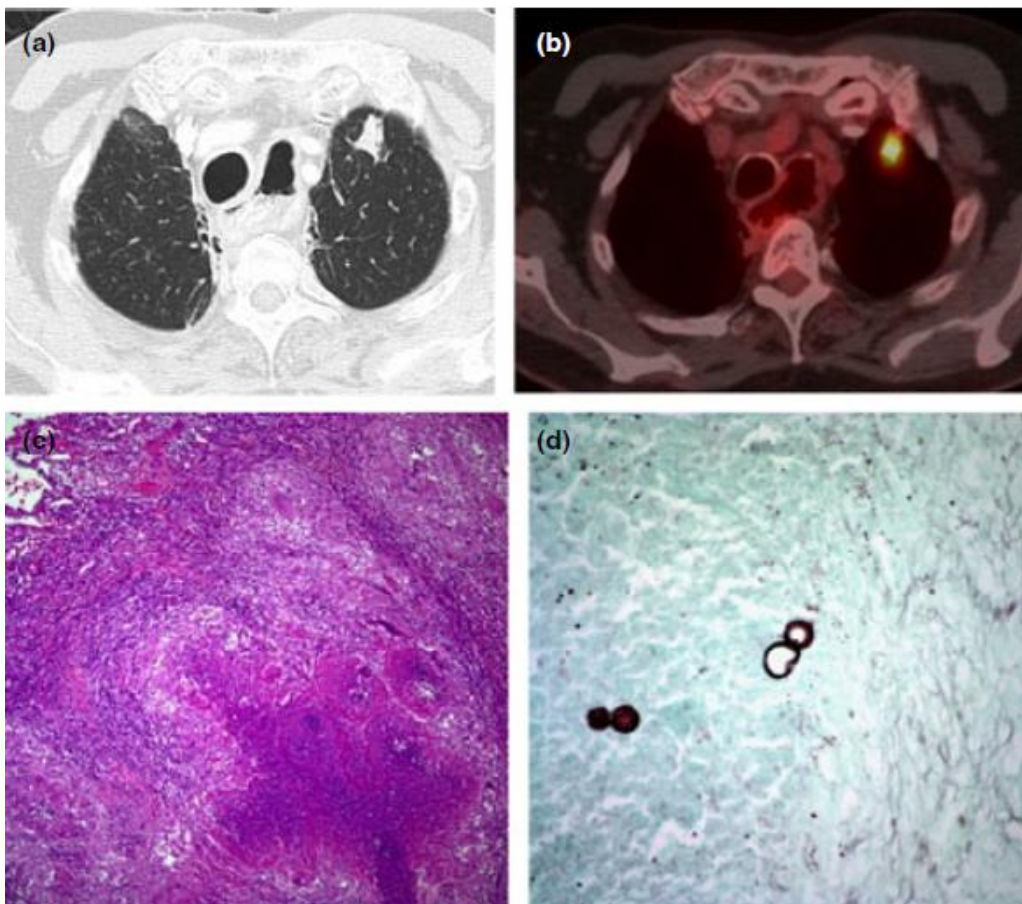


Table 1 Classical features in fungal diseases that assist in differential diagnosis with lung cancer.

Fungal disease	Pathogenesis	Areas of endemicity	Radiology	Diagnosis	Other
Paracoccidioidomycosis ^{8,9}	Primary pathogen/ Abnormal T-lymphocyte function	Latin America	Pleomorphic	Culture, biopsy, ID	Oral mucosal lesions
Histoplasmosis ^{3,17,19,27,29}	Primary pathogen/ Abnormal T-lymphocyte function	North America river valleys, several Caribbean islands, Central and South Americas	Solitary or multiple nodules with central calcification.	Culture, biopsy, ID, CF, Ag detection in serum/urine	Most common cancer mimicker
Cryptococcosis (<i>Cryptococcus gattii</i>) ^{30,31,32,35}	Primary pathogen/ Abnormal T- lymphocyte function	Ubiquitous	Solitary lung nodule or mass (cryptococcoma); multiple nodules	Culture, biopsy, direct examination of CSF, serum/CSF cryptococcal Ag	Immunocompetent; more likely to form cryptococcomas
Cryptococcosis (<i>C. neoformans</i>) ^{30,31,32,35}	Opportunistic pathogen/ Abnormal T-lymphocyte function	Ubiquitous	Multiple nodules, segmental or lobar consolidation, interstitial pneumonia	Culture, biopsy, direct examination of CSF, serum/CSF cryptococcal Ag	Immunocompromised; symptoms related to systemic dissemination, typically to the CNS predominate
Coccidioidomycosis ^{38,40,41}	Primary pathogen/ Abnormal T-lymphocyte function	<i>Coccidioides immitis</i> : California <i>C. posadasii</i> : all the remaining endemic areas of the American continent, from the southern United States to Argentina	Peripheral lung nodules that are predominantly cavitated	Culture, biopsy, ID	Simulates metastatic cancer and other granulomatous diseases
Aspergilloma ^{25,43,46}	Saprophytic/ Cavitary lung disease	Ubiquitous	Round mass with soft-tissue density within a cavity that moves when the patient changes position	Biopsy, direct microscopic exam and culture	Colonises a pulmonary cavity, forming a mass of intertwined fungal hyphae admixed with cellular debris
Angioinvasive Aspergillosis ^{25,43,44,46}	Opportunistic/ neutropenia	Ubiquitous	Halo sign, reversed halo sign, wedge- shaped consolidation	Biopsy, direct microscopic exam and culture	Neutropenia due to haematologic malignancies and HSCT
Mucormycosis ^{25,50,51}	Opportunistic/ neutropenia	Ubiquitous	Progressive lobar or multilobar consolidation, pulmonary masses and nodules	Biopsy, direct microscopic exam and culture	Rapidly progressive pneumonia in patients with haematologic malignancies
Blastomycosis ^{60,61,64}	Primary pathogen/ Abnormal T-lymphocyte function	Canada and the upper Midwest of the United States; Africa	Nodules or masses that tend to be paramediastinal or perihilar	Biopsy, direct microscopic exam and culture	Diagnosis is often delayed because it can mimic other diseases (bacterial pneumonia, malignancy and tuberculosis)

ID, immunodiffusion; CF, complement fixation; Ag, antigen; CSF, cerebrospinal fluid; CNS, central nervous system; HSCT, haematopoietic stem cell transplantation.